THE RESPONSE OF

KA ROIMATA O HINE HUKATERE

FRANZ JOSEF GLACIER

TO CLIMATE CHANGE

A thesis

submitted in fulfillment

of the requirements for the Degree

of

Doctor of Philosophy

in the

University of Canterbury

by

Brian Anderson

University of Canterbury

2003

Nestled among the rocky folds of the mighty Aorangi mountain is a white river of ice that creeps very slowly towards its father, Tangaroa. When the air is still and the sky is newly sprinkled with stars, a snow maiden picks her way through the debris and peers into the icy crevices of the glacier.

"Wawe," she calls. "Wawe, " she murmurs. "Where are you?"

Her voice is so chilly that those who have heard her calling have shuddered with dread and have held tight to each other saying, "It is Hine Hukatere, the snow maiden. She still looks for Wawe, her own true love."

"How can that be?" says someone.

"I'll tell you," says the One-who-knows.

Many years ago Hine Hukatere saw a young man walking in the foothills of Aorangi looking for cutting stones. He was very charming and she was so beautiful that they soon fell in love. However, every time Wawe tried to touch the Snow Maiden, she screamed in pain because his warm hands would melt her skin. Wawe would spring back in shock because she was so cold that his fingers would freeze instantly.

One day, Hine asked Wawe if he would go with her high into the mountains to ask Aorangi for warm breath and pink cheeks just like his.

Wawe was overjoyed and readily agreed and so they set out across the foothills and up into the mountain. As they climbed Wawe became afraid. His ancestors had forbidden everyone from climbing Aorangi. It was the home of the tribal gods who jealously guarded their resting place. Higher and higher they went. The air grew cold and thin. Hine Hukatere called to Wawe, "Isn't it beautiful? Could we not live up here together?"

Wawe was too cold to reply. His fingers and toes were numb. His face was blue and his eyelids were heavy with snow. He slowly turned to Hine and saw her skipping with pleasure over the snowy ground.

"Come on Wawe, not far to go."

"Wawe, not far to go."

Wawe stumbled towards her voice. He heard Tawhiri Matea scream in his head. "Get off this mountain, you mortal!"

He felt Hine touch his hand as Tawhiri Matea pushed him off the edge of the path. As he fell Hine Hukatere shook millions of snowflakes from her fingers so that Wawe would fall into their softness. But Tawhiri Matea blew the snowflakes over the mountain and Wawe plunged down to his death.

Hine Hukatere never leaves the mountains now. Nor does she seek the company of people anymore. Instead she wanders along the white river of ice peering between the thick blocks and walls hoping to find Wawe again.

And as she goes she cries and her tears are ice that fall into the glacier and move it ever so slowly towards Tangaroa.

Hana Weka

Source: Weka (2003).

Contents

Abstract

In the past century global climate warming has led to widespread glacier recession, which in turn has made a significant contribution to eustatic sea level rise. In the coming century, warming is projected to continue and small glacier melt will make a further contribution to sea level rise. In the monitoring of global glacier change and prediction of the response of glacier to climate change, the few well-studied Southern Hemisphere glaciers have an important role to play in elucidating global climate linkages, both in the information that they have left on past climate and glacier change, and the information the provide on future changes to the cryosphere.

Franz Josef Glacier, with the best record of terminus position in the Southern Hemisphere, has an important place in assessing global climate and glacier change. The aim of this thesis is examine the response of Franz Josef Glacier to climate change. This goal is achieved through the application of coupled mass balance and ice-flow models, verified with an extensive set of field measurements.

A range of previous studies have attempted to understand the linkages between climate and the advance and retreat of the glacier. Methods of examining the response of the glacier have progressed from simple correlations of climate variables and terminus position, to coupled mass balance - ice-flow models. Despite the large amount written about the glacier, there have been few direct measurements of ice velocity, almost a complete lack of mass balance measurements and no measurements of ice thickness. Without these measurements it is difficult to have confidence in the output of the models. A comparison of the output of these models indicates a wide range of predicted mass balance and ice velocity, the two essential components of glacier response to climate change.

The programme of field measurement indicates that Franz Josef Glacier has an extremely high mass turnover. Ablation at the terminus is more than 20 m/a w.e. and accumulation in the névé up to 7 m/a w.e. A degree-day mass balance model is able to simulate these measurements, but measured mass balance at the same elevation varies significantly, indicating that the assumption that the only spatial variation of mass balance is with elevation may not be valid here. Ice velocity reaches 2.5 m/day, which is high for a mid-latitude glacier. Temporal variations in velocity measurements indicate that basal sliding occurs year round with little seasonal variation, and a greater sliding velocity on the glacier tongue than in the accumulation area. An ice velocity model tuned to the ice velocity measurements confirms this pattern of sliding velocity.

The coupled mass balance and ice-flow simulates the overall 20th century glacier retreat, but does not simulate the terminus response well, a result of the mass balance model not producing accurate results for the period 1894-1940. The model, when run for a short period of time into the future, indicates that glacier response is independent of climate for a period of 5 years, and that Franz Josef Glacier will almost certainly retreat a further 1 km in the next 5 years. Longer term predictions are dependent on climate change scenarios, such that by 2100 the Franz Josef Glacier could be anywhere from a size similar to the present to two small glaciers perched on the highest peaks. The mean scenario indicates that by 2100 the glacier will have lost 20% of its volume and retreated 4 km to terminate near the present day Almer Glacier.

The possibly significant recession of the Franz Josef Glacier will have an impact on the local community and economy with recreation and tourism on the glacier becoming much more difficult. While the results of this study are particular to Franz Josef Glacier, they provide information on how other small glaciers respond to climate change.

List of Figures

List of Tables

List of Symbols

a	surface slope
a	ablation
A	area per elevation band
b	glacier bed elevation
B	mass balance
c	accumulation
D	effective diffusion
f_a	ablation factor
f_c	accumulation factor
f_d	deformation flow parameter
f_s	sliding flow parameter
g	acceleration due to gravity
F	shape factor
h	glacier surface elevation
H	ice thickness
k	degree-day factor
n	flow law exponent
N	effective pressure
q	valley side slope
r	density of ice
p	precipitation
p_{total}	total daily precipitation
P	wetted perimeter
q	sliding law exponent
r	sliding law exponent
S	cross-section area
t	time
T	temperature
T_{crit}	snow threshold temperature
T_{hourly}	hourly temperature
T_{mean}	mean daily temperature
T_{sum}	positive daily temperature sum
t_{xz}	basal shear stress
t_{xx}	longitudinal stress
t'_{xx}	longitudinal deviatoric stress
U	total velocity
U_d	deformation velocity
U_s	sliding velocity
w_b	glacier width at bed
w_s	glacier width at surface
x	coordinate in direction of ice flow
z	vertical coordinate/elevation

Acknowledgements

My parents and grandparents have instilled in their children a love and respect for the Aotearoa *New Zealand* mountains and glaciers, lakes and rivers, and the plants and animals that inhabit them. From them came the inspiration and support for this thesis.

Some other acknowledgements:

- Thanks to Becky Goodsell and lots of other field assistants for collecting data;
- Fieldwork was supported by University of Canterbury grant UC6474 and a Geography Department grant;
- Brett Mullan of NIWA kindly supplied climate change scenario data;
- Roddy Henderson, of NIWA, kindly supplied Almer Hut, Alex Knob and Douglas Hut rainfall data, of which the Douglas Hut data was jointly collected by Meridian Energy;
- Trevor Chinn, of NIWA, kindly supplied Almer Glacier EOSS data;
- The Department of Conservation permitted research on the glacier;
- Franz Josef Glacier Guides, and Mark Melsop in particular, provided encouragement and practical help on the glacier
- All of the local glacier guides kept access to the glacier open;
- The New Zealand Alpine Club provided accommodation in the névé;
- Modelling help was provided by R. Hindmarsh.

Finally, I acknowledge that during the time that this thesis took to write, approximately 1 million animals have been tortured in New Zealand in the name of science, vanity and greed. Of these, half were killed, and thousands more were subjected to ‘severe’ or ‘very severe’ suffering.

1 Introduction

1.1 Glacier response to climate change

The response of a glacier to climate change is a complex process made up of a number of steps which are generally non-linear (Figure 1.1). The general climate over a wide area depends on factors such as latitude and continentality. Local topography and glacier configuration influence the local glacier climate which controls the mass and energy exchanges at the glacier surface and ultimately results in the net mass balance of the glacier. The snow and ice is transported by ice flow, a process which is strongly controlled by the glacier bed topography, resulting in changes in glacier geometry, most commonly recorded as a terminus position change.

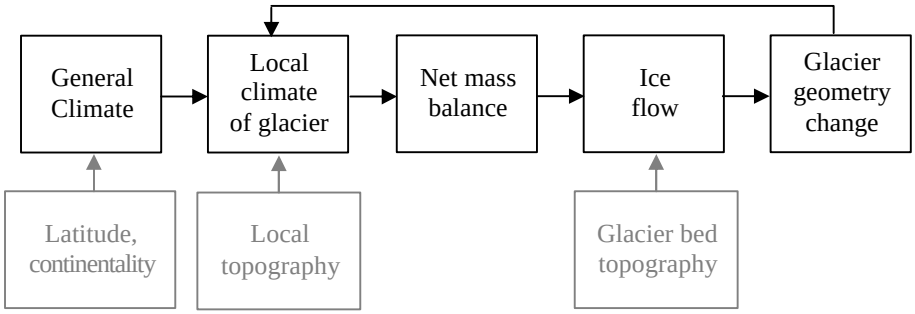

Figure 1.1. Aspects of the relationship between climate and glacier response. Modified from Paterson (1994).

In the coming century global mean air temperature is expected to rise by between 2°C and 4.5°C (IPCC, 2001). This temperature increase comes on top of an increase in temperature in the last century of between 0.4 to 0.8°C (IPCC 2001), which has lead to the worldwide shrinkage of many small glaciers (IPCC, 2001; Oerlemans, 2001). Small glaciers are defined here as any land ice outside the Greenland ice sheet and Antarctica (van de Wal and Wild, 2001). The increased warming rate expected in the coming century will consequently have a large effect on small glaciers (IPCC, 2001), and the response of small glaciers to climate change is an important issue on both a global and local scale.

On a global scale the recession of small glaciers in the last century is one of the main factors that has led to global sea-level rise (Meier, 1984; Warrick and Oerlemans, 1990; Wigley and Raper, 1993; IPCC, 2001). In the coming century one-third of the total sea level rise resulting from climate change will be from the world-wide melt of small glaciers (Gregory and Oerlemans, 1998; Van de Wal and Wild, 2001; IPCC, 2001).

On a local scale, water from glacierised basins is often used for irrigation and hydro-electric generation, and changes in run-off will have significant effects on these resource uses (e.g. Jóhannesson and others,

1995; Jóhannesson, 1997; Engeset and others, 2000). In many mountainous areas, glaciers also contribute to tourism and in some areas glacier recession will have a drastic impact on mountain tourism.

1.2 Evaluating glacier change

The impact of glacier changes on sea-level has led many researchers to attempt to assess glacier response on a global scale (Gregory and Oerlemans, 1998; Oerlemans and others, 1998; Van de Wal and Wild, 2001). However there are difficulties with this approach, in particular finding easily measured parameters for global glacier monitoring and predicting the distributions of glacier properties on a global scale (Bahr, 1997; Bahr and others, 1997; Dyurgerov and Bahr, 1999). In addition, individual glacier response is very dependent on the particular climatic and topographic setting of each glacier and it is therefore difficult to make generalisations about glacier response (Oerlemans and others, 1998). Hence many studies have concentrated on the response processes of individual glaciers (e.g. Greuell, 1992; Wallinga and Van de Wal, 1992; Schmeits and Oerlemans, 1997; Zuo and Oerlemans, 1997; Jóhannesson, 1997; Oerlemans, 2001).

The value of examining the response of individual glaciers to climate change is three-fold. Firstly, detailed knowledge of individual glacier response provides the basis for testing regional and global generalisations of glacier response (Oerlemans, 1997a). Secondly, if we understand climate-glacier response processes we can infer past climate from historical and geological evidence of glacier length. Thirdly, the local effects of glacier change are important to local communities for water and other resources.

1.3 The glaciers of New Zealand

The glaciers of New Zealand are of global interest in the study of climate change and glacier response because of the importance of interhemispheric relationships in climate change processes (e.g. Denton and others, 1999; Stocker, 2002). The small land area in the Southern Hemisphere compared to the Northern Hemisphere means that any Southern Hemisphere terrestrial evidence of past climate change is extremely valuable. A number of glaciers in New Zealand have had their terminus position recorded since the late 19th century which provides insight into recent climate and glacier fluctuations in the Southern Hemisphere (Grove, 1988). On a longer time scale, geomorphic data from Little Ice Age (Porter, 1975; McKinzey, 2001) and earlier glacier variations (Wardle, 1973; Denton and Hendy, 1994; Ivy-Ochs and others, 1999) are important evidence of the associated Southern Hemisphere climate changes. This evidence is particularly important with recent studies indicating that global climate processes may be driven from the Southern Hemisphere (Stocker, 2003).

To understand the response of glaciers to climate change on a global scale, we need to understand the response characteristics of the full range of glacier types. The mass turnover of the most maritime of the

New Zealand glaciers, those on the western side of the drainage divide, is high (Oerlemans, 2001). In particular, the Franz Josef Glacier appears to have a mass turnover which is unmatched by any other studied mid-latitude glacier (Oerlemans, 2001), providing the opportunity to understand how glaciers at the extreme high-end of the activity index scale (Andrews, 1975) respond to changes in climate.

There have been many studies on New Zealand glaciers, but they have tended to be rather sporadic (Fitzharris and others, 1999). There are relatively few mass balance measurements (Table 1.1), compared to other parts of the world where comprehensive mass balance programmes have been running for many decades (Haeberli and others, 1998). The only record of mass balance in New Zealand for an entire glacier for an entire year or more is from Ivory Glacier between 1969 and 1975. The other mass balance measurements have not been comprehensive enough to calculate net annual mass balance for any glacier for any year.

Table 1.1. A summary of glaciers with previous mass balance measurements in New Zealand.

Glacier	Location[(1)]	Study
Ivory Glacier	43°7'S,170°50'E west	Anderton and Chinn, 1978
Franz Josef Glacier	43°29'S,170°11'E west	Gunn, 1964; Marcus and others, 1985; Ishikawa and others, 1992; Owens and others, 1992; Kelliher and others, 1996; Ruddell, 1995
Fox Glacier	43°31'S,170°4'E west	Gunn, 1964; Ruddell, 1995
Tasman Glacier	43°43'S,170°10'E east	Goldthwait and McKellar, 1962; Chinn, 1969; Anderton, 1975; Kirkbride, 1995; Ruddell, 1995
Dart Glacier	44°29'S,169°35'E east	Bishop and Forsyth, 1988; Ruddell, 1995
Whakapapanui Glaciers	39°16'S,175°35'E North Island	Thompson and Kells, 1973

[(1)] The location column indicates whether the glaciers are to the west or east of the drainage divide for those glaciers in the South Island.

Franz Josef Glacier occupies 35 km^2 on the western flanks of the Southern Alps and its record of terminus position, since 1867, is the best in the Southern Hemisphere (Grove, 1988). The glacier is complex, with a compound névé and a number of tributary glaciers, and steep, as it falls 2500 m vertically in a length of 10.9 km. The high activity index (Andrews, 1975) of the Franz Josef Glacier is a result of the large névé, steep slopes and maritime climate (Oerlemans, 2001). Franz Josef Glacier is the best known of the New

Zealand glaciers both scientifically (e.g. Odell, 1955; Gunn, 1964; Denton and Hendy, 1994; Oerlemans, 1997b, 2001) and among tourists, with hundreds of people walking on the glacier every day in the summer.

Despite a wide range of studies on Franz Josef Glacier (Table 1.1), the only two aspects of the glacier response process (defined in Figure 1.1) which are known for Franz Josef Glacier are the general climate and the terminus position, an aspect of the glacier geometry. Consequently, a number of studies have attempted to correlate general climate variables with terminus position directly (Suggate, 1950; Soons, 1971; Hessell, 1983; Gellatly and Norton, 1984, Brazier and others, 1992) but with generally unconvincing results. Models have been constructed to refine the link between general climate and mass balance (Woo and Fitzharris, 1992; Ruddell 1995; and Oerlemans, 1997a) and between ice flow and glacier geometry changes (Ruddell 1995; and Oerlemans, 1997a), but have been limited by the absence of measurements of local climate, mass balance and bed topography. Our knowledge of the response of Franz Josef Glacier to climate change is rather disjointed.

1.4 Aims and Objectives

The Franz Josef Glacier has been chosen for this study for a number of reasons. The glacier has the best record of terminus position in the Southern Hemisphere (Grove, 1988), and this record coincides with the start of nearby instrumental climate records (Salinger, 1981), providing a valuable opportunity to verify a model of glacier response processes. In addition, there has been a significant amount of work and modelling done on the glacier already, which provides a solid basis to build upon.

The overall goal of this thesis is to assess the response of Franz Josef Glacier to climate change. The general approach to realise this goal is to use a degree-day mass balance model and a numerical flowline model, both firmly constrained by field measurements. The specific objectives are:

1. Synthesise the previous work regarding the climate - glacier linkages at Franz Josef Glacier in order to identify the key gaps and uncertainties in our knowledge of the response of the glacier to climate change.
2. Develop and verify a mass balance model which will explicitly account for the links between general climate, local glacier climate, and mass balance. Local glacier climate will be measured at a number of sites on the glacier to examine the link between general climate and local glacier climate. The link between local glacier climate and mass balance will be examined using simultaneous measurements of local climate and mass balance.
3. Develop and verify an ice-flow model which explicitly links mass balance and glacier geometry changes. Comprehensive ice thickness and ice-flow measurements will be used to tune a numerical flowline model incorporating multiple flowlines and the effect of longitudinal stresses.

4. Predict future glacier behaviour on the IPCC timescale, 2000-2100, using the coupled mass balance - ice-flow model.

The overall methodology to realise these objectives involves measuring the climate, mass balance, ice thickness, ice dynamics and terminus position in order to provide data for constructing and testing improved mass balance and ice dynamics models. Degree-day mass balance models, as used in this study, are used by other workers to assess the changes in mass balance that result from climate change (e.g. Jóhannesson, 1997; Braithwaite and Zhang, 2000). The required input data for this model is daily temperature and precipitation, which is available from a nearby climate station. The numerical flowline ice-flow model, as used in this study, is similar to that used to assess the response of glaciers to climate change (e.g. Greuell, 1992; Wallinga and Van de Wal, 1998; Schmeits and Oerlemans, 1997; Zuo and Oerlemans, 1997; Jóhannesson, 1997; Oerlemans, 2001). Together, the mass balance and ice-flow models will simulate the processes of glacier response (Figure 1.1) explicitly, and allow the response of the glacier to climate change to be assessed in a quantitative manner.

1.5 Thesis structure

This thesis is divided into six chapters. The next chapter synthesises the work that has been undertaken on glacier - climate linkages at Franz Josef Glacier, and identifies the key gaps and uncertainties in our knowledge.

The third chapter examines mass balance, and uses measurements of local glacier climate, accumulation and ablation to construct and verify a degree-day model of mass balance. The verified model is then used to assess the changes in mass balance at Franz Josef Glacier over the last century, and likely changes in the next century resulting from IPCC (2001) climate change scenarios. The fourth chapter examines the processes of ice dynamics at Franz Josef Glacier, and uses measurements of ice thickness and ice velocity to construct a model of ice flow.

The fifth chapter brings together the models of mass balance and ice flow into a coupled model to assess glacier response. The coupled mass balance - ice flow model is used to examine the response of the glacier to climate changes of the last century, and predict what the past response means for the short-term future behaviour of the glacier. Long-term climate scenarios (IPCC, 2001; Mullan and others, 2001) are then used as input to the coupled model to predict the effect of climate change on the glacier in the coming century.

The final chapter provides a summary of the key results of the thesis and puts them in the wider context of global response of glaciers to climate change.

2 A synthesis of previous work on glacier-climate linkages at Franz Josef Glacier *Ka Roimata O Hine Hukatere*

2.1 Introduction

Franz Josef Glacier is a temperate maritime glacier in the Southern Hemisphere. Since the first human habitation of New Zealand it has aroused interest because of its steep descent into temperate rainforest. The, at times, dramatic advance and retreat of the glacier over thousands of metres has been recorded since the mid 19th century making it the longest record of terminus position in New Zealand (Chinn, 1989), and the Southern Hemisphere (Grove, 1988). The advance and retreat of the glacier has also led many researchers to examine the relationship between climate and terminus position at Franz Josef Glacier, but the results have been largely inconclusive.

As well as the long terminus position record, Franz Josef Glacier is of interest to glaciologists and climatologists for a number of reasons, including:

- it is one of relatively few well studied glaciers in the mid-latitudes of the Southern Hemisphere, and as such provides an important proxy climate record for examining past climate changes in the Southern Hemisphere (Denton and others, 1999),
- it is a steep maritime glacier at the high end of the activity index scale (Andrews, 1975), and its study helps us understand the behaviour of these types of glaciers,
- unlike many glaciers it has actively advanced and retreated since the end of the Little Ice Age (LIA).

This chapter synthesises more than 100 years of research on the glacier, establishing what is already known about the response of the glacier to climate changes. Gaps in our understanding of these response processes will be highlighted, and the way in which this thesis aims to address these uncertainties will be outlined.

2.2 Description

The Franz Josef Glacier is presently (2003) 11 km long and occupies 35 km^2 on the western flanks of the Southern Alps of New Zealand (Figure 2.1) at 43^o29' S, 170^o11' E. The maximum elevation of the glacier is 2900 m above sea level (a.s.l.), although the areas at this elevation are small, consisting of snow and ice perched on steep mountain sides. The upper névé consists of broad gently sloping snowfields at elevations

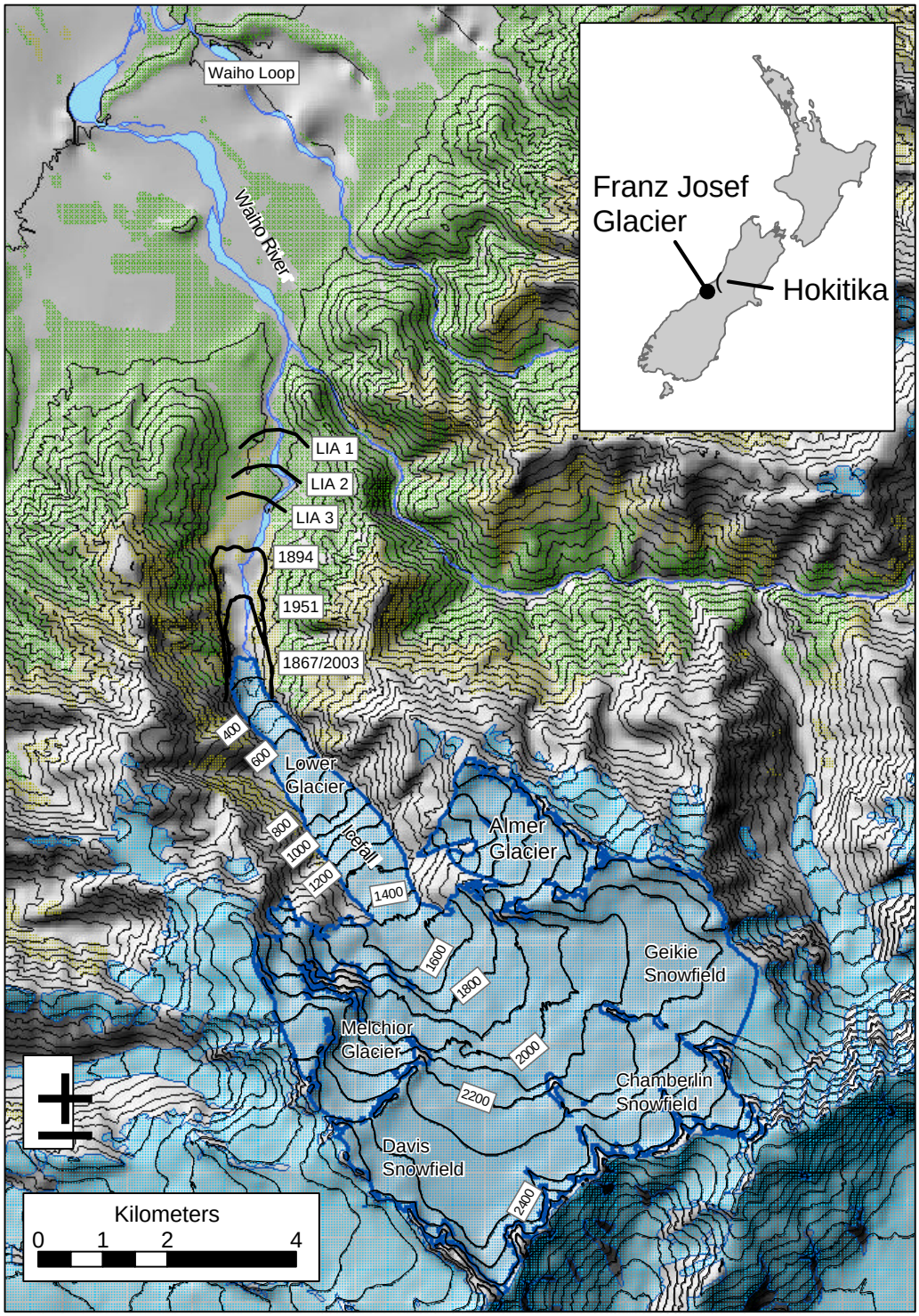

Figure 2.1. A map of the Franz Josef Glacier showing its location on the West Coast of the South Island of New Zealand. The glacier is mapped at its 2003 length, which is almost identical to its length in 1967. The source of other mapped terminus positions is given in the text.

between 2600 m a.s.l. and 2000 m a.s.l (Figure 2.2). Between 2000 m a.s.l. and 1600 m a.s.l., these snowfields converge in a heavily crevassed area, below which the glacier consists of a steep narrow tongue comprising a series of icefalls (Figure 2.3). The glacier presently (2003) terminates at 300 m a.s.l., approximately 20 km from the Tasman Sea, and has been retreating since early 1999. The tongue below 1600 m is referred to as the 'lower glacier', and the area above 1600 m the 'névé'.

The glacier is in a maritime climatic environment with a measured precipitation maximum of 10.6 m/a on the glacier tongue (Griffiths and McSaveney, 1983), and a mean annual temperature of 11.3 ^{o}C measured at Franz Josef village (Hessell, 1982), 7 km from the glacier terminus. The lower glacier tongue experiences year round ablation, estimated at over 20 m/a water equivalent (w.e.) (Woo and Fitzharris, 1992; Oerlemans 1997b).

2.3 History

Ka Roimata O Hine Hukatere was well known to Maori. The name translates roughly to 'The tears of Hine Hukatere', which can be understood by reading the story of Weka (2003) which is reproduced at the start of this thesis.

The first European record of the Franz Josef Glacier is from the log book of the sailing vessel *Mary Louisa*, written while sailing along the West Coast in 1859 (Sara, 1979). Sir Julius von Haast visited the glacier in 1865 (Sara, 1970), and took the liberty of renaming the glacier in honour of the then Emperor of Austria-Hungary, Franz Josef. Haast sketched the glacier during his visit and a water colour was painted by Sir William Fox in 1872 (Grove, 1988). The first photograph was also taken of the terminal face around this time (Figure 2.4).

Since these early visits, the scenery and the dynamic nature of the glacier have attracted tourists and scientists alike. The large and rapid variations in terminus position recorded since these first observations in the late 1800s have focused interest on the relationship between climate and glacier behaviour.

2.4 Terminus position

The first formal survey of the glacier was carried out by Douglas and Harper in 1893 (Douglas, 1894; Harper, 1894). While early surveys were carried out on many of the major glaciers of New Zealand around or before this time (summarised by Gellatly, 1985), what sets the record from the Franz Josef Glacier apart is the continued measurements made up until the 1940s, largely thanks to the efforts of Speight (Bell, 1910; Speight 1914, 1921, 1935 and 1941). Little was recorded about other New Zealand glaciers during this time, but at Franz Josef Glacier the terminus position was recorded every 10 years or so up to and during the first major retreat which started in 1934.

Figure 2.2. The névé of the Franz Josef Glacier from the south, December 2000.

Figure 2.3. The tongue of the Franz Josef Glacier, March, 2003. Source: D Nobes.

Figure 2.4. A copy of the photograph taken by T. Pringle in 1867. The rock on the right of the picture is Sentinel Rock, one of the *roches moutonnées* in the glacier forefield.

The short period of recorded human history in New Zealand means that the direct records of terminus position (Figure 2.5) are short compared to glaciers in Europe and Scandinavia, where records go back to 1534 (Schmeits and Oerlemans, 1997). However, the 20th century record at Franz Josef Glacier has good temporal resolution, and the geomorphic record provides information on glacier fluctuations though the Little Ice Age (McKinzey, 2001) and earlier (Wardle, 1973; Denton and Hughes, 1994).

2.4.1 Moraine dating

The first records of terminus position come from the dating of vegetation and moraine features. The earliest record of the glacier is from radiocarbon dating at Omoeroa Bluff (on the coast south of the Waiho River mouth) which shows that ice went beyond the present coast line, 20 km away from the 1909 position, some 14 000 years BP (Wardle, 1973).

The next recorded date comes from the Waiho Loop, a forest covered moraine on the Waiho river flats approximately 8 km from the 1909 position (Figure 2.6). The loop itself defied many early attempts at dating (Wardle, 1973), but Denton and Hendy (1994) reported corrected radiocarbon dates of 11 050 ± 14 years BP from wood fragments buried beneath till at nearby Canavans Knob (Figure 2.6) and cited this as evidence for the global synchroneity of the Younger Dryas late glacial advance. However, there is some debate both about the precision of the dates, and therefore synchroneity with the North Hemisphere (Mabin 1995; Denton and Hendy, 1995), and whether the advance was caused by a cooling or an increase in precipitation (Singer and others, 1998).

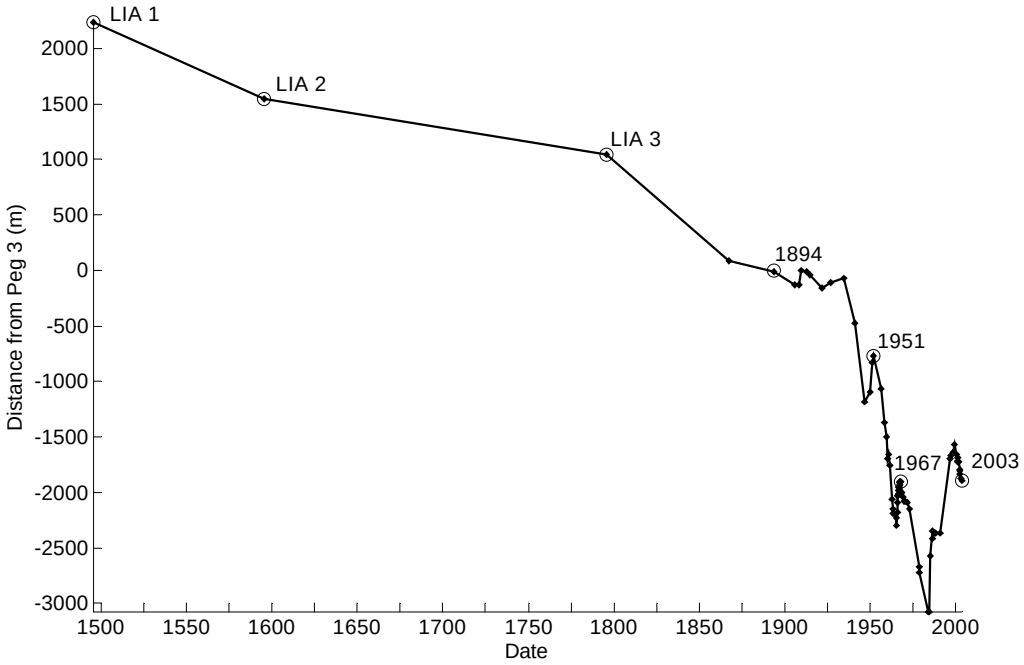

Figure 2.5. Length variations of the Franz Josef Glacier from the Little Ice Age (LIA) to the present. Distances are measured from an iron peg (no. 3) placed by Jack Clarke and Alec Graham in 1909 (Bell, 1910). The terminus positions marked with an open circle have been mapped in Figure 2.1. Sources: McKinzey (2001), Ruddell (1995), I.Owens (pers. comm.) and this study.

Figure 2.6. Oblique aerial photo of the Franz Josef Glacier (right) and the Waiho Loop (centre foreground). Canavans Knob is the bush covered knob immediately behind the right hand end of the Waiho Loop. Source: Broecker (1997).

The next dated glacial events come from a number of moraines in the upper Waiho Valley, 3 km and less from the glacier position recorded in 1909. Different researchers have assigned different dates to these moraines, although they have all used vegetation dating techniques (Lawrence and Lawrence, 1965; Wardle, 1973; Burrows, 1990; McKinzey, 2001). The most comprehensive study is provided by McKinzey (2001), who presents a revised Little Ice Age (LIA) chronology for the Franz Josef Glacier. Three LIA advances have been identified, marked as LIA 1-3 in Figure 2.1. LIA 1 is dated at 1480 - 1510, LIA 2 at 1580-1610 and LIA 3 at 1770-1820 (Figure 2.5).

2.4.2 Historic Records

The first historic record of terminus position of the glacier is the early photograph by T Pringle (Figure 2.4), dated at 1867 (Sara, 1979). The glacier almost completely covered the prominent *roches moutonnées* now in the glacier forefield. The glacier retreated by about 100 metres (Harper, 1926) before Explorer Charlie Douglas and Arthur Harper surveyed the glacier in 1893 (Harper, 1894). As well as surveying terminus position, they also marked the lateral extent of the glacier and plotted a number of surface elevation profiles. After this survey there was a retreat for a few years, but the glacier was advancing in 1905 (Speight, 1921) and in 1907 the ice suddenly thickened and pushed forward, wrecking a recently built viewing gallery on Gallery Rock, near the 1894 glacier position (Harper, 1926).

The glacier was in a similar position to 1893 when surveyed again by Greville in 1908 and Clarke in 1909 (Bell, 1910). The glacier started retreating again in 1910 (Speight 1921) and was still retreating in 1926 although an advance seemed imminent (Harper, 1926). The advance started in 1931 and continued until the measurement by Speight in 1934 (Speight, 1935).

The first major retreat of the glacier in the 20th century started in 1934 and continued until 1946, reaching a position a little less than 1000 m upstream of the position of 1909 (Suggate, 1950). The glacier advanced almost 400 m between 1947 and 1950 (Suggate, 1952), before receding again, losing 600 m by 1963. A vigorous but short-lived advance from 1965 until mid 1967 advanced the glacier some 400 m. Frequent surveys from 1951 to 1971 by the NZGS (Sara 1968, 1979) have ensured that this period was well recorded. Since this time the glacier continued to retreat to its 20th century minimum, in 1983, some 3000 m upstream of the position recorded in 1909.

In 1983 the glacier started a long advance, which continued until early 1999 with a total advance of 1500 m. Annual surveys of terminus position using the global positioning system (GPS) since 1996 show a continuing steady retreat from 1999 to April 2002, totalling 250 m and bringing the glacier to a position 1800 m upstream the 1909 position (I.Owens, unpublished data).

Overall, Franz Josef Glacier showed a very rapid retreat from 1934 to 1983, interspersed with some vigorous readvances at rates of up to 1.7 m/day (Sara, 1979). The glacier advance starting in 1983 was also rapid at 1.5 m/day at its peak between 1984 and 1985 (Ruddell, 1995). Other maritime glaciers such as Nigardsbreen, Norway, have also advanced during this period (Oerlemans, 2001) but did not match this rate of advance.

2.5 Ice dynamics

Ice flow is the process by which the glacier advances or retreats in response to changes in mass balance and therefore climate. While none of the previous published measurements of ice dynamics at Franz Josef Glacier have examined glacier movement in this light, nonetheless they provide information on ice dynamics since 1893. Ruddell (1995) and Oerlemans (1997b) have constructed ice flow models and used these to examine the response processes.

2.5.1 Measurements

Any synthesis of previous ice velocity measurements at Franz Josef Glacier is difficult because published measurements of ice velocity have been made in different places, and measurement periods have varied from less than one hour to several years (Table 2.1).

Gunn (1964) examined the spatial variation of ice velocity over most of the glacier, with the goal of linking velocity variations to structures in the ice. The pattern of velocity showed low velocities in the névé, increasing to a maximum in the main ice fall and reducing rapidly towards the terminus.

An attempt to examine temporal variations in velocity was made by McSaveney and Gage (1968) on a small area of the glacier at an elevation of 400 m a.s.l. Most of their measured velocities were between 1 and 1.5 m/day, with some seasonal and daily variations apparent. Variations were expected to occur as a result of changes in the supply of water to lubricate the bed. Velocities measured over one hour on April 10, 1966, were between 2.3 and 7.9 m/day, although measurement errors were estimated at up to 30% when extrapolated to a full day. The authors attributed the high velocity values to exceptionally high rainfall.

These studies provide us with a general knowledge of the spatial patterns of velocity on the glacier, and tell us that velocity varies significantly on a number of time scales. On a long time scale the surface ice velocity depends on the size of the glacier. For example as the glacier has retreated the maximum velocity has dropped from over 5 m/day in 1893 (Harper, 1894; Line II) to 0.59 m/day in the same place in 1956 (Gunn, 1964; Line 6). On a shorter time scale, the velocities measured in 1956 (Gunn, 1964; Line 8) were half that measured in 1966 in the same area (McSaveney and Gage, 1968; Lines 1-5), which is consistent with the change from a retreating to advancing phase. On a smaller scale again, there are marked velocity variations on a daily scale (McSaveney and Gage, 1968).

Table 2.1. A summary of velocity measurements from the Franz Josef Glacier.

Date	Station/ Line	Elevation (m a.s.l.) [1]	Measurement Period	Speed (m/day) [2]	Note	Source
1893	Line I	250	4-20 days	0.13-3.37		Harper (1894)
	Line II	600	3 days	0.60-5.26		
1908	Line 1	200	24-134 days	0.24-0.61		Bell (1910)
1914		200		1		Speight (1914)
1921		400	200 days	1		Speight (1921)
1943-1952		1300-250	7 years	1.5	Aircraft wreckage	Suggate (1952)
		1300	2 years	2.5	Aircraft wreckage	
1948		250		0.9		Gunn (1964)
1950-1955		1300	5 years	1.5-1.8	Aircraft wreckage	Odell (1955)
March 1956	1,2 and 3	2000	24-48 hours	0.03-0.20		Gunn (1964)
	4	1300	6-48 hours	0.51-2.45		
	5	800	24-48 hours	0.08-0.66		
	6	600	24-48 hours	0.41-0.59		
	7	500	24-48 hours	0.05-0.37		
	8	400	24-48 hours	0.07-0.37		
	9	250	24-48 hours	0.06-0.09		
April - August 1966	(1) - (4)	500	1 hour	2.3-7.9	1 hour on April 10	McSaveney and Gage (1968)
	1-5	400	5 months	0.73-1.48		
	6-12,15-19	300	5 months	0.47-1.53		
February-March 1991	1-5	2000	13.8 days	0.18-0.33		Ruddell (1995)
	1-5	2200	13.8 days	0.29-0.36		
	1-4	2300	13.9 days	0.11		
	1-6	2300	13.9 days	0.12-0.21		

[1] Locations of measurements are given as elevations on the present day glacier (Figure 2.1).

[2] The precision of the measurements varies enormously, and so the measurements are quoted as in the original publication.

The velocities recorded for the Franz Josef Glacier are high for a mid latitude glacier, a result of the very high mass turnover indicated by its maritime environment and the steep bed of the glacier (Oerlemans, 2001). As a result, one would expect that the glacier would respond to climate changes rapidly (Woo and Fitzharris, 1992; Oerlemans, 2001)

2.5.2 Ice flow modelling

As part of a wider study, Ruddell (1995) constructed a flow line model for Franz Josef Glacier where velocity was calculated along a glacier flowline. The chosen flowline went from the head of the Chamberlin Snowfield to the terminus, with a 500 m grid spacing. A critical parameter for all ice flow modelling is glacier bed elevation; in the absence of measurements of bed elevation, Ruddell (1995) calculated the glacier bed elevation from balance velocities. Ruddell (1995) compared the calculated ice

velocities with previous measurements of ice velocity on the glacier and found that the modelled velocities were often too low because of model limitations.

Oerlemans (1997b) applied a similar model but his flowline started at the head of the Davis Snowfield, and used a higher spatial resolution of 100 m. The glacier bed was calculated from an assumption of constant basal shear stress. Oerlemans (1997b) does not compare the calculated velocities with existing measurements from the glacier, and a cursory comparison with the results of Gunn (1964) show that the modelled velocities are too low in the névé and ice fall. No comparison on the lower glacier can be made because of the different terminus position at the time of the measurements of Gunn (1964) and in the model of Oerlemans (1997b).

2.6 Climate - glacier interactions

A large part of the work on Franz Josef Glacier has been focused on understanding climate-glacier linkages. These studies have been undertaken on three scales: point measurements, glacier wide linkages and global circulation changes.

2.6.1 Small scale mass and energy transfers

A series of papers in the 1980s and 1990s examined the exchanges of energy and mass at the surface of the Franz Josef Glacier. These papers first looked at the seasonality of ablation at Franz Josef Glacier, by conducting measurements on the bare ice of the lower glacier for short periods June, July, August, October and December 1981 (Owens and others, 1984; Marcus and others, 1985). A seasonality in the amount of energy available for melt was detected. However this was masked to some degree by synoptic scale conditions, in particular an intense rainstorm during the June measurement period (306 mm in 19 hours). During this event measured ablation was twice as much as a summer average of 82 mm/day given by Gunn (1964). The seasonality of ablation was better displayed in a study over 3 days in June 1988 and 3-4 days in February 1990 (Owens and others, 1992; Ishikawa and others, 1992). There was an average 13.7 cm/day melt in February 1990 compared to 1.7 cm/day in June 1988. There was a corresponding six-fold decrease in solar radiation during the winter period.

Although a complete picture is not possible because data from only short periods were available, these studies indicate that warm, humid, windy and cloudy conditions lead to the domination of the energy balance by turbulent transfers, particularly sensible heat, on the lower glacier. At high elevations, colder temperatures and reduced atmospheric absorption mean that net radiation is the most important energy source (Kelliher and others, 1996). The increase in the importance of radiation with elevation is in line with measurements from other glaciers. The dominance of turbulent transfers at low elevation is characteristic of maritime glaciers (Oerlemans, 2001), but the large magnitude of ablation at Franz Josef Glacier is unusual.

2.6.2 Relating terminus position to precipitation or temperature

Suggate (1950, 1952) attempted to relate low-altitude rainfall to glacier behaviour. A positive relationship was tentatively suggested between rainfall measured in Hokitika (100 km north of the glacier) and glacier retreat and advance. Suggate was the first to suggest a 5-year lag for changes in climate to be manifested at the terminus. Further analysis using precipitation measured in Franz Josef village and winter precipitation did not improve the correlation (Suggate in Sara, 1968).

Soons (1971), Hessell (1983), Brazier and others (1992) and Hooker and Fitzharris (1999) followed up the line of investigation started by Suggate (1950) by comparing precipitation to terminus position. Soons (1971) concluded that an excess of winter precipitation is a necessary but not a sufficient condition for advance, while Brazier and others (1992) concluded that there was insufficient data to pick out either temperature or precipitation as a driver of glacier change. Hessell (1983) claimed a statistically significant relationship between glacier retreat and Hokitika precipitation. In addition he found no significant relationship between temperature and glacier retreat although Gellatly and Norton (1984) have questioned his statistical methods and the way that he adjusted the temperature record. Hooker and Fitzharris (1999) found significant differences in rainfall and temperature at the equilibrium line altitude (ELA) between retreat and advance phases.

In general, these studies did little to elucidate glacier response processes, and the mostly unconvincing relationships suggested between temperature or precipitation and terminus position are not surprising considering the gross simplification of glacier behaviour implied by a direct correlation between climate and terminus position. It is common to correlate mass balance to climate directly (e.g. Holmlund, 1987; Chen and Funk, 1990). However, in general, the link between mass balance and terminus position is a function of glacier geometry which cannot be accurately parameterised by a simple lag time.

2.6.3 Mass balance modelling

Although there are few mass balance measurements from the glacier, there have been a number of attempts to calculate mass balance from climate variables. Woo and Fitzharris (1992) used a degree-day mass balance model where ablation was calculated from a relationship between positive temperature sums and ablation. As in all mass balance models, accumulation is calculated from precipitation with a temperature threshold to discriminate snow from rain. Woo and Fitzharris (1992) based the precipitation on the Griffiths and McSaveney (1983) distribution who predicted an increase in precipitation up to the main divide at 2500-3000 m a.s.l. In all of these mass balance models, temperature distribution is calculated using a constant lapse rate. The mass balance model was used to reconstruct mass balance variations for the glacier using the Hokitika climate record (temperature and precipitation) from 1913 to 1989. The model was noted to give unrealistically positive mass balance, a problem that could not be resolved without field measurements

Another degree-day model was constructed by Ruddell (1995). The model covered the entire Southern Alps, and used the equivalence of ablation, which is relatively easy to calculate, and accumulation at the ELA to infer precipitation distribution. The result was a decrease in precipitation from the lower glacier to the ELA, and a further reduction to the main divide. The model was verified using measurements of net accumulation from Franz Josef and other glaciers, before being used to reconstruct mass balance from Hokitika for the period 1894-1989. The total glacier mass balance appeared to be realistic, judging by the correct prediction of glacier length (Section 2.6.5). However, the ablation at low elevation seems unrealistically high, compared with the other two mass balance models (Table 2.2).

A different type of mass balance model, where ablation was estimated from energy balance calculations, was constructed by Oerlemans (1997b). In order for ablation to be calculated, a number of assumptions about cloudiness, albedo and other input parameters were used, although no reference was made to earlier energy balance studies at Franz Josef Glacier. Accumulation was calculated in a similar way to Woo and Fitzharris (1992) and Ruddell (1995), although much lower precipitation at high elevation was assumed. Oerlemans (1997b) did not run his model with a time series of climate data, but rather used a single set of annual average temperature and precipitation values from Franz Josef Village. The model was used to assess the sensitivity of the glacier to changes in temperature and precipitation.

A comparison of the output of these models, for the mean values of annual precipitation and temperature at Franz Josef Village, indicates that the variation in calculated accumulation and ablation between these models is large (Table 2.2). There are no measurements of annual mass balance with which to compare these results. Ruddell (1995) estimates ablation at over 40 m/a w.e., twice that of the other models. This ablation rate corresponds to a mean daily ablation rate of 0.11 m/day which is clearly too high given that the only published long-term ablation rate is 0.082 m/day measured in summer (Gunn, 1964). Accumulation calculations between the models also vary by a factor of two, giving little overall confidence in the accuracy of these models.

Table 2.2. Maximum net annual ablation and maximum net annual accumulation calculated by mass balance models for Franz Josef Glacier, from mean annual temperature and precipitation at Franz Josef Village.

Study	Maximum net annual ablation (m w.e.)	Maximum net annual accumulation (m w.e.) [2]
Woo and Fitzharris (1992)[1]	20	10
Ruddell (1995)	40	8
Oerlemans (1997)	25	5

[1] Maximum annual ablation is not explicitly stated by Woo and Fitzharris, and is calculated from parameters given in that study.

[2] Maximum net annual accumulation is estimated from the maximum precipitation above 2500 m, where little ablation is experienced (Oerlemans, 1997b).

2.6.4 Global circulation and glacier behaviour

The configuration and location of the Southern Alps, surrounded by ocean with the main range trending across the prevailing westerlies, means that the glaciers of New Zealand are well placed to respond to changes in atmospheric circulation (Hessell, 1983; Fitzharris and Hay, 1989; Fitzharris and others, 1992; 1997; Tyson and others, 1997; Hooker and Fitzharris, 1999). As the glacier with the best record of terminus position variations, Franz Josef has naturally been used in some of these studies to represent New Zealand glacier behaviour.

The effect of circulation patterns on glacier behaviour in New Zealand was first investigated by Hessell (1983) who found a relationship between pressure gradients normal to the predominant westerlies and glacier retreat. A preliminary investigation by Fitzharris and Hay (1989) indicated that winter snow accumulation is related to the strength of the westerly flow and hence orographic precipitation. A reconstruction of variations in sea level pressure patterns back to 1911 and circulation indices back to 1860 shows that glacier terminus behaviour is strongly linked to circulation changes, especially in summer (Fitzharris and others, 1992). Hooker and Fitzharris (1999) also examined global circulation patterns in an attempt to find correlation between climate parameters and the retreat and advance of the glacier. They found statistically significant relations between zonal pressure difference in the accumulation season, southern oscillation index (SOI) in both seasons and latitude of the subtropical high in the ablation season and retreat/advance phases.

One example of the influences of circulation changes is an abrupt shift around 1950 that increased the northerly flow component and encouraged ablation, and glacier retreat (Figure 2.5) (Fitzharris and others, 1997). Another example is the two strong El Niño events in the 1980s which were linked to a summer shift

to southerly flow and therefore glacier advance (Figure 2.5) (Fitzharris and others, 1997). The circulation changes also result in teleconnections between glacier advance and retreat in New Zealand and extended dry periods in South Africa (Tyson and others, 1997).

The changes in temperature and precipitation which have been linked to variations in Franz Josef Glacier terminus position with varying success (Suggate, 1952; Soons, 1971; Hessell, 1983; Brazier and others, 1992; Hooker and Fitzharris, 1999) appear to be the result of circulation changes, which often occur on a decadal scale (Fitzharris and others, 1997).

2.6.5 Coupled mass balance - ice flow models

While Woo and Fitzharris (1992) did not use an ice flow model, they compared cumulative mass balance to terminus positions over the period 1913 to 1989. Ice flow was accounted for by applying a constant lag between climate and terminus response of 5 years. The changes in cumulative mass balance showed broad agreement with terminus advance and retreat, and provide the strongest support for the often-cited 5-year response time of the glacier. However, Woo and Fitzharris (1992) called for an ice flow model to be used to link mass balance changes to terminus position changes.

Ruddell (1995) coupled his mass balance and ice flow models and ran a simulation of terminus position variations from 1894 - 1990. The simulation was compared with the recorded terminus position, and showed a broad agreement with the general pattern of retreat, given the limitations identified in the mass balance and ice flow models, although the result was tuned by calculation of the bedrock topography using balance velocities. Details such as the readvances in the late 1940s, 1960s, and 1980s (Figure 2.5) were not shown in the model output, possibly a result of the very coarse grid resolution of 500 m used.

Ruddell (1995) also ran an experiment where the temperature input to the model was held constant at its mean for the period 1895-1990 and only the precipitation allowed to vary. The result was a glacier length change of a few percent, showing little similarity to the measured terminus position. In comparison, the experiment was run with the precipitation held constant at its mean and the temperature allowed to vary. The result indicated that almost all of the terminus position variation from 1895 to 1990 can be explained by variations in temperature, and that the glacier is not notably sensitive to changes in precipitation.

Oerlemans (1997b) used the coupled mass balance - ice flow model to assess the sensitivity of Franz Josef Glacier to changes in climate by perturbing the climate around its present regime. The length sensitivity of the glacier is approximately 3 km per ^{o}C warming and 2 km per ^{o}C cooling and about 1 km per 10% increase or decrease in precipitation. Oerlemans concludes that a 30% increase in precipitation is required to offset a 1 K increase in temperature, and that his results do not support the idea that the glacier is notably sensitive to precipitation changes.

The work of Oerlemans (1997b) and Ruddell (1995) provides an answer to the questions surrounding statistical relationships between temperature, precipitation and terminus position (Suggate, 1950; Hessell 1983; Gellatly and Norton, 1984). Both Ruddell (1995) and Oerlemans (1997b) show that terminus position is sensitive to changes in temperature and not notably sensitive to changes in precipitation. As these later studies account for the processes of mass accumulation, ablation and ice flow explicitly, which the earlier statistical studies do not, the results are more convincing. Oerlemans (1997b) notes that his results support the general theory that the sensitivity of terminus position to temperature increases when the climate regime is wetter (Oerlemans and Fortuin, 1992).

Oerlemans and others (1998) used the Franz Josef Glacier model in a global study of glacier sensitivity to climate change, using 12 study glaciers. An interesting, and somewhat unlikely, result shows that if the climate was maintained at the average for the period 1961-1990, the Franz Josef Glacier would advance to its position of the 1930s, before the drastic retreats of the 20th century. The model was used to further predict that if warming at the rate of 0.02 ^{o}C/a is imposed the glacier would reduce to around 70% of its present volume by 2100.

2.6.6 Response Time

These coupled mass balance – ice flow models allow us to examine response time of the glacier. Suggate (1950) and Soons (1971) originally postulated a 5 year response time, and the most convincing evidence for this comes from the correspondence between cumulative mass balance (with a 5 year lag) and terminus position presented by Woo and Fitzharris (1992). Both Ruddell (1995) and Oerlemans (1997b) have used their models to measure the time between a step change in mass balance and a return to equilibrium. The result is the static response time and strictly only applies to a step change between two equilibrium states. Both estimate a time between 10 and 25 years, significantly longer than the previously used 5 years. The dynamic response time, more likely to correspond to an observed lag between a constantly changing climate and terminus position, is not a characteristic of the glacier geometry alone, but depends on the mass balance history of the glacier (Oerlemans, 2001). Therefore, the static and dynamic response times are not necessarily comparable.

2.7 Conclusion

The last century has seen a large amount of work on Franz Josef Glacier, much of it related to the way in which the glacier responds to changes in climate. Early work concentrated on recording the terminus position and ice velocity. The dramatic retreat and advance which characterised glacier behaviour in the 20th century led researchers to try to understand the cause of these fluctuations. Early attempts to link changes in temperature or precipitation to terminus position were unconvincing (Suggate, 1950; Soons,

1971; Hessell, 1983; Brazier and others, 1992). The lack of direct correlation between climate variables and terminus position is not surprising considering the complexity and non-linearity of the processes of accumulation, ablation and ice flow which are accounted for only implicitly in the statistical approach. In the last 10 years, mass balance and ice flow modelling techniques have been used to assess the links between climate, mass balance and terminus position, and a clearer picture of glacier response to climate change has emerged. However, there are large uncertainties and inconsistencies between the results of these models, largely as a result of the lack of ground measurements of the key glaciological parameters of accumulation, ablation and ice thickness.

In terms of glacier flow there are a significant number of measurements of ice velocity, and we have enough information to make general statements about ice velocity distributions and how they change through time. While ice flow is the link between changes in mass balance and changes in terminus position, our knowledge of it is patchy in space and time, and with the exception of Ruddell (1995), no attempt has been made to link these measurements of ice flow to glacier response and climate change in the last century. The ice flow models applied to Franz Josef Glacier (Ruddell, 1995; Oerlemans, 1997b) have significant uncertainties, in particular the calculation of ice velocities in these models is sensitive to ice thickness and there have been no ice thickness measurements available.

There is also some information about mass balance. The detailed studies of energy balance done on the glacier (Owens and others, 1984; Marcus and others, 1985; Owens and others, 1992; Ishikawa and others, 1992; Kelliher and others, 1996) allow us to understand in some detail the energy balance and resultant mass transfer processes that operate at the ice surface. However these are point measurements, and there are difficulties in extrapolating them to a larger scale, either in time or in space.

While Oerlemans (1997b) applied an energy balance model to the Franz Josef Glacier, he made no reference to these earlier energy balance studies, and the only climate data that he used were annual temperature and precipitation from a nearby climate station. The mass balance models of Woo and Fitzharris (1992) and Ruddell (1995) used a degree-day method. Together these three models spanned a factor of two in their calculations of accumulation and ablation, with no one model standing out as being more accurate than the others. Hence the conclusions drawn from these models must be treated with caution, especially since there are no direct measurements with which to compare them.

The uncertainties in these mass balance and ice flow models indicate that there is still much work to be done to understand the response of Franz Josef Glacier to climate change. A comparison of the previous mass balance model results (Woo and Fitzharris, 1992; Ruddell, 1995; Oerlemans, 1997b) indicates that both accumulation in the névé, and ablation at the terminus are poorly constrained (Table 2.2). The uncertainties in accumulation and ablation can best be resolved by measuring these quantities directly. The

ice flow models also have large uncertainties, in particular the ice thickness, for which there have been no measurements available, and the spatial and temporal variations in ice velocity, for which there are few systematic measurements. The uncertainties in ice flow are also best resolved by direct measurements of ice thickness and ice velocity measurement.

3 Climate - mass balance linkages at the Franz Josef Glacier *Ka Roimata O Hine Hukatere*

3.1 Introduction

Measurements of mass balance at Franz Josef Glacier are few, but indicative of high mass turnover. Gunn (1964) measured a summer average (January to April) ablation rate of 0.082 m/day on the glacier tongue. A series of short-term energy balance studies (Marcus and others, 1985; Ishikawa and others, 1992; Owens and others, 1992; Kelliher and others, 1996) indicate that ablation is strongly seasonal, and that significant year round ablation occurs on the lower part of the glacier. The highest ablation rate measured was 0.196 m/day on the glacier tongue (Marcus and others, 1985). The only accumulation measurements for the glacier are from Ruddell (1995) who measured net annual accumulation of up to 6.8 m/a water equivalent (w.e.) in the Chamberlin snowfield.

These few measurements are not extensive enough in either time or space to indicate the overall mass balance regime of the Franz Josef Glacier. For the complete picture we have to turn to mass balance models (Woo and Fitzharris, 1992; Ruddell, 1995; Oerlemans, 1997b). However, these models all calculate different ablation and accumulation rates (Table 2.2). The ablation rates calculated at the terminus by each of the models, between 20 and 40 m/a w.e., are extremely high, higher than measured on any glacier reported in the most recent Mass Balance Bulletin (Haeberli and others, 2001), the closest being Nigardsbreen, Norway, at 11 m/a w.e.

Published estimates of the equilibrium line altitude (ELA) of Franz Josef Glacier also vary widely, as might be expected from the wide variation in calculated mass balance, between 1600 m (Hooker and Fitzharris, 1999), 1680 m (Oerlemans, 1997b) and 2000 m (Ruddell, 1995). While some of the variation in estimated ELA is due to different definitions and methods, none of these estimates are robust and the most that can be said is that the ELA probably falls within the range 1600-2000 m.

One of the most valuable sources of mass balance information for New Zealand is the record of the end-of-summer snowline (EOSS) elevation (Chinn, 1995; Chinn and Salinger, 2001). The EOSS lies at the elevation where the annual mass balance is zero, and is also referred to as the 'annual ELA' (Meier and Post, 1962). The EOSS elevation has been recorded since 1977 for 48 ‘index’ glaciers (Chinn and Salinger, 2001). The EOSS elevation for each glacier is compared to an estimated long-term ELA to provide an

index of mass balance fluctuations throughout the Southern Alps. The Franz Josef Glacier is not included in this survey because the EOSS is hard to see from the air due to the crevassed nature of the area where the EOSS lies. However the Almer Glacier, which is in the Franz Josef Glacier catchment, is included in the survey, and potentially provides valuable information on the mass balance of the Franz Josef Glacier itself.

Attempts to explain the advance and retreat of the Franz Josef Glacier in the past without mass balance data have been inconclusive (Suggate, 1952; Soons, 1971; Hessell, 1983; Gellatly and Norton, 1984; Brazier and others, 1992), while mass balance models (Woo and Fitzharris, 1992; Ruddell, 1995; Oerlemans, 1997b) have produced widely varying outputs. Woo and Fitzharris (1992) calculated a consistently positive mass balance for the period 1913 to 1989, which they noted as being unrealistic given the general retreat of the glacier. Ruddell (1995) calculated a more realistic total mass balance for the glacier, but had to resort to an extremely high ablation rate of more than 40 m/a near the terminus. A first step in linking terminus position to climate is to reconstruct a realistic mass balance record for the last 100 years.

The future advance and retreat of the glacier is important on a local scale for tourism, and on a global scale as an indicator of the behaviour of maritime and Southern Hemisphere glaciers and the impact they will have on sea level changes. The IPCC has developed future climate scenarios for the next century (IPCC 2001). A first step in assessing the effect of these future climate scenarios on the future advance and retreat of the Franz Josef Glacier is to understand the effect that these climate change scenarios will have on glacier mass balance.

The overall aim of this chapter is to establish the relationship between climate processes and mass balance at Franz Josef Glacier, in order understand the variations of the glacier over the last century, and to use that relationship to predict the change in mass balance in the next century. The specific objectives of this chapter are:

- To understand the present-day regime of climate and mass balance at Franz Josef Glacier;
- To assess whether the Almer Glacier EOSS can be used as an indicator of Franz Josef Glacier mass balance;
- To examine how mass balance has varied in the last century, given the measured terminus position variations; and
- To predict how mass balance will vary in the next century, given various predictions of future climate change scenarios.

The overall approach to realise these objectives is to use detailed climate and mass balance measurements on and near the glacier to construct and verify a mass balance model and to then use the model to assess the effect of climate variations on the mass balance and EOSS of Franz Josef Glacier.

The methodology used in this chapter will first be outlined, including a description of a degree-day mass balance model, and the climate and mass balance measurements that have been made on the glacier to calculate model parameters. The model and measurements are then combined in the development and application of the mass balance model to the Franz Josef Glacier. This model is verified with field measurements, and the relationship between the Almer Glacier EOSS and total annual mass balance of Franz Josef Glacier is explored. Finally, the variations in mass balance over the last 100 years are qualitatively compared to glacier advance and retreat, and the effect of future climate change scenarios on the mass balance at Franz Josef Glacier is described.

3.2 Degree-day mass balance model

In order to establish the links between climate and mass balance at Franz Josef Glacier, a degree-day mass balance model is used. This model calculates accumulation and ablation from climate parameters, and is based on those used by Jóhannesson and others (1995) and Braithwaite and Zhang (2000). In these models spatial variation in mass balance is a function of elevation alone, a consequence of the parameterisation of temperature and precipitation as functions of elevation.

In general, degree-day models are known to predict ablation well on medium to long time scales (months – years) and have modest requirements for input data (Laumann and Reeh, 1993). Temperature and precipitation are the only climatic input data required for the model. For Franz Josef Glacier, temperature and precipitation are readily available from long-term climate stations.

The uncertainties in previous mass balance models (Woo and Fitzharris, 1992; Ruddell, 1995; Oerlemans, 1997b) are addressed by measuring climate and mass balance on the glacier and using these measurements to constrain and verify the model.

If we assume that the spatial variation in mass balance is a function of elevation alone, the mass balance rate may be described as the sum of the accumulation rate and ablation rate:

$$\dot{B}(t,z) = \dot{c}(t,z) + \dot{a}(t,z) \qquad (1)$$

where $\dot{B}$ is the balance rate, $\dot{c}$ the accumulation rate, and $\dot{a}$ the ablation rate at time t and elevation z.

In the degree-day model, accumulation occurs when the temperature T is less than a threshold T_{crit} and the precipitation p is greater than zero. The threshold T_{crit} is usually taken in the range 0 – 2°C. Accumulation is calculated on a daily basis, from daily temperature T_{mean} and daily precipitation, p_{total}. Many accumulation events occur on sub-daily timescales, and some knowledge of the variation of temperature T and precipitation p within the day is required. An empirically-derived function f_c, termed the accumulation

factor, is introduced and defined as the proportion of daily precipitation p_{total} that falls when the hourly temperature $T_{hourly}<T_{crit}$ during the day. In this way the daily accumulation c can be calculated:

$$c(z) = f_c(T_{mean})\, p_{total}(z) \qquad (2)$$

In the degree-day model the daily ablation a is assumed to be proportional to the sum of positive temperatures per day:

$$a(z) = kT_{sum}(z) \qquad (3)$$

where k is the degree-day factor. Ablation events also occur on time scales less than the daily temporal resolution of the model, so the positive temperature sum T_{sum} is related to hourly temperatures T_{hourly}:

$$T_{sum}(z) = \frac{1}{24}\sum_{1}^{24} T_{hourly}(z) \quad T_{hourly}(z) > 0 \qquad (4)$$

An empirically derived function f_a is introduced which allows the positive temperature sum T_{sum} to be calculated from mean temperature T_{mean} for the period:

$$T_{sum}(z) = f_a T_{mean} \qquad (5)$$

A temporal discretisation has been imposed by calculating accumulation and ablation on a daily basis, where variations in temperature T and precipitation p on a sub-daily basis are accounted for with the accumulation and ablation factors f_c and f_a. Spatial discretisation is achieved by imposing elevation bands on the spatial variable z, which is justified providing that the elevation band z is small enough. The spatial resolution used is in the order of the accuracy of the measured glacier surface elevation, 20 m at Franz Josef Glacier.

To calculate mass balance B over the entire glacier for the balance year, taken as 1 April to 31 March (Chinn, 1995), the daily totals of accumulation and ablation for each elevation band are summed:

$$B = \sum_{t=1\,April}^{31\,March} \sum_{i=1}^{n} A(z_i)\big(c(t, z_i) + a(t, z_i)\big) \qquad (6)$$

where the elevation range of the glacier (z_{min}, z_{max}) is split into n, elevation bands, z_i is the mid elevation of elevation band i and $A(z_i)$ is the area of the glacier in the elevation band i.

This model is run on a daily basis, whereas most degree-day mass balance models operate on a monthly basis (Woo and Fitzharris, 1992; Laumann and Reeh, 1993; Jóhannesson and others, 1995; Braithwaite and Zhang, 2000). In these models, assumptions are made about the proportion of temperatures during the month being low enough for snowfall, and the positive temperature sums, based on a normal distribution of temperatures within the month (Braithwaite and Zhang, 2000). In order to remove these assumptions, we run the model on a daily basis and use the measured variation of temperature within a day. Note that this increased temporal resolution will not necessarily provide accurate short-term (days – weeks) estimates of

mass balance because of the inability of the degree-day model to resolve ablation on short time scales (Laumann and Reeh, 1993).

3.3 Input data

The input data required for this model to calculate the variation of mass balance with elevation are daily mean temperature T_{mean} and daily total precipitation p_{total}. These data are available from long-term climate stations close to the glacier.

The model parameters which need to be calculated are:

- The variation of temperature T and precipitation p with elevation
- The accumulation factor f_c which relates daily mean temperature T_{mean} to the proportion of precipitation falling when $T<T_{crit}$
- The ablation factor f_a which relates daily mean temperature T_{mean} to the daily positive temperature sum T_{sum}.
- The degree day factor k.

To calculate these parameters, measurements of the spatial variation of temperature and precipitation on the glacier are required. In addition, to calculate the degree-day factor k, concurrent ablation measurements are required. It is assumed that the spatial variation of temperature and precipitation, and the degree-day factors will not change with time (Jóhannesson and others, 1995). Therefore the measurements of the basic variables of temperature, precipitation and ablation on the glacier need only be long enough that a representative sample is obtained.

3.3.1 Climate data

The nearest long-term rainfall and temperature data available are from Franz Josef village, about 7 km north of the glacier terminus (Figure 3.1), at a station maintained by the National Institute for Water and Atmospheric Research (NIWA). The records are only substantially complete since 1954 and the site has often been in poor condition (Salinger, 1981). The record is used in this study from 1982 to 2003, a period in which there were no site changes, both to calibrate the longer term Hokitika data and to compare the model output between runs using the Franz Josef Village and Hokitika data. The long term station at Hokitika, 100 km north of the glacier, is reliable from 1894 to the present. A transformation is applied to the data recorded at Hokitika and used for model input. The transformation is described in the next section.

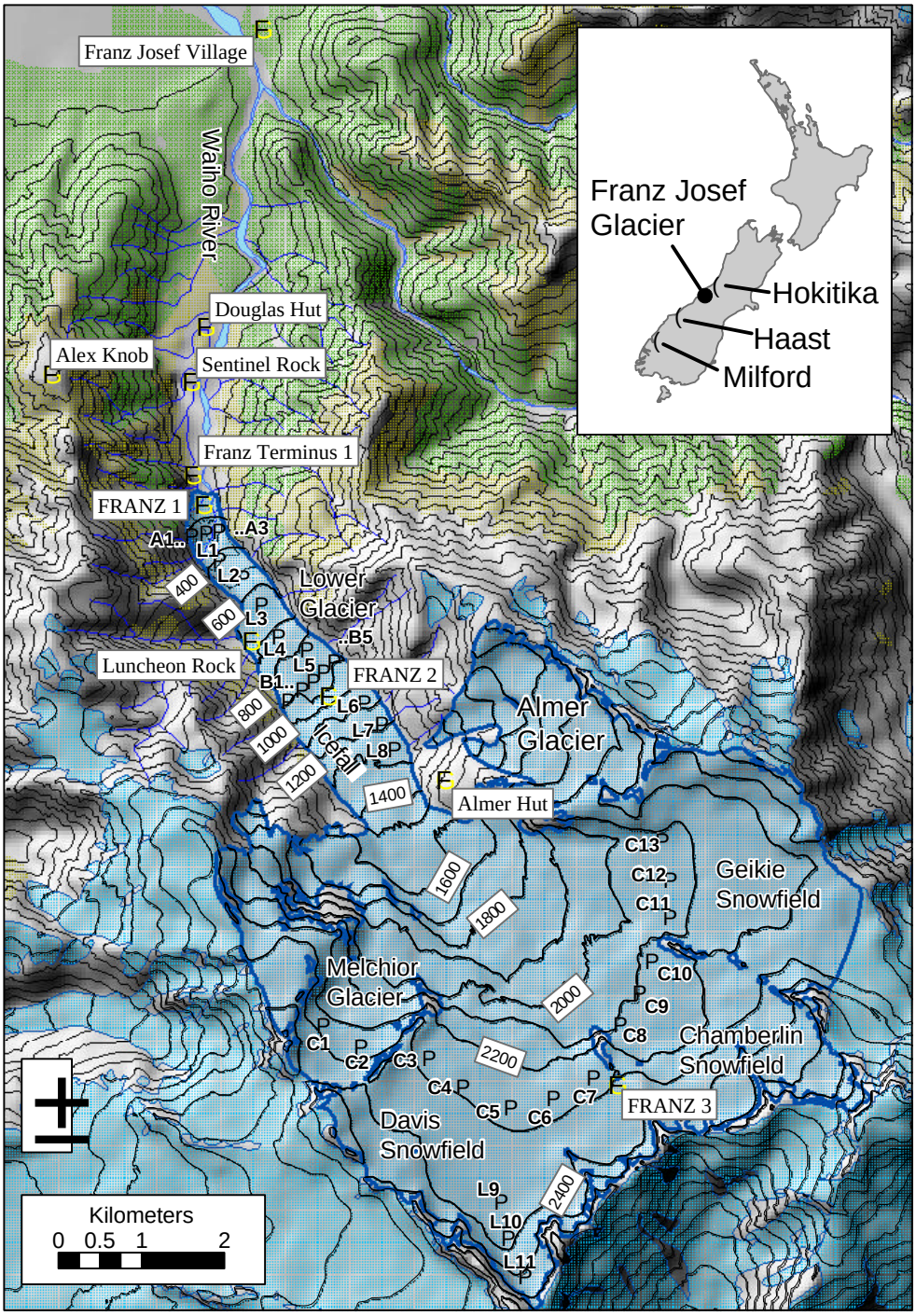

Figure 3.1. A map showing the location of Franz Josef Glacier. The location of the long-term climate stations at Franz Josef village and Hokitika are shown, along with short-term measurement sites in Table 3.1. The stations FRANZ1-3 were installed as a part of this study. The location of the rainfall measurement transects (Henderson and Thompson, 1999) near Hokitika, Haast and Milford are shown.

In order to assess the spatial and temporal distribution of temperature and precipitation on the glacier, required to calculate model parameters, a network of three climate stations (FRANZ 1-3) was deployed on the glacier between October 2000 and March 2003. The distribution of these stations was based on the expectation that the dominant variation in temperature, precipitation and thence mass balance would be with elevation (Paterson, 1994; Fountain and Vecchia, 1999). Hence the stations are placed to cover as much of the altitudinal range of the glacier as possible. However, due to difficulties with precipitation measurements the stations are used only to determine the temperature distribution on the glacier.

Precipitation distribution is determined from measurements by Westland National Park (WNP), NIWA and Meridian Energy within the glacier valley. A summary of the main characteristics of all of the stations used in this study is presented in Table 3.1, and their locations are plotted in Figure 3.1.

Table 3.1. A summary of the climate records used in this study and the purposes for which they are used. Rainfall normals from the Westland National Park (WNP) stations are from Griffiths and McSaveney (1983). Data from the NIWA stations are sourced from the National Climate Database.

	Station	Source	Elevation (m)	Start date	End date	Measurement interval	Purpose
Long- term stations	Franz Josef village	NIWA	155	1982	2003	1 day	local data for calibration
	Hokitika	NIWA	39	1894	2003	<1 day	input data for mass balance model
Short-term stations	Almer Hut	NIWA	1700	1992	1995	1 day	calculate precipitation variation
	Alex Knob	NIWA	1200	1992	1995	1 day	
	Luncheon Rock	WNP	600	Annal precipitation normalised to the 1940-1971 period available			
	Franz Terminus 1	WNP	328				
	Sentinel Rock	WNP	230				
	Douglas Hut	NIWA/ Meridian	200	1992	1995	1 day	
This Study	FRANZ 1	this study	400	2000	2002	1 hour	calculate temperature lapse rates
	FRANZ 2	this study	800	2000	2003	1 hour	
	FRANZ 3	this study	2200	2000	2003	1 hour	

The relationship between Hokitika and Franz Josef village climate

The model described in Section 3.2 provides the ability to predict ablation and accumulation at any elevation on the glacier, based on the daily temperature and rainfall recorded in Franz Josef village. As already noted, the records from this station do not go as far back in time as those from Hokitika. Hence to calculate mass balance as far back as 1894, the relationship between climate at Franz Josef village and Hokitika is needed.

An analysis of monthly rainfall records shows a strong seasonal variation in rainfall between Franz and Hokitika. The Franz Josef village rainfall data show a marked winter minimum which is not apparent in the Hokitika record. This variation is accounted for in the model by using a seasonally-variable ratio between Hokitika rainfall and Franz Josef village rainfall (Tangborn; 1980; Woo and Fitzharris, 1992). The ratios are calculated using monthly average rainfall from the two stations (Table 3.2) for the period 1982 to 2003. This period is chosen to avoid any inconsistencies in the Franz Josef village record which had a site change in 1982.

A comparison of daily temperatures measured in Franz Josef village and daily temperatures measured in Hokitika shows that there is also large seasonal variation in the temperature differences between Hokitika and Franz. The temperature difference is greatest in the warmer months, and least in the coldest months.

Table 3.2. A comparison of mean monthly temperature and rainfall measured at Franz Josef village and Hokitika. The ratios are Franz Josef / Hokitika, and differences are Franz Josef - Hokitika.

Month	Temperature difference	Rainfall ratio
January	-0.80	2.17
February	-0.67	2.22
March	-0.65	2.35
April	-0.46	1.73
May	-0.38	1.76
June	-0.16	1.85
July	-0.35	1.61
August	-0.48	1.87
September	-0.47	1.79
October	-0.54	2.33
November	-0.64	2.17
December	-0.72	2.27

These temperature differences and rainfall ratios are used to calculate the Franz Josef village temperature and rainfall using Hokitika data for periods when the Franz Josef village data are not available.

3.3.2 Mass balance data

Mass balance data are used to calculate degree-day factors and to verify the model output. Mass balance measurement was started at Franz Josef Glacier in October 2000 and continued until April 2003. The

measurement interval was initially 10-20 days, but this was increased to 30-45 days in 2001. Measurements were made using stakes and crevasse stratigraphy.

Measurements were made at 34 stakes made of 25 mm diameter PVC pipe; 18 on the lower glacier and 16 in the névé (Figure 3.1). Stakes were positioned based on the premise that the dominant influence on mass balance is elevation (Fountain and Vecchia, 1999). A longitudinal profile, line L, covers as much of the altitudinal range as possible, although in the vicinity of the ELA the extensive heavily crevassed area means that no measurements can be made, except a visual assessment of the EOSS. To test the premise that most variation is with elevation, three transverse profiles, lines A, B and C, were maintained to allow comparison of mass balance at the same elevation.

On snow covered parts of the glacier, the surface snow density was measured at the same time as stake height and was used for calculating the water equivalent of subsequent ablation. On bare ice, the density was assumed to be 917 kg/m^3.

Net accumulation in the névé was measured by crevasse stratigraphy. While this method has limitations (Meier and others, 1997) it is a valuable tool in measuring accumulation in high snowfall areas (Pelto, 1996, 1997). Measurements were taken at 14 sites in March 2001, and 14 in March 2003. The water equivalent of the snow layer thickness measurements was calculated using a relationship between mean density of the first annual snow layer r and elevation developed from density measurements on the adjacent Tasman Glacier (Ruddell, 1995) as follows:

$$r = 44.75z^{-0.557} \qquad (7)$$

where z is the surface elevation. The density falls in the range 600 to 690 kg m^{-3} for all of the measurements in this study.

3.3.3 Glacier geometry

The glacier hypsometry $A(z)$ is required to calculated the total mass balance on the glacier. No glacier geometry adjustment is attempted in this chapter because the most straightforward and rigorous way to do this is using a flow model in which the geometry is adjusted according to ice flow, and this is done in Chapter 5. Mass balance calculated on a fixed geometry is a direct indicator of the climatic variables which affect glacier behaviour, whereas mass balance calculated on a varying glacier geometry is not, as the glacier constantly adjusts its geometry towards a zero mass balance state (Oerlemans, 2001). Similarly, the EOSS is a direct indicator of climate which is independent of glacier geometry.

The most recent contour map of the Franz Josef Glacier has a scale of 1:50 000 and is based on aerial photography taken in 1986 (NZMS 261, H35 and H36). The digital elevation model (DEM) created from this map is used for mass balance calculations. The uncertainty in elevation of the resulting digital elevation model (DEM) is ± 10 m. The elevation band width used for the mass balance model calculation is 20 m, the same order of accuracy as the elevation data.

3.4 A mass balance model for Franz Josef Glacier

In order to apply the degree-day mass balance model outlined in Section 3.2 to Franz Josef Glacier we use measured glacier climate and mass balance (Section 3.3) to calculate model parameters.

3.4.1 Precipitation variation

The variation of precipitation with elevation *p(z)* at Franz Josef Glacier is critical to the calculation of mass balance. In other parts of the Southern Alps, a peak in precipitation has been identified within a narrow band well to the west of the main divide (Chinn, 1979; Griffiths and McSaveney, 1983; Henderson and Thompson, 1999). The location of this band has been identified along three profiles, near Hokitika, Haast and Milford (see Figure 3.1 for locations), and is remarkably consistent along the Southern Alps. All of the precipitation maxima have been measured within a band 10 km wide and centred 10 km south east of the alpine fault (Henderson and Thompson, 1999).

A precipitation measurement profile also exists in the Franz Josef Glacier valley (Griffiths and McSaveney, 1983; Henderson and Thompson, 1999), but the highly glacierised nature of the area makes precipitation measurements at high elevation difficult, and the location of the precipitation peak has not been identified. Precipitation data have been collected within the Franz Josef Glacier valley at a number of sites (Table 3.1, Figure 3.1). The maximum recorded rainfall is 10.6 m/a at Luncheon Rock (600 m a.s.l. on the western glacier margin, Figure 3.1).

Here we analyse past precipitation measurements to identify the location of the peak in precipitation at Franz Josef Glacier. High elevation precipitation measurements were collected between 1992-1995 at Almer Hut at 1700 m a.s.l. on the eastern glacier margin (Figure 3.1) by NIWA, but the site is difficult due to its exposed nature and heavy winter snowfalls, resulting in undercatch (Henderson, 1998). In order to assess the reliability of the record from Almer Hut, it is compared with the record from Alex Knob, a similarly exposed site at 1200 m a.s.l., and Douglas Hut, a sheltered site at 200 m a.s.l. on the valley floor (for locations see Figure 3.1, data supplied by R. Henderson).

The correspondence between precipitation at the Alex Knob, Douglas Hut and Almer Hut in the months December to March is striking (Figure 3.2). The Almer Hut raingauge shows a winter minimum in measured precipitation, most likely due to snowfall blocking the gauge. Monthly precipitation for Almer

Hut in the months December to April from 1991 to 1995 is strongly correlated with Alex Knob (r^2=0.96) and Douglas Hut (r^2=0.96) precipitation, indicating that the Almer Hut record is consistent with other measurements in the catchment during the summer, although it clearly is not in the winter. The mean precipitation ratio for December to April calculated between Almer Hut and Franz Josef village (1.6) is assumed to apply throughout the year in the absence of any other information about winter precipitation.

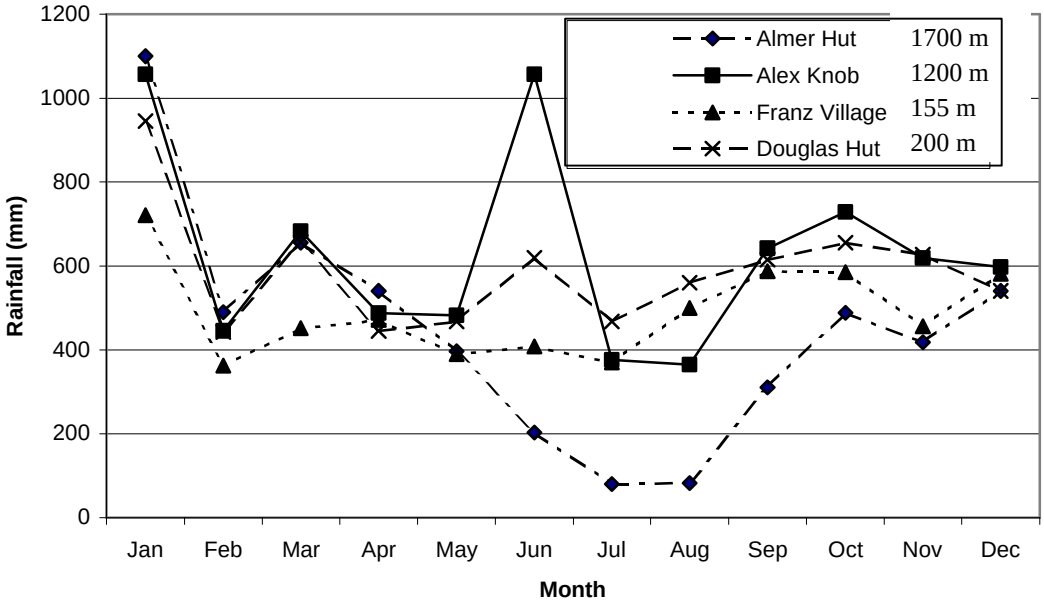

Figure 3.2. Monthly mean precipitation totals for Alex Knob, Almer Hut and Franz Josef village raingauges for the period 1992 to 1995.

Ratios of precipitation between other stations in the valley and that at Franz Josef village have been calculated (Table 3.3). At low elevations up to 600 m a.s.l, ratios are calculated using the precipitation normals in Griffiths and McSaveney (1983) and New Zealand Meteorological Service (1973). From comparison with the other precipitation profiles in the Southern Alps (Henderson and Thompson, 1999) and these ratios it is apparent that the precipitation maximum occurs between Luncheon Rock (600 m a.s.l.) and Almer Hut (1700 m a.s.l.), above which precipitation most likely reduces towards the glacier head (2500-3000 m a.s.l.). There is no information on the precipitation at the glacier head, and the ratio is adjusted so that the modelled net accumulation matches measured net accumulation (Section 3.5.3), resulting in a ratio of 0.7.

This reduction in precipitation above 1700 m is consistent with the pattern apparent in the other precipitation profiles (Henderson and Thompson, 1999), and the decreasing net accumulation with elevation measured by Ruddell (1995) on the adjacent Fox Glacier. A polynomial is fitted to the resulting variation of precipitation with elevation:

$$p(z) = 3.176 \times 10^{-16} z^5 - 3.279 \times 10^{-12} z^4 + 1.397 \times 10^{-8} z^3 - 2.995 \times 10^{-5} z^2 + 0.0276 z + 2.163 \quad (8)$$

This precipitation distribution is shown Figure 3.3 for the 1940-1971 normal period, along with those assumed in previous studies. None of these previous studies used the Almer Hut precipitation record, and so precipitation above 600 m was speculative, although Woo and Fitzharris (1992) and Oerlemans (1997b) did not use other precipitation records from within the glacier valley either.

Table 3.3. Annual mean precipitation for stations near Franz Josef Glacier. Source: Griffiths and McSaveney (1983) and Henderson and Thompson (1999).

Station	Elevation (m a.s.l.)	Annual mean precipitation (m/a)	Ratio to Franz Josef village precipitation
Franz Josef village	122	5.13	1.00
Sentinel Rock	230	7.02	1.37
Franz Terminal 1	328	8.47	1.65
Luncheon Rock	600	10.56	2.06
Almer Hut	1700	5.64	1.61

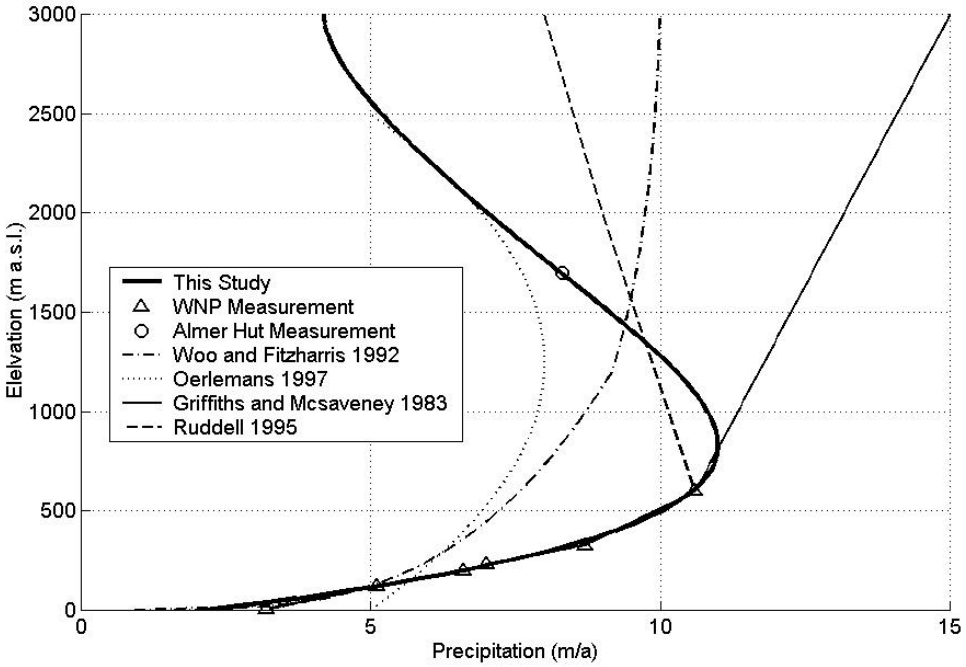

Figure 3.3. Precipitation variation with elevation *p(z)* estimated for Franz Josef Glacier. The Westland National Park (WNP) measurements are presented in Griffiths and McSaveney (1983), and the Almer Hut measurement calculated in this study. The curves of Woo and Fitzharris (1992), Ruddell (1995) and Oerlemans (1997) have been used in mass balance models.

3.4.2 Temperature variation

The variation of temperature with elevation *T(z)* is another key parameter required by the mass balance model which allows the calculation of ablation and accumulation variation with elevation.

Temperature lapse rates are calculated between stations on the glacier (Table 3.4). For the relationship between temperature measured at Franz Josef village and on the glacier the best station for comparison is FRANZ2 because it has the most continuous record (see Figure 3.1 for location). The lapse rates measured on the glacier are consistent with those measured by Barringer (1989) between high elevation stations in a non-glacierised alpine site in New Zealand (0.005 ^{o}C/m) and that calculated by Ruddell (1995) from Franz Josef village to Tasman Saddle (0.0054 ^{o}C/m).

Table 3.4. Lapse rates calculated between climate stations on the glacier.

From station	Elevation (m a.s.l.)	To station	Elevation (m a.s.l.)	Lapse rate (^{o}C/m)	Number of observations
FRANZ1	400	Franz2	800	0.0051	3246 hourly
FRANZ1	400	Franz3	2200	0.0050	5477 hourly
FRANZ2	800	Franz3	2200	0.0047	2730 hourly
Village	155	Franz2	800	0.0069	218 daily

The lapse rates between Franz Josef village and the station Franz1 (0.0069^{o}C/m) and between the stations on the glacier (close to 0.005^{o}C/m) are markedly different. The reason for this difference is most likely that there is a step in temperature between the Franz Josef village, located outside the glacier valley, and the glacier. Russell (1989) found that inside the valley, glacier winds dominated the wind regime, while out on the coastal plain, where Franz Josef village is located, sea breezes dominate, suggesting a temperature front between the glacier terminus and the Franz Josef village. Workers on other glaciers have found a similar effect (e.g. Conway and others, 1999). Given this inferred temperature step and the difference in lapse rates between the lowland station and the glacier, and within the glacier valley, the following function for temperature variation in the model is used

$$T(z) = T_{fjv} - T_s - 0.005(z - z_{fjv}) \qquad (9)$$

where T_{fjv} is the temperature measured at Franz Josef village, and z_{fjv} is the elevation of Franz Josef village (155 m a.s.l.). The constant temperature step T_s is calculated at 1.2^{o}C, derived from the elevation difference between Franz Josef village and FRANZ1 and the difference between the lapse rates on and off the glacier.

The mean annual average temperature at the glacier terminus (300 m a.s.l.) is then 8.9°C, and at 2900 m a.s.l., the highest elevation on the glacier, -4.1°C (based on the 10.8°C mean annual average temperature at Franz Josef village; Hessell, 1982)

3.4.3 Ablation parameters

As well as the variation of temperature with elevation over the glacier surface *T(z)*, the ablation factor f_a is required by the model to calculate positive temperature sums T_{sum} from daily temperature (equation 5). These daily temperature sums are then related to ablation rates by calculating the degree-day factor *k*.

Relationship between daily temperature and positive temperature sums.

The temperature lapse rate presented above allows calculation of daily temperature at any elevation on the glacier. To calculate ablation using the degree-day method, this daily temperature needs to be related to the daily positive temperature sum T_{sum}. The temperatures measured daily at the long-term climate stations at Franz Josef village and Hokitika are 0900 temperatures and minimum/maximum temperatures (0900 to 0900). The mean of the daily minimum and maximum temperatures is chosen as the input to the degree-day model because experimentation show there is a better correlation between this quantity and mean daily temperature at each of the stations Franz1-3 on the glacier (r^2=0.98) than between 0900 temperatures and mean daily temperature at the stations Franz1-3 on the glacier (r^2=0.94).

In order to calculate the relationship between the daily mean temperature T_{mean} and the daily positive temperature sum T_{sum}, the mean of minimum and maximum daily temperatures measured at each of the stations Franz1-3 on the glacier is compared with the daily temperature sum, measured hourly, at the same station. A strong piecewise linear relationship (r^2=0.98) is found of the form:

$$T_{sum} = \begin{cases} 0 & T_{mean} < 0.4 \\ T_{mean} - 0.4 & T_{mean} \geq 0.4 \end{cases} \qquad (9)$$

Combined with equation (9) for *T(z)*, the positive temperature sum $T_{sum}(z)$ can now be calculated at any elevation on the glacier, using the daily minimum and maximum temperatures at Franz Josef village.

Degree-day factors

Temperature and ablation were measured simultaneously on the Franz Josef Glacier to enable the direct calculation of the degree-day factor *k*. For each mass balance stake measurement, temperature is lapsed from the nearest climate station on the glacier at the previously calculated glacier lapse rate of 0.005 °C/m to the mass balance stake elevation and the positive temperature sum T_{sum} for the period calculated. The resultant ablation and positive temperature sums for each mass balance measurement period allows the degree-day factor to be calculated (Figure 3.4)

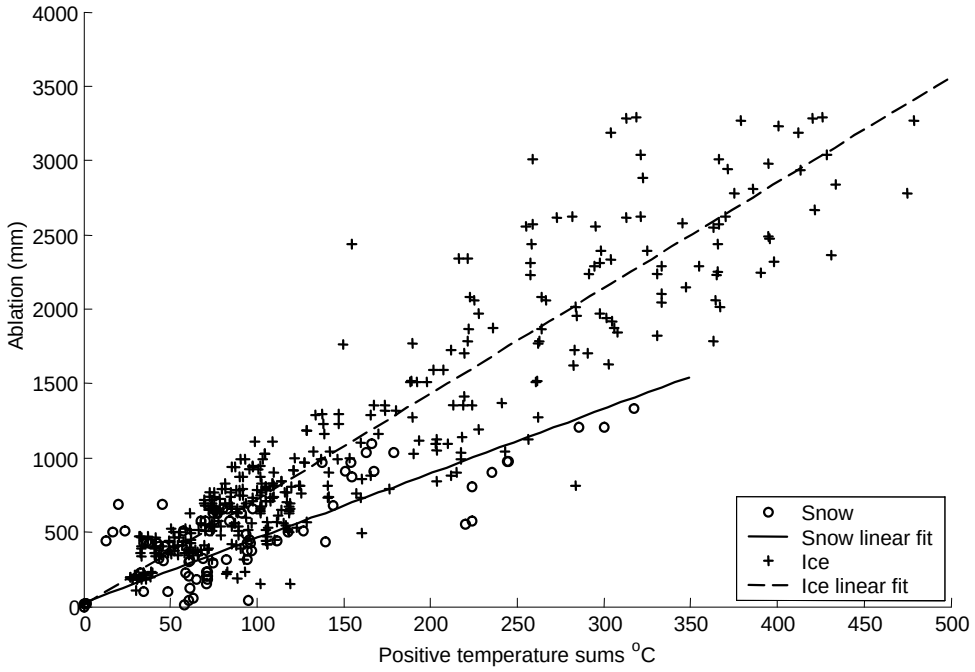

Figure 3.4. The relationship between positive temperature sums and measured ablation.

A t-test indicates that the intercept in the regression of positive temperature sums against ablation is not significantly different from zero, and so the regression is forced through zero (Figure 3.4). The gradient of the two regression lines is then the degree-day factor *k* for snow and for ice (Braithwaite, 1985; 1995). The result is a degree-day factor k_i = 7.1 mm day^{-1} deg^{-1} for ice and k_s = 4.5 mm day^{-1} deg^{-1} for snow. These values are comparable with those found in the literature (Braithwaite and Zhang, 1999) and somewhat higher than the k_i = 6 mm day^{-1} deg^{-1} for ice and k_s = 3 mm day^{-1} deg^{-1} for snow used for Franz Josef Glacier by Woo and Fitzharris (1992).

Due to the differential melting of snow and ice, it is necessary to record the thickness of the snowpack over the glacier so that ablation can be calculated correctly based on the different degree-day factors for snow and ice. To manage the transition from snow to ice in irregular topography, where the snow thickness is less than a certain value, in this case, 0.1 m w.e. (Jóhannesson, 1997), the degree-day factor is varied linearly between the snow and the ice degree-day factor.

3.4.4 Accumulation parameter

As indicated in Section 3.2, accumulation is modelled by assuming that precipitation that falls when $T(z) < T_{crit}$ falls as snow. The relationship between daily temperature and proportion of hourly temperatures less

that T_{crit} is now explored (Figure 3.5). Other snow accumulation models (Moore and Owens, 1984; Barringer, 1989) have found that a value for T_{crit} close to 1°C is the most appropriate for New Zealand conditions, and that value is used here.

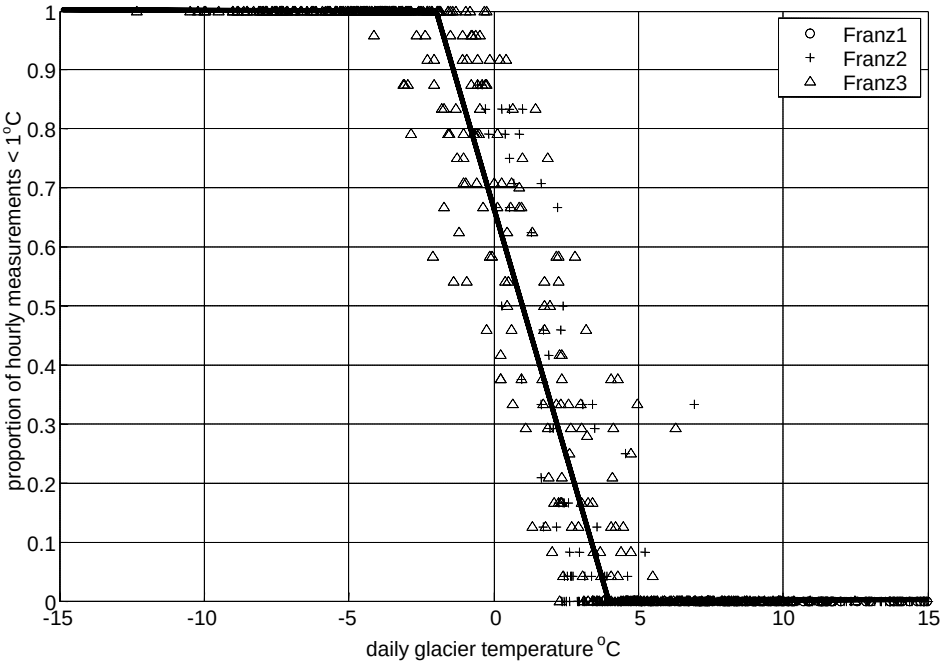

Figure 3.5. The relationship between daily temperature (mean of the maximum and minimum temperatures) measured at a glacier station and the proportion of hourly temperature measurements that are less than T_{crit} = 1°C.

A piecewise linear function f_c is fitted to the relationship between the proportion of hourly measurements where $T_{hourly} < T_{crit}$ and daily glacier temperature T:

$$f_c(T_{mean}) = \begin{cases} 1 & T_{mean} < -2 \\ -\dfrac{T_{mean} + 4}{6} & -2 \le T_{mean} < 4 \\ 0 & T_{mean} \ge 4 \end{cases} \qquad (10)$$

When the temperature is less than -2°C all precipitation falls as snow, when the temperature is greater than 4°C all precipitation falls as rain. In between the proportions vary between these extremes. This accumulation factor f_c, in combination with *T(z)* and *p(z)*, allows the calculation of accumulation at any elevation on the glacier.

3.5 Mass balance model verification

In order to verify that the mass balance model and the input data outlined in the preceeding sections models mass balance on the Franz Josef Glacier accurately, the model is run for the period of mass balance measurement, the three balance years from 1 April 2000 to 31 March 2003, to compare the results of the model with measurements. The model is run using input climate data from both Franz Josef village and from Hokitika to verify that mass balance can be modelled using the adjusted Hokitika data.

3.5.1 Comparison with short-term mass balance measurements

For each of the three years of mass balance calculations there are a large number of individual mass balance measurements, taken at elevations from 400 m a.s.l. to more than 2600 m a.s.l. The measurements have been taken over time periods varying from 10 days to 60 days. For each one of these measurements, the modelled mass balance for the period is extracted, and compared to the measurement (Figure 3.6).

There is a good correspondence between measured and modelled mass balance (Figure 3.6). The set of parameters used to calculate mass balance is not unique (Laumann and Reeh, 1993; Braithwaite and Zhang, 1999). In particular the choice of temperature lapse rates and degree-day factors are not independent. Hence it is expected that measured ablation rates will match modelled ablation within the variability apparent in Figure 3.4.

In the first two balance years, 2000-2001 and 2001-2002, the model underestimates mass balance for a significant proportion of the measurements (Figure 3.6a and b). In 2002-2003, the mean measurement interval increased to 45 day and there is a better correspondence between measured and calculated mass balance rates. The underestimate here is not apparent in the net annual ablation measurements presented in Section 3.5.3.

The mass balance model results are consistent with the set of short-term mass balance measurements, although limitations of the degree-day method mean that individual measurements are not calculated well, unless the measurement period is greater than about 30 days. Modelled mass balance using Hokitika climate data do not appear to be significantly different from modelled mass balance using Franz Josef village on this time scale.

3.5.2 Comparison of snowline elevations

Another mass balance model verification tool is comparison of the modelled transient snow line elevation with observations. The only observations of snowline apart from the EOSS were made in the balance year April 2000 – March 2001 (Figure 3.7).

a) 2000-2001

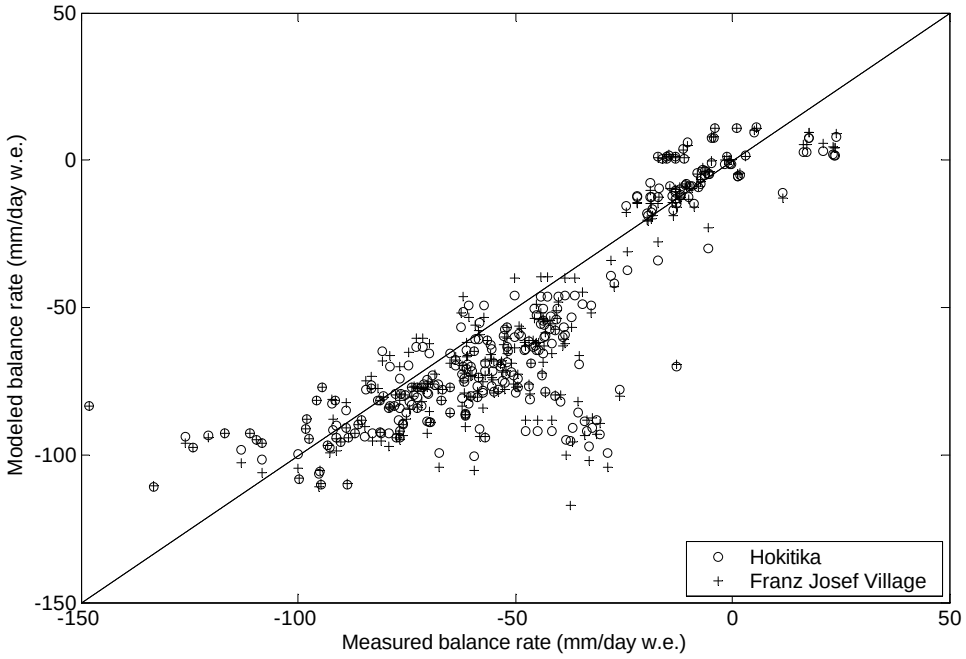

b) 2001-2002

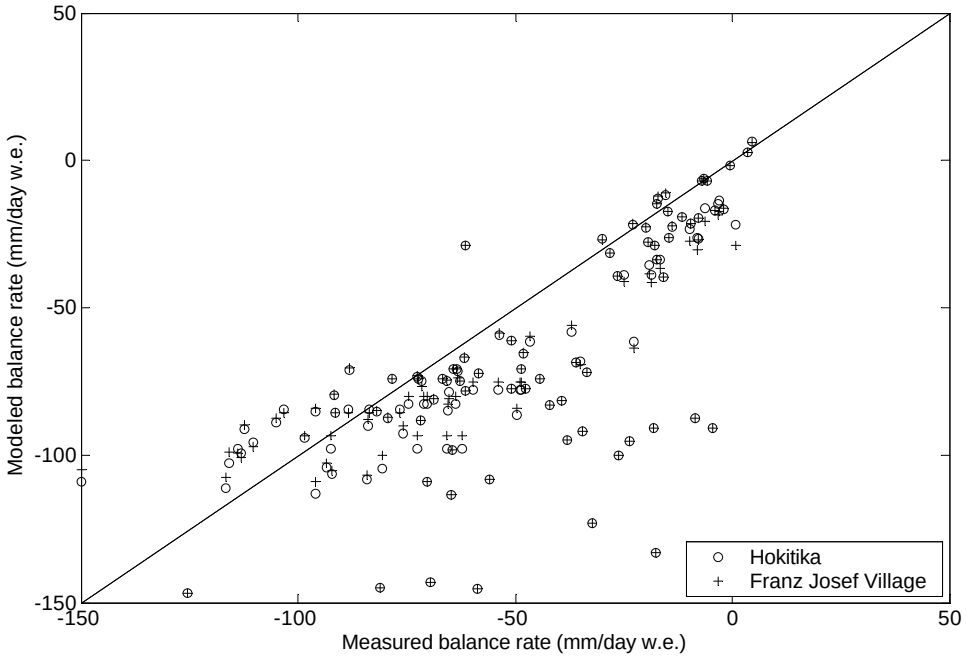

continued over..

c) 2002-2003

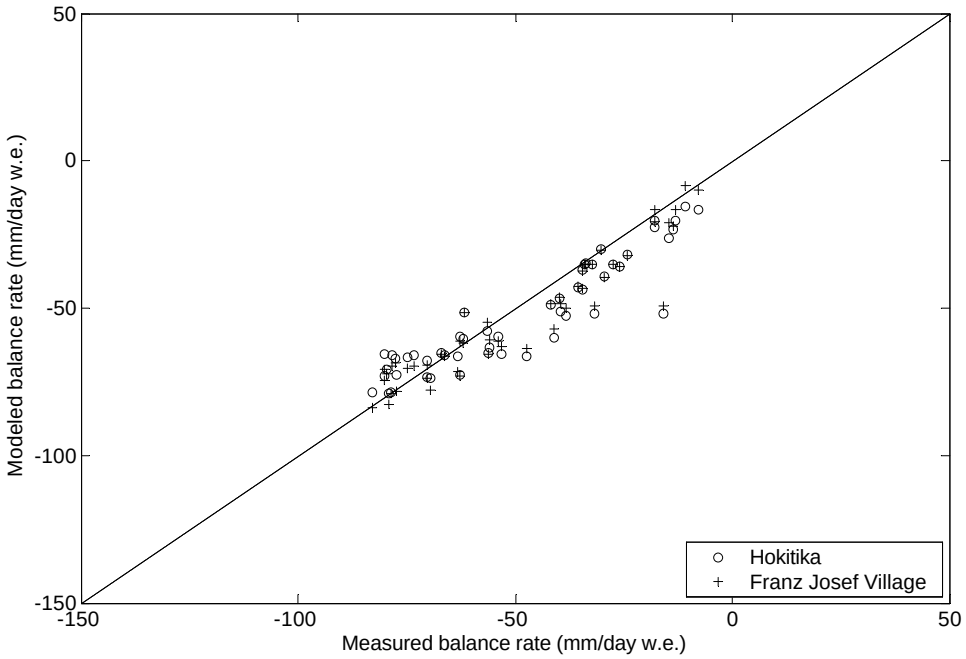

Figure 3.6. A comparison of measured and modelled mass balance. The dashed line is the line of modelled = measured mass balance. The mass balance is modelled using Hokitika and Franz Josef village climate records for the purposes of comparison of model output.

The predicted transient snowline matches observation well when the model is run using Franz Josef village input data. The differences may be a result of the poor short-term ablation calculation mentioned previously.

There is a difference between the transient snowline calculated using the Franz Josef village and the Hokitika climate data of 100 m. The reason for the difference is that the adjusted Hokitika climate record does not match the Franz Josef village record perfectly. A precipitation event in June occurred in Franz Josef village but not in Hokitika, which resulted in the snowline difference of about 100 m which persisted to the end of the balance year.

A comparison between measured and modelled EOSS elevations for 2000-2003 is given in Table 3.5. The patterns of change in measured and calculated EOSS are the same, but the actual values differ by up to 160 m, with the measured EOSS almost always lower than the calculated EOSS. The reason for this difference is that the mass balance model does not account for snow transport by ice flow. Velocities in the vicinity of the EOSS exceed 1 m/day (Section 4.4) which combined with the relatively steep slopes mean that snow is transported more than 400 m horizontally and 100 m vertically through the course of the year. Hence it is to be expected that measured EOSS is lower than calculated EOSS by about 100 m for this reason

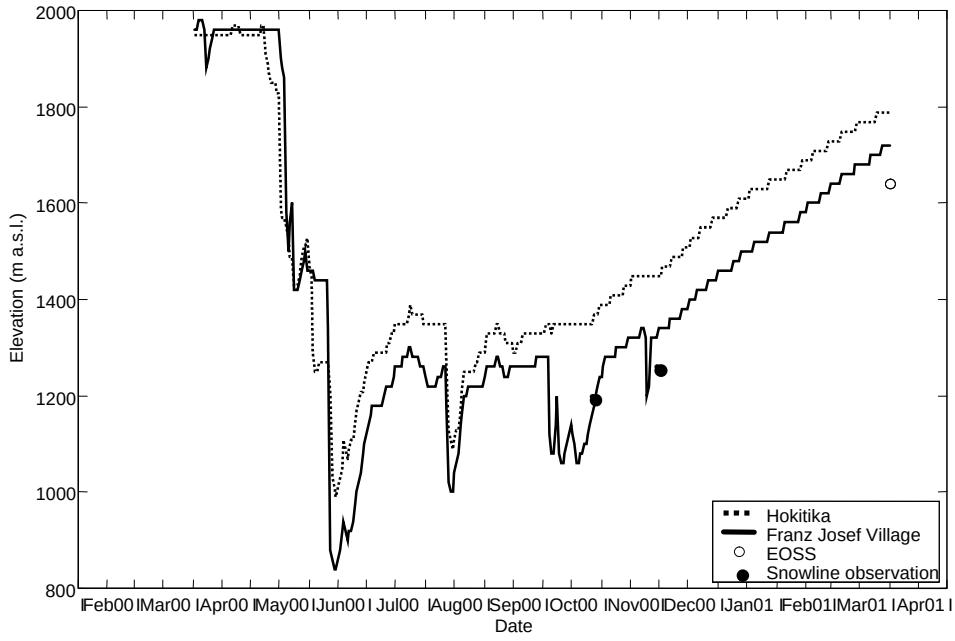

Figure 3.7. Modelled and measured snowline elevation for April 2000 – March 2001.

Table 3.5. Modelled and measured EOSS elevations.

Year	EOSS observation (m a.s.l.)	EOSS calculation (m a.s.l)	
		Franz Josef village	Hokitika
2001	1640	1720	1800
2002	1760	1900	1920
2003	1560	1540	1680

The difference between snowlines calculated using the Franz Josef village and Hokitika climate data is again put down to an imperfect match between the adjusted Hokitika and actual Franz Josef village data. The close correspondence for the 2002 balance year is partly a result of 164 days of missing records from Franz Josef village which were filled using the transformed Hokitika data.

3.5.3 Comparison with net annual balance

The most important output of the model in terms of overall glacier response is the net annual mass balance variation with elevation, calculated using equation (6). Comparison of this modelled net annual mass

balance with measurements indicates that the measured and modelled annual ablation match well (Figure 3.8). Note that there are no net ablation results available for 2000-2001 and no net accumulation results for 2002-2003. The match between measured and modelled annual accumulation is more difficult to judge. The calculated accumulation is within the range of measured accumulation. However, measurements of net annual accumulation show a large variation of up to 5 m/a w.e. in a small elevation range, especially in the 2002-2003 balance year (Figure 3.8c), providing only a weak verification for the modelled accumulation.

The mass balance measurements show that there is significant variation in mass balance at the same elevation. The variations show no systematic pattern, and so are ascribed to site specific conditions. On the lower glacier these are:

- proximity of steep rock walls, which can both enhance ablation through re-radiation and reduce ablation through shading,
- concentration of surface debris, which can also enhance or reduce ablation depending on its thickness, and
- surface drainage patterns which can locally enhance ablation dramatically through water erosion.

On the névé these processes occur to a much lesser extent, and the variations in mass balance are ascribed to variations in snow accumulation, primarily through redistribution by wind and avalanche.

The modelled total mass balance for the glacier indicates that there are significant differences between results from the model run using Hokitika and Franz Josef village climate data input (Table 3.6). The Hokitika and Franz Josef village results show the same pattern, with a positive mass balance year in 2000-2001, a slightly negative year in 2001-2002 and the most positive year being 2002-2003. In all years the Hokitika input results in a lower mass balance, the difference being 0.64 m/a w.e. in 2000-2001, 0.10 m/a w.e. in 2001-2002 and 0.65 m/a w.e. in 2002-2003.

The measurements and model together provide a good understanding of the present-day regime of climate and mass balance at Franz Josef Glacier. While the model does not reproduce the measured mass balance perfectly, the wide range of mass balance measured in a small range of elevation means that the model provides the best fit possible within the constraints of the measurements of climate on the glacier and the assumption that the spatial variability in mass balance varies with elevation alone.

The parameters in the mass balance model are generally constrained by field measurements of climate and mass balance, rather than being tuned to a measured mass balance profile. However, it is still instructive to examine the effect of errors and uncertainties in model parameters on the model output. Annual ablation is modelled fairly well on the lower glacier, and since only a small area experiences net ablation (17% of the glacier was below the EOSS of 1640 m in 2001), uncertainties in net ablation on the lower glacier will have little effect on overall glacier behaviour. The model is much more sensitive to the net accumulation

calculation due to the large accumulation area. As mention in section 3.4.1, precipitation above 1800 m a.s.l. has been tuned so that measured and modelled mass balance are comparable. Due to the large variability in the net accumulation measurements, this is not a tight constraint, and so the model is further verified in Section 5.5 where it is apparent that for present day conditions the coupled mass balance-ice flow model predicts a length close to that observed at present. The sensitivity of the model to accumulation means that some care has been taken in adjusting the unmeasured part of the precipitation curve.

The model is now used to examine the relationship between the EOSS elevation and total mass balance, and analyse the past and expected future changes in mass balance at Franz Josef Glacier.

a) 2000-2001

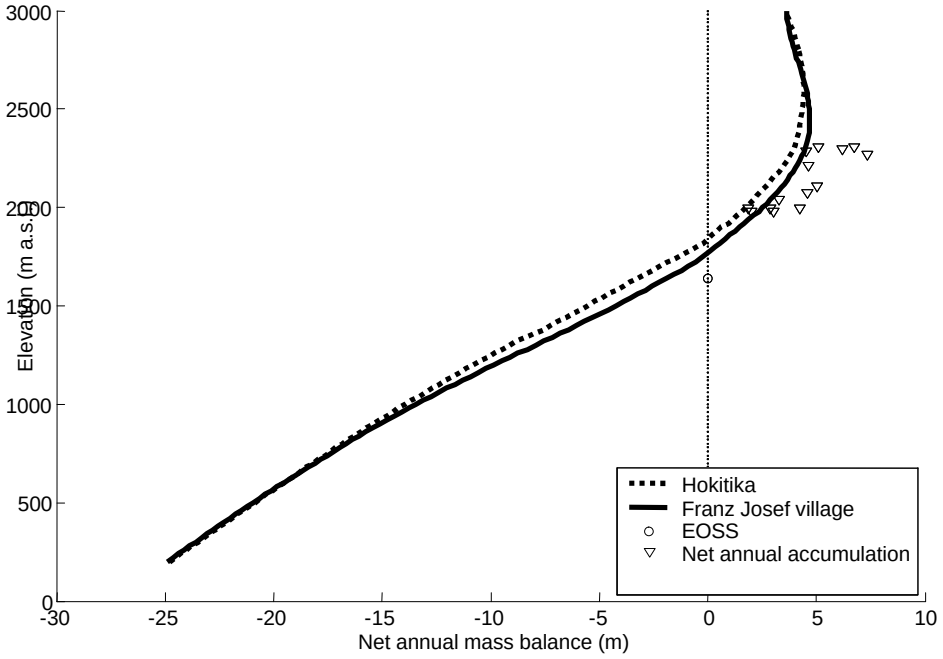

continued over..

b) 2001-2002

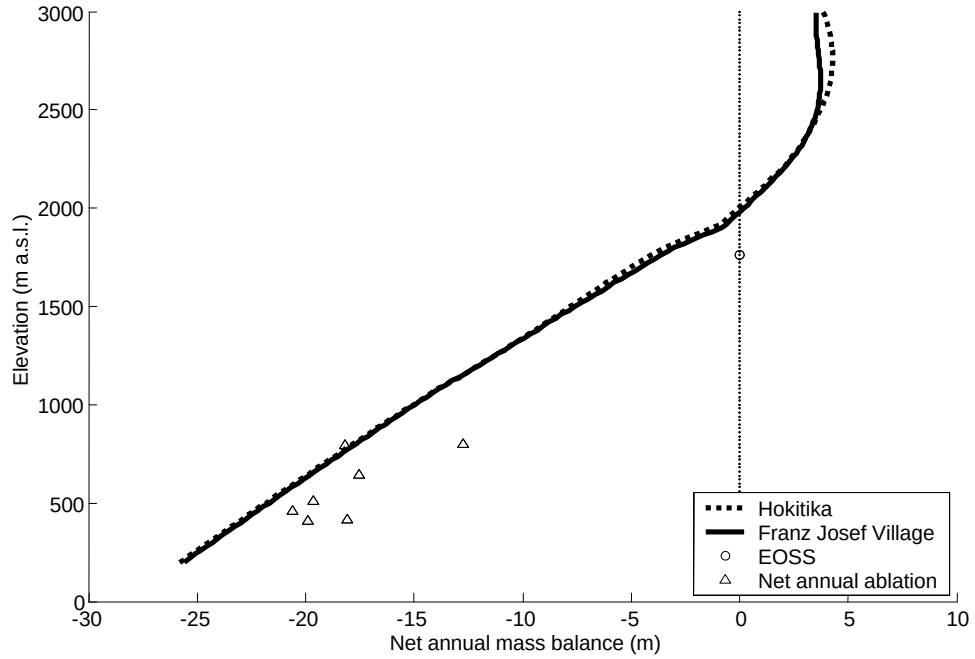

c) 2002-2003

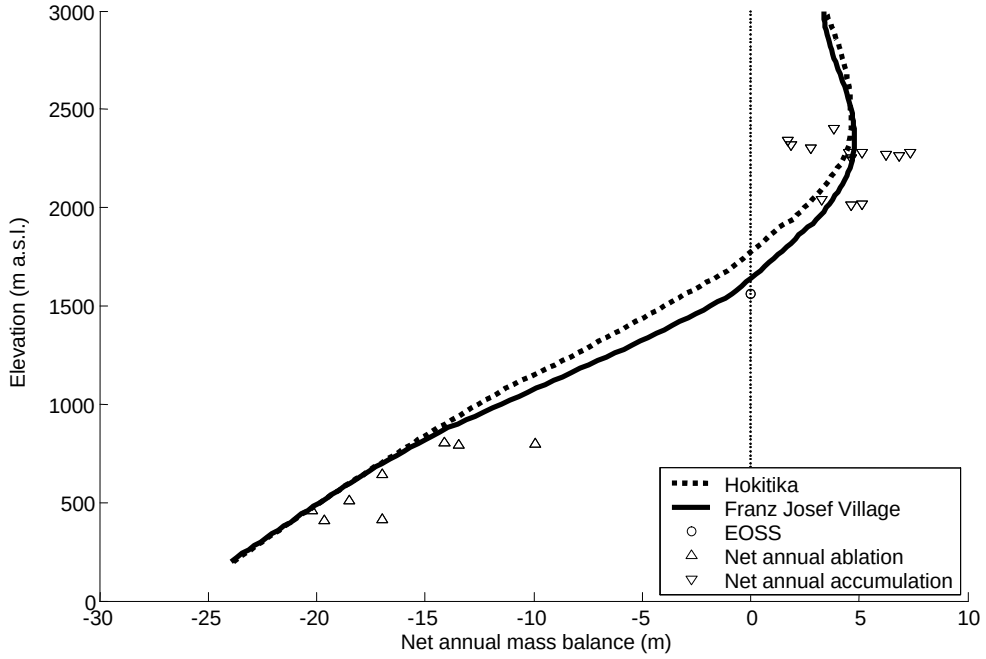

Figure 3.8. Net annual balance modelled over the elevation range of the glacier. a) April 2000 – March 2001 b) April 2001 – March 2002 c) April 2002 – March 2003.

Table 3.6. Modelled net annual mass balance for the three years of measurement.

Year	Mass balance (m/a w.e.)	
	Franz Josef village	Hokitika
2000 – 2001	1.60	0.94
2001 – 2002	-0.43	-0.53
2002 – 2003	2.30	1.65

3.6 Relating end of summer snowlines to net annual balance

The mass balance model has been verified against measurements, and is now employed to realise the second objective of this chapter, namely to ascertain whether the Almer Glacier EOSS (Figure 3.9), measured since 1977 (Chinn and Salinger, 2001), can be used to predict the mass balance of the Franz Josef Glacier. To do this the model is run for the full period of available climate measurements, April 1894 to March 2003 (Figure 3.10).

There is a strong linear relationship ($r^2 = 0.91$) between modelled Franz Josef Glacier mass balance and modelled Franz Josef Glacier EOSS. The intercept of the best fit line is 1820 m (Figure 3.10) which corresponds to the EOSS elevation when the mass balance is zero, or the ELA for the 1986 geometry on which the mass balance is calculated (Section 3.3). An uncertainty of ±50 m is assigned to the ELA, based on the width of the 95% prediction interval (Figure 3.10). The width of the 95% prediction interval also indicates that the regression can be used to predict mass balance from calculated EOSS with an uncertainty of ±1 m/a w.e.

As already noted, the measured Franz Josef Glacier EOSS is consistently lower than the modelled Franz Josef Glacier EOSS, and the three years of measured Franz Josef Glacier EOSS are insufficient to draw a relationship between measured Franz Josef Glacier EOSS and calculated mass balance.

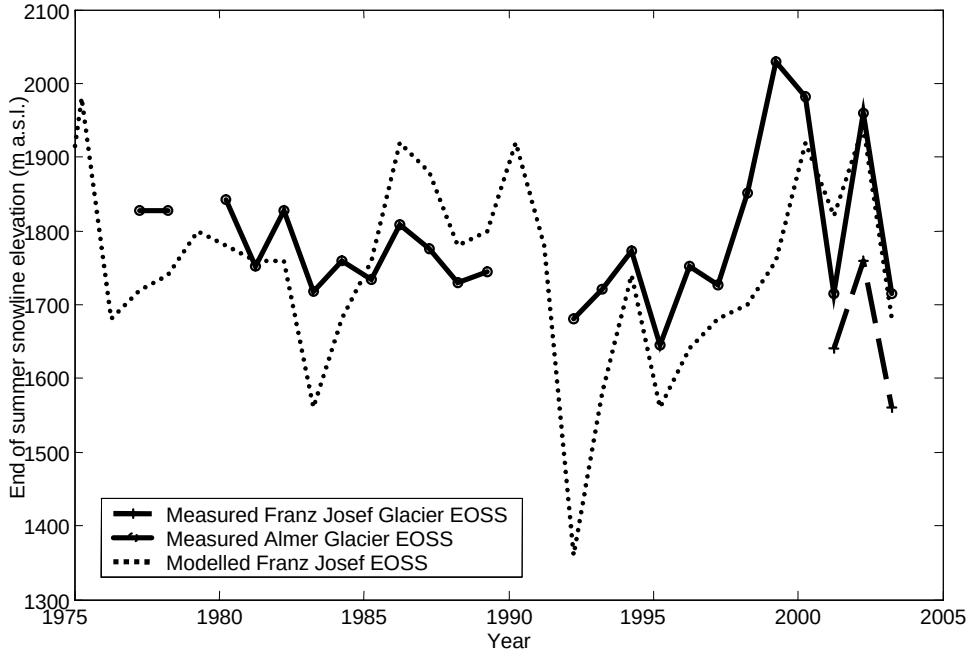

Figure 3.9. Time series of the modelled EOSS for Franz Josef Glacier, the measured EOSS for Franz Josef Glacier and the measured EOSS for Almer Glacier.

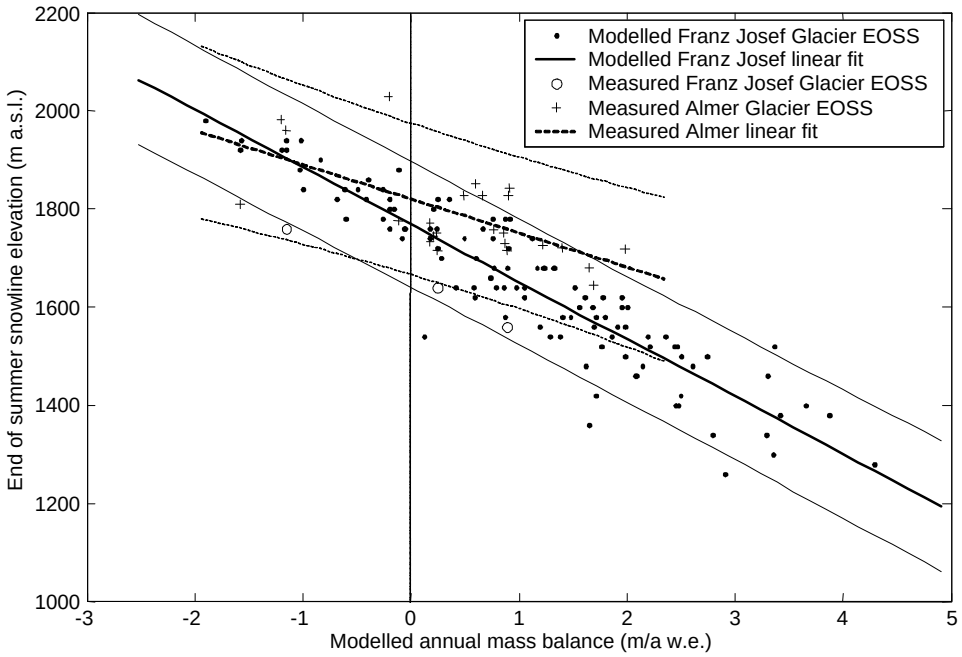

Figure 3.10. The relationship between modelled Franz Josef Glacier total annual mass balance and EOSS elevation modelled for Franz Josef Glacier and measured on the Franz Josef and Almer Glaciers. The thin lines are the 95% prediction interval.

The relationship between the measured Almer Glacier EOSS elevation and calculated Franz Josef Glacier mass balance (Figure 3.10) is not as strong ($r^2 = 0.65$). There is a range of 2.5 m/a w.e. in Franz Josef Glacier mass balance within a range of 60 m of Almer Glacier EOSS (Figure 3.10), and the resulting 95% prediction interval is too wide to predict Franz Josef Glacier mass balance from Almer Glacier EOSS.

While the Almer and Franz Josef Glaciers are close geographically, it is not possible to predict Franz Josef Glacier mass balance from the Almer Glacier EOSS. The Almer Glacier EOSS cannot even be used to determine the sign of the Franz Josef Glacier mass balance.

3.7 Past mass balance variation

The third objective of this chapter is to examine variations of mass balance at Franz Josef Glacier over the last century. In order to achieve this objective, the mass balance model is run with daily values of rainfall and temperature collected in Hokitika (Figure 3.11). The Hokitika input data are used instead of the Franz Josef village data because they are more reliable (Salinger, 1981) and extend back to 1894.

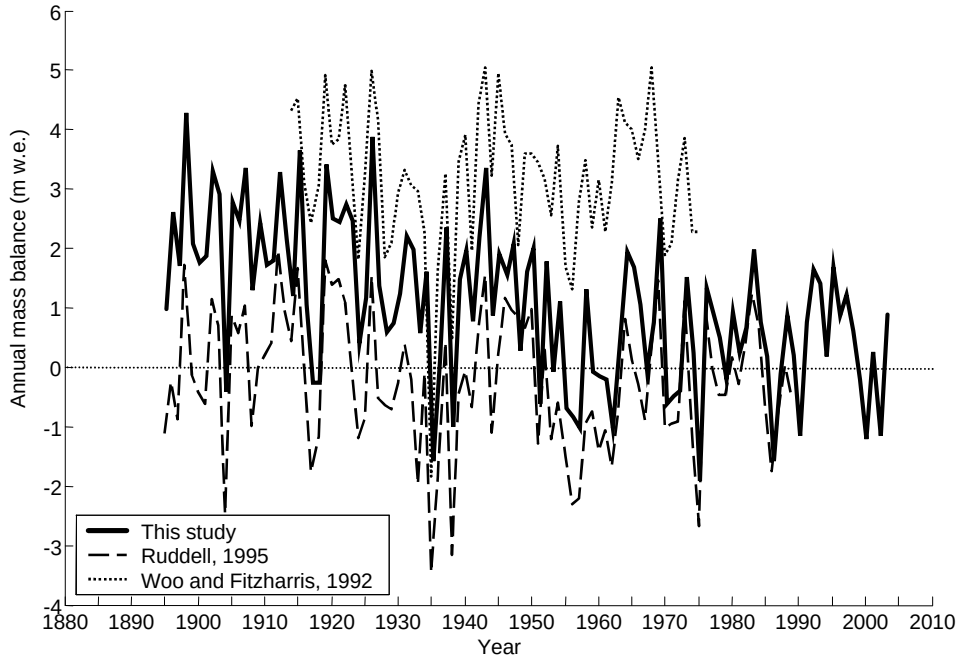

Figure 3.11. The modelled total annual mass balance for Franz Josef Glacier from 1894 to 2003.

The modelled mass balance for the period 1894 to 2003 shows a trend of -0.02 m/a^2 w.e.(Figure 3.11), indicating that during this period the variations in temperature and precipitation have led to a reduction in

mass balance over the glacier. Note that the mass balance is calculated on a fixed geometry (the 1986 geometry described in Section 3.3), whereas if mass balance was calculated on a varying geometry there would not be such a strong trend as the glacier continuously advances and retreats towards a state of zero mass balance (Oerlemans, 2001).

The mass balance modelled here is compared with that modelled by Woo and Fitzharris (1992) and Ruddell (1995). While all three mass balance reconstructions show similar year to year patterns, the comparison demonstrates the significant differences between previous mass balance models at Franz Josef Glacier. The mean difference between the mass balance calculated by Woo and Fitzharris (1992) and Ruddell (1995) from 1913 to 1989 is 3.2 m/a w.e., of the same order as the variation from 1894 to 2003 calculated in this study. The geometry adjustment through time used by Woo and Fitzharris (1992) and Ruddell (1995) means that the calculated mass balance can only be compared directly for all three studies in the 1980s when the glacier geometry was close to that of 1986. The comparison reveals that the model in this study calculates a mass balance always more positive than that of Ruddell (1995), but by less than 1 m/a w.e. and always more than 2 m/a w.e. less than Woo and Fitzharris (1992).

3.8 Future mass balance scenarios

The final objective of this chapter is to examine the likely changes in mass balance that will be experienced by the glacier in the next century. The period to 2100 is used by the IPCC for the construction of future climate scenarios, and that period is used here in constructing glacier mass balance scenarios.

3.8.1 Climate change scenarios

Different types of General Circulation Models (GCM) and methods of regional downscaling for the New Zealand situation are described by Mullan and others (2001). They use a transient coupled ocean-atmosphere model, which predicts an increase in the westerlies across New Zealand in the next century, resulting in a significant increase in precipitation as the temperature increases.

A simple approach to applying the changes in temperature and precipitation predicted by Mullan and others (2001) to a particular site is to take projections for that site of rainfall and temperature scaled per degree of global warming from a number of GCM models. The magnitude of global warming for different emission scenarios is then used to calculate climate change scenarios for that site.

The global temperature changes predicted by the IPCC (2001) are plotted in Figure 3.12. The range of predicted temperatures for a number of scenarios has been characterised by the minimum, mean and maximum temperature change encompassed by the scenarios in each year.

The expected changes from the present-day normal period (1970-1999) to the next century (2070-2099) in rainfall and temperature per degree global warming for Hokitika (Figure 3.13) have been calculated by statistical downscaling of transient GCM runs (Mullan and others, 2001; data provided on a decadal basis by B. Mullan). The warming predicted for Hokitika is significantly less than the global average and there are seasonal differences in the predicted changes with an increase in winter precipitation and temperature.

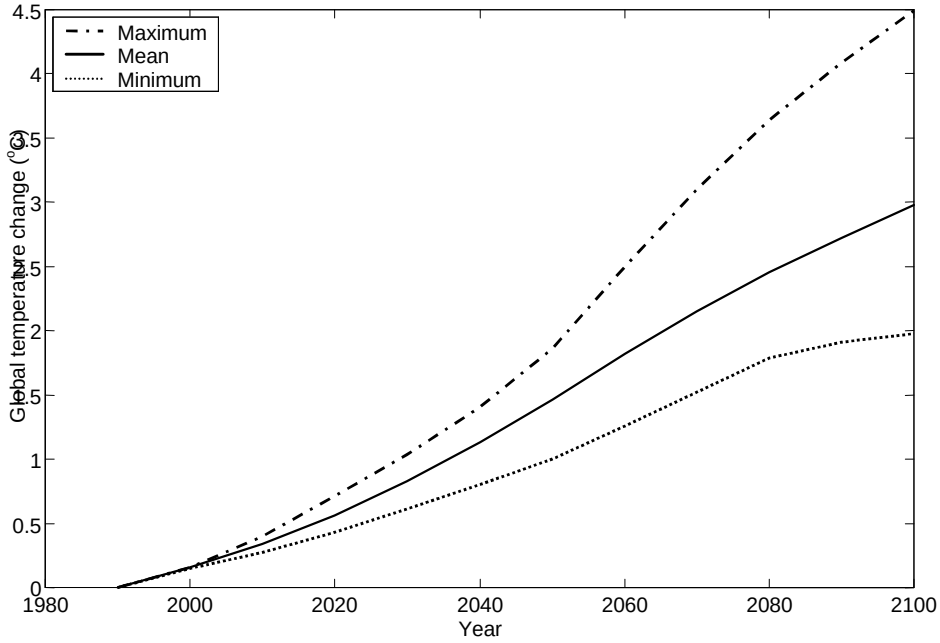

Figure 3.12. Predicted global temperature change for the scenarios. The plotted lines are the minimum, maximum and mean temperature change for each year. Source IPCC 2001.

3.8.2 Mass balance scenarios

These future climate change scenarios are now used as the basis for input to the mass balance model in order to assess the likely changes in glacier mass balance between the present-day and 2100. The mass balance model is run for each year from 2003 to 2100 using the global temperature changes in Figure 3.12 and the local seasonal changes in temperature and precipitation in Figure 3.13. The calculation is organised into four different scenarios:

1. The 'no warming' scenario where temperature and rainfall are held at their means for the 1970-1999 normal period.
2. The 'mean warming' scenario where the mean global warming scenario is used.
3. The 'minimum warming' scenario where the minimum global warming scenario is used.
4. The 'maximum warming' scenario where the maximum global warming scenario is used.

The 'mean warming' scenario incorporates the mean precipitation change. In order to assess the full envelope of future mass balance encompassed by these scenarios, in the 'minimum warming' scenario

incorporates the maximum precipitation increase, and the 'maximum warming' scenario incorporates the minimum precipitation increase.

The changes in mass balance under these scenarios are described by the change in EOSS, since this is a measure of the mass balance which is independent of changing glacier geometry. The results of the mass balance model run with the 'mean warming' scenario (Figure 3.14) indicates that the EOSS (contour of zero mass balance) will rise from 1820 m in the year 2000 to 1960 m in the year 2100. The mass balance model, when run with the 'no warming' scenario, results in an EOSS of 1820 m.

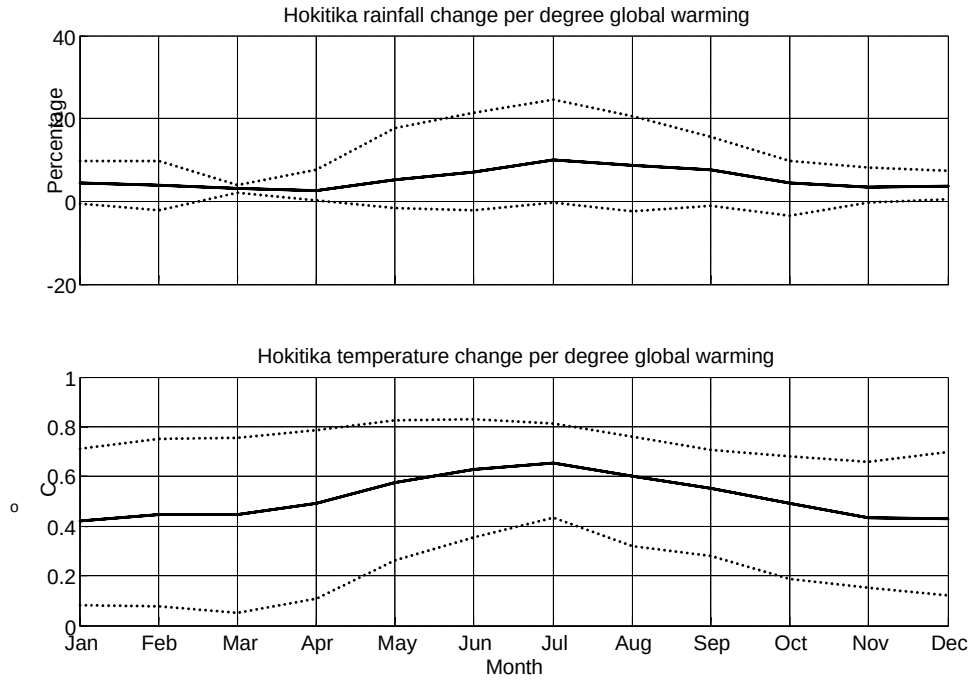

Figure 3.13. Changes in temperature and rainfall per degree global warming projected for Hokitika. The mean, maximum and minimum values are used to characterise the output of four GCMs (CCC, CSIRO, Hadley, Japan). The data are smoothed with a three-month running mean.

The range of calculated EOSS elevations for the other scenarios (Figure 3.15) is large. The ‘minimum warming’ scenario results in a minor reduction of the EOSS from the 'no warming' scenario, as the smaller increase in temperature (1^{o}C by 2100) is offset by the large increase in precipitation (annual mean increase of 26%). The 'maximum scenario' results in the EOSS rising to over 2600 m, above 98% of the 1986 glacier area (Figure 3.15).

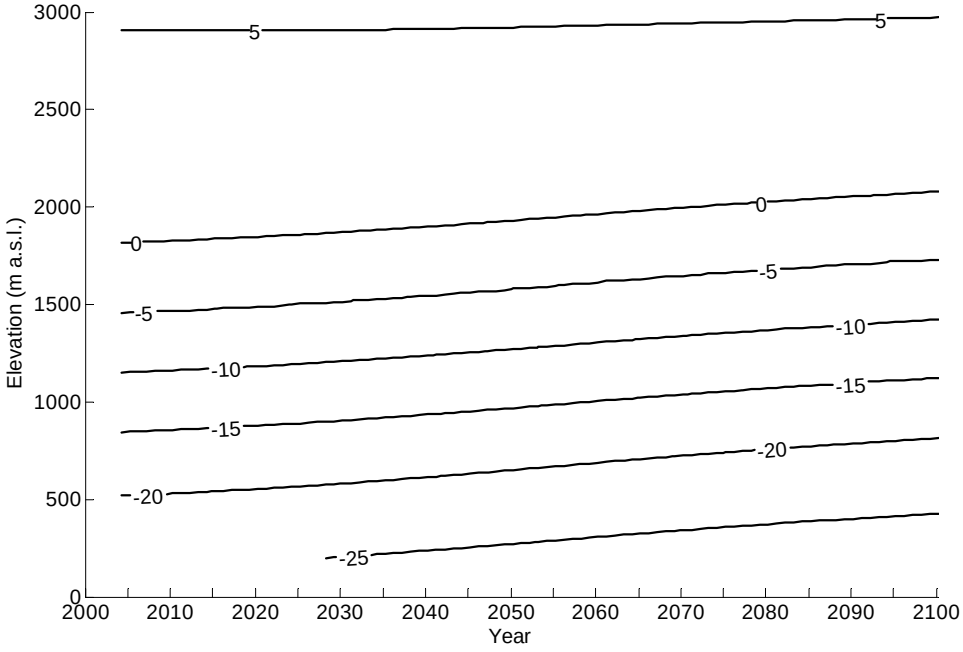

Figure 3.14. A contour plot of the expected change in mass balance for the 'mean warming' future climate scenario.

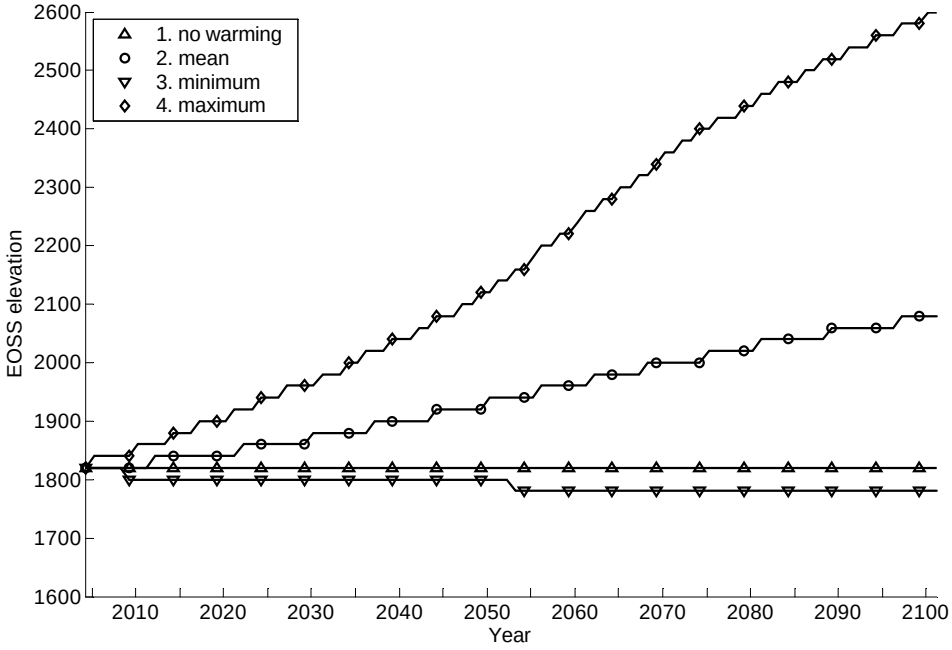

Figure 3.15. The range of EOSS variations for the period 2003-2100 calculated using each of the four climate change scenarios.

3.9 Discussion

3.9.1 Present-day climate and mass balance

An analysis of precipitation at Franz Josef Glacier indicates that the variation of precipitation with elevation is quite different from what has been assumed by previous studies, with a maximum in precipitation near 1200 m a.s.l. in elevation of approximately 11 m/a reducing above this to 5.6 m/a at 1700 m a.s.l. Above this elevation precipitation reduces to 3.6 m/a at the glacier head, between 2500 to 3000 m a.s.l., although this precipitation is established from net accumulation measurements and may include effects such as the reduction in accumulation resulting from wind redistribution of snow.

These high precipitation rates result in measured and modelled net annual accumulation in the névé of up to 7 m/a w.e. (Figure 3.8). Measured and modelled net annual ablation at the terminus of the Franz Josef Glacier is approximately 20 m/a w.e. (Figure 3.8). The Franz Josef Glacier is a maritime glacier, and to compare its behaviour to other glaciers, we look to other glaciers in moist, mid-latitude areas such as south Alaska, western Norway and Patagonia (Benn and Evans, 1998). A summary of mass balance measurements in Alaska (Mayo, 1984) indicates that the Colombia Glacier has the highest accumulation rates here, peaking at 5 m/a w.e. and net ablation of 9 m/a w.e. The Taku Glacier, Alaska, and Nisqually Glacier, Washington State, have similarly high ablation rates of 10 m/a w.e. Nigardsbreen has the highest measured accumulation and ablation rates in western Norway (Nesje and Dahl, 2001), experiencing up to 4 m/a w.e. net accumulation and 11 m/a net ablation (Haeberli and others, 2001). There are very few measurements of mass balance in Patagonia. Hence, we can conclude that of the well known and well measured glaciers of the world, Franz Josef Glacier appears to have the highest measured accumulation and ablation rates.

The relationship between measured mass balance and elevation at Franz Josef Glacier (Figure 3.8) is not as strong as for many glaciers (e.g. Jóhannesson and others, 1995; Braithwaite and Zhang, 2000). The variability is similar to that measured on South Cascade Glacier, Washington State, USA, and somewhat less than that measured on the McClure Glacier, California, USA, (Fountain and Vecchia, 1999). The relatively weak relationship between measured mass balance and elevation at Franz Josef Glacier is a result of shading and heating from the steep rock valley sides on the lower glacier, and the redistribution of wind blown snow and differing aspects of different parts of the névé.

The mass balance model shows a good correspondence with measurements, which improves as the comparisons become longer term. However, the large variation of measured mass balance in a small elevation range (Figure 3.8) and the assumption in the model that spatial variability can be modelled by elevation alone means that the match is not as good as that of mass balance models on other glaciers. For example, Jóhannesson and others (1995) and Braithwaite and Zhang (2000) obtained a good match between

measured and modelled mass balance on glaciers in Northern Europe and Switzerland respectively. Both of these studies have tuned the mass balance model parameters to fit the measured mass balance. In this study model parameters have been derived from measurements of temperature, precipitation and mass balance, and tuning has only been used in the precipitation variation at high elevation (Section 3.4.1).

3.9.2 The use of EOSS as an indicator of mass balance

The use of the Almer Glacier EOSS as an indicator of Franz Josef Glacier mass balance was investigated with the aim of reconstructing Franz Josef Glacier mass balance for the period 1977-2003 using Almer Glacier EOSS (Chinn and Salinger, 2001) and the Franz Josef Glacier mass balance curve (Figure 3.8).

The mass balance model used in this study defines a strong relationship between EOSS elevation and mass balance for Franz Josef Glacier (Figure 3.10), as expected (Braithwaite, 1984). However, the relationship between measured EOSS and mass balance is not as strong. With only the three years of Franz Josef Glacier EOSS elevation, measured in this study, there are insufficient data to define a relationship between Franz Josef Glacier EOSS and mass balance. The record of Almer Glacier EOSS since 1977 (Chinn and Salinger, 2001; Chinn, pers. comm.) is also not able to be used as a predictor of Franz Josef Glacier mass balance (Figure 3.10). Even the sign of the Franz Josef Glacier mass balance cannot be determined from the Almer Glacier EOSS.

3.9.3 Past mass balance

The record of climate and reconstructed mass balance since 1894 allows a qualitative analysis of the large overall retreat of the glacier since 1894 (Figure 3.16). The mass balance calculated on a fixed geometry (1986) shows a strong negative trend for the period of -0.02 m/a^2. The first major retreat of the glacier after 1935 (Speight, 1941) coincides with the negative mass balance years in the 1930s (Figure 3.11). In the 1940s the mass balance recovered to its levels before in the 1930s, and there was a small advance in the late 1940s. In the 1950s the mass balance was negative again for some years, and the retreat continued. Another recovery of mass balance in the 1960s leads a glacier advance in the late 1960s. A more positive mass balance in the late 1970s and mid 1990s appears to force the sustained advance from 1983 to 1999. It is clear that there is a relationship between reconstructed mass balance and terminus position, which in the past has been qualitatively linked through a constant lag time of 5 years (Woo and Fitzharris, 1992). The simplification of the processes of ice flow by a constant lag time is avoided here by the use of an ice flow model which is developed in Chapter 1 and applied in Chapter 5 of this thesis.

3.9.4 Future mass balance scenarios

The mass balance model calculates a wide variety of glacier mass balance possibilities based on future climate scenarios. The 'mean warming' scenario indicates that the increase in temperature of 1.5^{o}C by the

year 2100 assumed in this scenario, even when combined with the increase in precipitation of 16%, results in an increase in EOSS of 140 m. The 'minimum warming' scenario results in a 40 m lowering of the EOSS from the 1970-1999 normal period by the year 2100 (Figure 3.15). This result indicates that the negative effect on mass balance of an increase in temperature of 1°C has been outweighed by the positive effect on mass balance of a mean annual increase in precipitation of 26% (Figure 3.12 and 3.13). The 'maximum warming' scenario would lead to a glacier with an EOSS of 2600 m a.s.l. (Figure 3.15), indicating that the combination of an increase in temperature of 2.2°C and small decrease in precipitation (-5%) will lead to drastic glacier recession, considering that only 2% of the present day glacier is above the elevation of 2600 m a.s.l. (Figure 3.1).

(a)

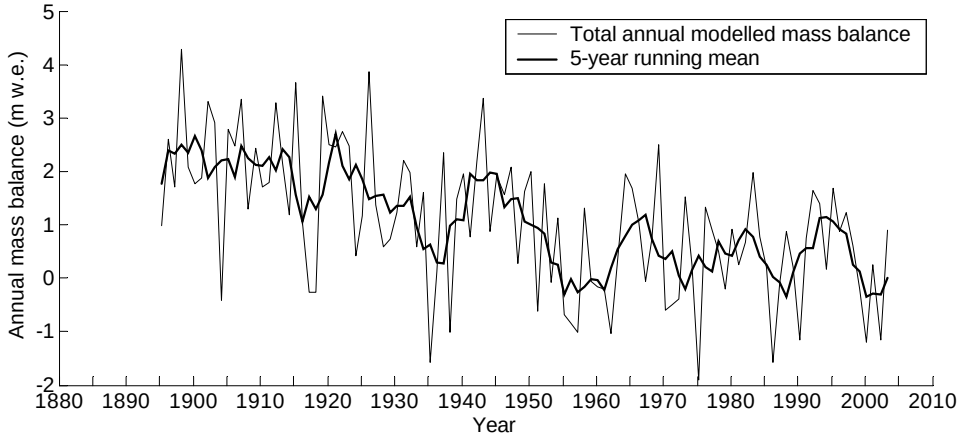

(b)

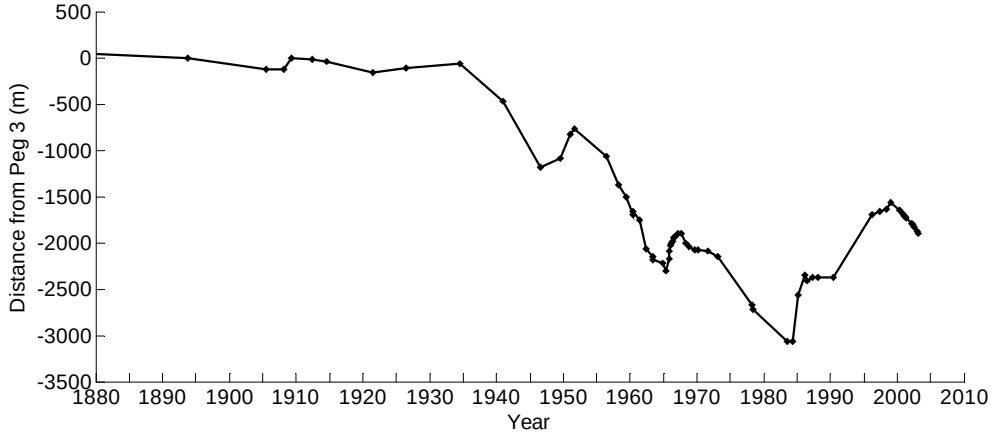

Figure 3.16. A comparison of (a) reconstructed mass balance and (b) terminus position.

The wide range of mass balance scenarios presented here is a result of the sensitivity of Franz Josef Glacier to climate change (Oerlemans, 2001). Many studies (e.g. Oerlemans, 1992; Laumann and Reeh, 1993; Oerlemans, 1997a; Jóhannesson 1997; Fleming and others, 1997; Oerlemans and others, 1998; Braithwaite

and Zhang, 2000; Engeset and others 2000) have shown that glaciers are sensitive, to varying degrees, to changes in precipitation and temperature, and predictions of future mass balance are sensitive to the particular changes specified.

3.9.5 General

A pervasive problem in previous mass balance models at Franz Josef Glacier is that the mass balance calculation is consistently positive. Without any annual mass balance measurements against which to compare their calculations Woo and Fitzharris (1992) suggested that perhaps some parts of the glacier did not contribute to the mass balance, suggesting that the accumulation area is smaller than thought.

Ruddell (1995) avoided the problem of consistently positive mass balance, by specifying an unrealistic ablation rate at the terminus. Ruddell (1995) took some measurements of net annual accumulation from crevasse stratigraphy in the névé, of up to 6.8 m w.e. In order to avoid a consistently positive mass balance, to ensure consistency with net accumulation measurements, and in the absence of net annual balance measurements at the terminus, he predicted 40 m/a w.e. ablation at the terminus. When applied to an ice-flow model the predicted glacier length was close to that observed.

Oerlemans (1997b) predicted an unrealistically positive mass balance, and reduced his maximum precipitation to 8 m/a from 10 m/a to reduce accumulation. This was despite the measured maximum precipitation being 10.6 m/a (Griffiths and McSaveney, 1983) and the net annual accumulation measurements of Ruddell (1995). The resulting mass balance was still too positive, and when applied to an ice-flow model predicted an equilibrium glacier more than 1 km longer than present.

In this context we must question whether the model presented in this study has overcome the overestimated mass balance problem. The model has calculated 86 years of positive mass balance out of a total of 110 years (Figure 3.10). This is not alarming, since the 1986 geometry on which the mass balance was calculated was close to the smallest the glacier was during that period, indicating that almost any year would be positive mass balance on this geometry. In addition, the mass balance calculated for the three years of measurement, 2000-2003 is close to that measured, so we can conclude that at least under present day conditions the mass balance model does not overestimate mass balance.

3.10 Conclusion

The Franz Josef Glacier experiences high precipitation rates which vary from 5.1 m/a at Franz Josef village (155 m a.s.l.) to a maximum of approximately 11 m/a at 1200 m a.s.l. on the glacier tongue before reducing to 3.6 m/a at the glacier head, between 2500 - 3000 m a.s.l. (Figure 3.3). The terminus experiences a mean annual temperature of 8.7 ^{o}C. The result of these high precipitation rates and temperatures are extreme annual ablation and accumulation rates. Net annual accumulation varies between 2-7 m w.e. in the

elevation range 1800-2300 m a.s.l. (Figure 3.8), while ablation rates of 20 m/a w.e. have been measured at the terminus (Figure 3.8). The accumulation and ablation data indicate there is significant spatial variation in mass balance independent of elevation. The ELA for the 1986 glacier was 1820 ± 50 m a.s.l.

The Almer Glacier EOSS, which has been measured since 1977 (Chinn and Salinger, 2001) is a poor predictor of Franz Josef Glacier mass balance, despite the fact that the two glaciers are in the same catchment. This result precludes the use of the Almer Glacier EOSS record for any further analysis of the past mass balance variations of the Franz Josef Glacier.

The retreat of the glacier over the last century is qualitatively linked with a strong reduction in the mass balance over this period. The link between mass balance changes and glacier advance and retreat can only be quantitatively examined with an ice-flow model, which is done in Chapter 5.

Future mass balance scenarios indicate that the mass balance is almost certain to continue to reduce over the next century. However, the uncertainty in the climate projections leads to a large uncertainty in the mass balance. The resulting range of EOSS change will be between a 40 m lowering over the next 100 years, to an 800 m rise over the next 100 years. The mean scenario leads to a 140 m rise in EOSS by 2100. The resulting glacier length will be anywhere between similar to the present day length, to small remnant glaciers on the highest peaks.

4 Modelling glacier dynamics at Franz Josef Glacier *Ka Roimata O Hine Hukatere*

4.1 Introduction

Ice flow is the process by which changes in mass balance, described in the previous chapter, lead to changes in glacier geometry, including terminus position. In this chapter we examine these ice flow processes and develop a model which will simulate ice flow for Franz Josef Glacier.

The response of a glacier to climate change is a dynamic response to a constantly changing mass balance. Many studies of the sensitivity of glaciers to climate change consider the static response, where step changes in mass balance lead to an resulting equilibrium glacier length change (Oerlemans, 1986, 1997b; Stroeven, 1996; Wallinga and van de Wal, 1998). In this case precise calculation of glacier dynamics is not critical (Oerlemans, 2001). When the dynamic response of the glacier to constantly changing mass balance is considered, however, the correct calculation of glacier velocity is vital (Greuell, 1992).

Glacier velocity models are sensitive to ice thickness, as deformation rates vary with the fourth power of thickness, and sliding rates with the second power (Paterson, 1994). Since ice thickness has not been measured on Franz Josef Glacier before, thickness has previously had to be calculated. Ruddell (1995) used a steady state analysis where ice thickness was calculated from balance velocities. Oerlemans (1997) used an assumption of constant basal shear stress to calculate ice thickness. With the ice thickness measurements presented in this chapter, we can examine the effect of these assumptions on calculated velocities.

It is generally accepted that longitudinal stresses also play an important role in the flow of mountain glaciers (Greuell, 1992; Willis, 1995; Hubbard, 2000). However, longitudinal stresses are almost universally neglected in coupled mass balance-ice-flow models (e.g. Wallinga and Van de Wal, 1998; Schmeits and Oerlemans, 1997; Zuo and Oerlemans, 1997), partly because of the additional computational cost involved in their calculation. Longitudinal stresses would be expected to be significant at Franz Josef Glacier due to its steep and rapidly changing surface slope, and will be examined in this chapter.

The Franz Josef Glacier is somewhat unusual in that it descends to a low altitude in a warm maritime environment. As a result, the lower ~ 2 km (300 -800 m a.s.l.) of the glacier experiences year round ablation of up to approximately 20 m/a (Figure 3.8) and measured mean annual rainfall peaks at about 12 m/a (Figure 3.3) at 1200 m a.s.l. which falls throughout the year. The plentiful supply of water throughout

the year raises the question of whether the generalised sliding law can be used to calculate the sliding velocity for this glacier.

This chapter builds on the measurements of Gunn (1964) and the models of Ruddell (1995) and Oerlemans (1997b). The overall goal is to understand the dynamics of Franz Josef, in order to provide a sound foundation for modeling the dynamic response of the glacier to climate change and to more accurately predict future glacier behaviour. Our objectives are to:

1. Establish the variability of measured velocity, both spatially and temporally (at submonthly and seasonal timescales), in order to determine the role and variability of basal sliding in motion;
2. Examine the links between sliding variability and rainfall events;
3. Use measured velocities to establish flow parameters that appropriately characterise the velocity field;
4. Quantify the proportions of measured velocity that can be attributed to internal deformation and to sliding;
5. Evaluate the role of longitudinal stress in motion; and
6. Evaluate the results of previous studies in the context of the results of this more detailed analysis.

These objectives are achieved by comparison of measured velocities with velocities of internal deformation and sliding predicted from stress distributions. Stress distributions are calculated from standard relationships (Paterson, 1994), using measured ice depths that are presented in this chapter. Movement mechanisms considered are sliding and internal deformation. Sediment deformation, which is unlikely to be important at Franz Josef Glacier, is not included in the analysis.

4.2 Ice flow mechanisms

Ice flow in glaciers is composed of two components, internal deformation and basal motion. Surface movement is the combination of these two processes. Basal motion can be comprised of sliding and sediment deformation. Based on observations at the margins and recently deglacierised areas, Franz Josef Glacier, in common with many mountain glaciers, appears to rest largely on bedrock. While there may be pockets of sediment under parts of the glacier, sediment deformation is not expected to be a significant process and is neglected here, following similar studies elsewhere (e.g. Greuell, 1992; Schmeits and Oerlemans, 1997).

4.2.1 Internal deformation

Internal deformation is caused by a number of processes within the ice; primarily glide along crystal basal planes and to a smaller extent anisotropic deformation. Numerous theoretical analyses (Nye 1951, 1952, 1953), laboratory studies (Glen, 1955) and field studies in deformation of boreholes and tunnels (Nye, 1953, 1957; Paterson, 1977) have given us a good understanding of these processes.

Velocity on the centreline U_d due to internal deformation velocity can be calculated quite reliably for a given glacier geometry (Paterson, 1994):

$$U_d = f_d \tau_{xz}^n H \qquad (1)$$

where f_d is the deformation flow parameter, n the flow law exponent, H the ice thickness, x is in the direction of flow, z the vertical coordinate and τ_{xz} the driving stress, defined for a valley glacier such as Franz Josef Glacier by:

$$\tau_{xz} = -F\rho gH \sin\alpha \qquad (2)$$

where F is the shape factor, ρ is the density of ice, and α the surface slope. The shape factor F can be calculated (Paterson, 1994):

$$F = \frac{S}{HP} \qquad (3)$$

where S is the cross-section area and P the wetted perimeter of the cross-section. In this study the cross-section is modelled as a trapezium defined by the width of the glacier at the surface w_s, ice thickness H, and valley side slope θ (Figure 4.1).

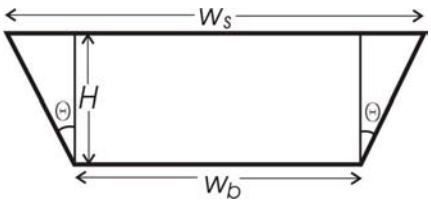

Figure 4.1. Glacier cross-section representation.

There are difficulties in determining the value of some of the parameters in the relationship, in particular f_d and n, but in practice f_d varies little between different glaciers and the value of 1.9 x 10^{-24} $Pa^{-3}s^{-1}$ (Budd and others, 1979) is often used, and a value of 3 is taken for n (Paterson, 1994).

Equation (2) implies that ice velocity depends only on local variables, and longitudinal stress gradients are neglected. For mountain glaciers in particular this is unrealistic (Greuell, 1992; Hubbard, 2000). Longitudinal stresses can be calculated by a number of methods (van der Veen, 1987; Blatter, 1995; Hubbard, 2000), the simplest of which is described by Paterson (1994) and termed the 'ice stretching approximation' by Hubbard (2000). Longitudinal stresses are calculated along a flowline, where the surface

elevation *h* and the bed elevation *b* are defined. The driving stress τ_{xz} in equation (2) is then modified by the addition of a correction term:

$$\tau_{xz} = -\rho g H \sin\alpha + 2\int_{b}^{h} \frac{\tau'_{xx}}{\partial x}\partial z \qquad (4)$$

where τ'_{xx} is the deviatoric longitudinal stress, *x* the direction of flow, *b* the bed, *h* the surface and *z* the vertical coordinate. Hubbard (2000) describes a scheme by which the correction can be calculated. This scheme is used here and model results include the effect of the longitudinal stress calculation.

4.2.2 Basal sliding

Basal sliding is difficult to measure, because it is a process that occurs at an inaccessible part of a glacier. Some studies have measured sliding velocities directly (e.g. Hooke and others, 1992; Blake and others, 1992, Copland and others, 1997; Hubbard, 2002). A major difficulty in calculating sliding velocities is that sliding shows large variability on a number of spatial and temporal scales, largely a result of changes in the subglacial drainage system (Iken and others, 1983; Mair and others, 2001). While there have been analyses linking subglacial water pressure to sliding velocities (Röthlisberger, 1972; Fowler, 1987), subglacial water pressure itself is difficult to calculate.

A number of theoretical treatments of sliding have been presented (Weertman, 1964; Nye, 1969, 1970; Kamb 1970). These analyses have lead to the development of a generalised sliding law (Paterson, 1994):

$$U_s = f_s \tau_{xz}^{q} N^{-r} \qquad (5)$$

where f_s is the sliding parameter, *N* the effective pressure (ice overburden less water pressure) and *q* and *r* are small integers. Calculating *N* is a difficult matter (Röthlisberger, 1972; Bindschadler, 1983; Greuell, 1992), and so *r* is often set to zero, with the result that variations of water pressure are neglected, although the bulk effect is incorporated in the other parameters. A value of 2 for *q* arises from regelation, and 3 for the viscous flow of ice around bumps (Paterson, 1994).

While this sliding law has been generally discredited (e.g. Paterson, 1994; Vincent and others, 2000) it is in general use in ice flow models in the absence of any better method. The parameters f_s and *q* are tuned to fit the velocity profile of a particular glacier.

4.3 Methods

The overall method for the analysis of dynamics is to compare the measured spatial and temporal patterns of glacier velocity with modelled glacier velocities. Glacier velocity was measured for the period October

2000 to March 2002. Ice thickness has also been measured, as an important input to a glacier velocity model.

4.3.1 Velocity measurement

Ice velocity was measured by repeat high precision survey of a network of stakes (Figure 4.2). The spatial distribution of the stakes is one longitudinal line and three transverse lines, although there is a large gap in longitudinal stake coverage where the four main basins converge and form a large icefall. The highly crevassed nature of this area precludes ground measurements.

The stakes were maintained at fixed locations throughout the measurement period. When each stake had moved more than approximately 50 m from its original site, it was relocated to the original site. This approach was necessitated by the limited safe areas available for stakes, and their rapid movement into crevassed areas.

The surveying was undertaken using Trimble 4700 Global Positioning System (GPS) receivers. The GPS data were processed using Trimble software, which typically reported horizontal errors in position in the range 0.01-0.02 m. The maximum horizontal error in stake displacement between two measurements of 0.2m is made up of a GPS error of 0.04 m, an antenna positioning error of 0.06 m and an error arising from the stakes not being perfectly vertical of 0.10 m. Error bars are plotted on all graphs of ice velocity, but are often too small to be seen.

Stake position measurement interval varied in different years of the study (Table 4.1). The overall goal was to examine sub-monthly velocity variations from November 2000- March 2001, and continue measurements from November 2001-October 2002 to allow analysis of longer term velocity variations. Measurement frequency in the névé is limited by logistics, so there is no information on sub-monthly velocity variations from this area.

Table 4.1. The average number of days between measurements during different periods of the study. The * denotes a single measurement period of 30 hours in July 2002.

year	2000		2001												2002									
month	11	12	1	2	3	4	5	6	7	8	9	10	11	12	1	2	3	4	5	6	7	8	9	10
névé	30												30								*			
lower	10-20												30					45						

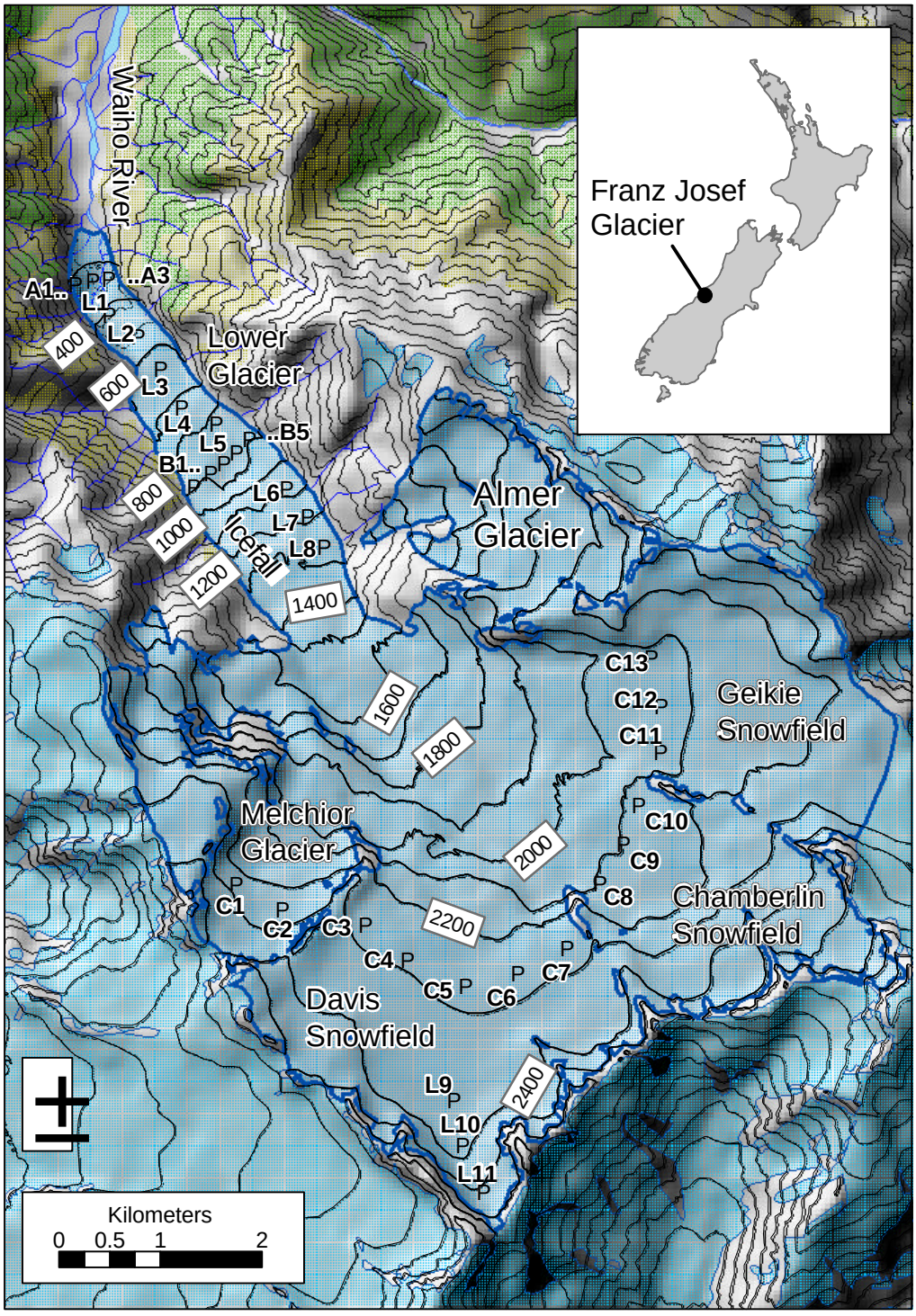

Figure 4.2. Franz Josef Glacier and its location in the South Island, New Zealand. The location of velocity measurements stakes are shown and labelled. Contours are at 100 m intervals.

4.3.2 Ice velocity modelling

In order to establish flow parameters f_d and f_s which best fit measured velocity, the equations presented in Section 4.2 are used to calculate velocities caused by internal deformation and basal sliding along the centreline of the glacier, which are compared with measurements of velocity. The ice velocity modelling is also used to assess the contribution of basal sliding to surface velocity and the influence of longitudinal stresses on the velocity field.

The calculation is carried out every 100 m along the glacier on the line marked in Figure 4.3. The input data required for the ice flow model, glacier geometry, is defined by the surface elevation *h*, the bedrock elevation *b*, the glacier width w_s and w_b, and the valley side slopes *?*.

Surface elevation

Surface elevation data are available in the form of a digital elevation model prepared from a contour map which was drawn from aerial photography in 1986 (NZMS 261, G35 and H35). The vertical accuracy of the DEM grid is 25 m, and the horizontal resolution 20 m. Further surface elevation data from GPS profiles near the head and terminus of the glacier, recorded during the period 2000-2003, are incorporated in the DEM to ensure that the glacier model accurately represents the current geometry of the glacier. The surface elevation *h* is calculated from this DEM at each of the flowline grid points (Figure 4.3)

Bedrock elevation

Two radio-echo sounding (RES) systems were employed in different parts of the glacier to measure ice thickness and thence bedrock elevation. In the névé, data were collected using an impulse transmitter (Narod and Clarke, 1994) with resistively loaded antennae at 5 MHz. Spatial location was determined from a GPS in kinematic mode. This system was unable to resolve the bed on the lower glacier tongue, most likely a result of the close, steep valley walls and the heavily crevassed and wet nature of the lower glacier. On the lower glacier GPR data were collected using a ‘Sensors and Software Pulse Ekko 100’ GPR system with 25 MHz antennae. Spatial location was determined from interpolation of GPS positions taken every 50 m along the profiles.

The bed return is defined by strong spatially continuous response in the trace record. Where there was no such return no attempt at interpretation has been made. A wave velocity of 168 m/μs was used to calculate ice thickness (Murray and others, 2000). No migration was attempted due to difficulties that have been encountered on other temperate glaciers due to the non-uniformity of radio wave velocity due to differing water content (Murray and others, 2000; Goodsell and others, 2002).

The resulting ice thickness data are shown in Figure 4.4. Ice thickness in the middle reaches of the glacier was interpolated using an assumption of a constant basal shear stress t of 150 kPa in equation 2

(Oerlemans, 1997). The measured and calculated ice thickness measurements do not coincide exactly, so a five-point moving average is used to smooth the glacier bed and remove any discontinuities.

Glacier width and side slopes

Glacier width is calculated using the DEM in conjunction with the glacier outline from the same map (NZMS 261, G35 and H35). Valley side slope q is calculated from the elevation change over a distance of 100 m outside the glacier outline. The mean slope of the two sides of the glacier is the valley side slope q .

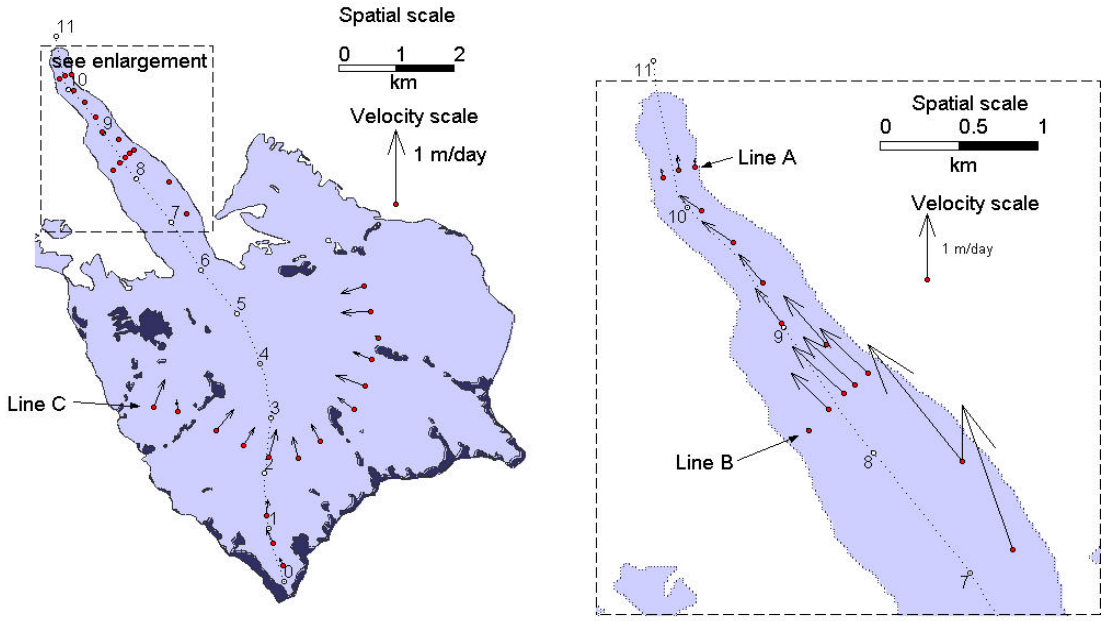

Figure 4.3. Vector plot of measured mean velocity from November 2000 to March 2001. The centreline along which velocity is calculated and plotted is shown with numbers every 1 km along the line.

4.4 Spatial variations in measured ice velocity

To examine the spatial variations in ice velocity on Franz Josef Glacier, the means of velocity measurements for each stake from November 2000 to March 2001 are examined. This period was chosen because there are measurements from all stakes for this period, whereas winter velocities from the névé are few. It will later be shown (Section 4.5.2) that there is little seasonal variation in velocity at Franz Josef Glacier and that measurements from this period are representative of the overall velocity regime.

The most striking feature of the spatial pattern of velocity (Figure 4.3) is the convergence from the four névé basins, the Melchior Glacier, Davis, Chamberlin and Geikie Snowfields into the lower névé area (Figure 4.3).

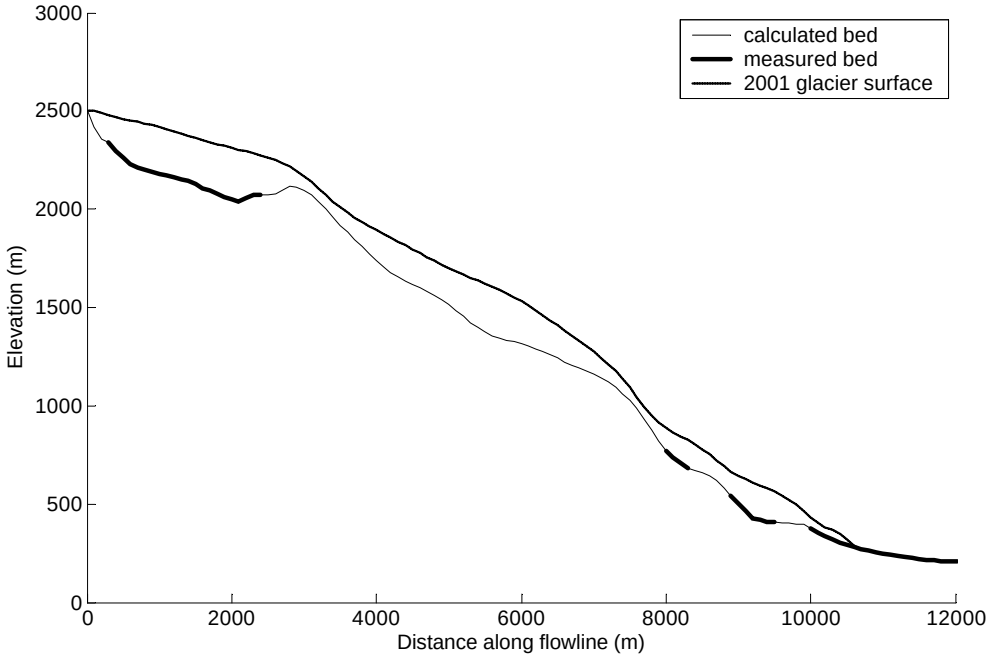

Figure 4.4. Surface and bed elevation along the velocity calculation centreline. The location of the centreline is shown in Figure 4.3.

Flow velocity in the névé increases from 0.11 m/day near the head of the glacier to 0.38 m/day at the lowest measurement sites in the névé (Figure 4.5). It is likely that the velocity then increases as the flow from the four accumulation basins converge at the head of the main icefall (6 km along the centreline), but cannot be measured by ground methods due to extensive crevassing. The nearest measured velocity is 2.3 m/day at stake L7, 7 km along the centreline. This stake is not on the glacier centreline but in the nearest accessible area, and provides the highest velocity measured on the glacier. Ice velocity reduces downglacier of the icefall to a minimum of 0.17 m/day near the terminus.

Of the previous measurements of ice velocity at Franz Josef Glacier (Table 2.1), the only study which measured ice velocity over a significant portion of the glacier surface is that of Gunn (1964). A comparison of the measurements of Gunn (1964) and measurements in this study (Figure 4.5), indicates that the general pattern of ice velocity was similar in 1956 (Gunn, 1964) and 2003 (this study). The glacier was approximately 1 km longer in 1956 than 2003 and in a retreating phase (Figure 2.1). The fact that the glacier was longer in 1956 explains why the velocities measured beyond 10 km along the centreline were higher in 1956 than 2003.

Maximum ice velocity is consistent across the four accumulation basins on line C (Figure 4.6), at approximately 0.4 m/day. The low velocities measured on the true right of the Melchior Glacier and true left of the Geikie Snowfield are a consequence of the close proximity of the glacier margins. These measurements indicate that there is little marginal slip in these areas, which suggests that the sliding velocities may also be low in the névé.

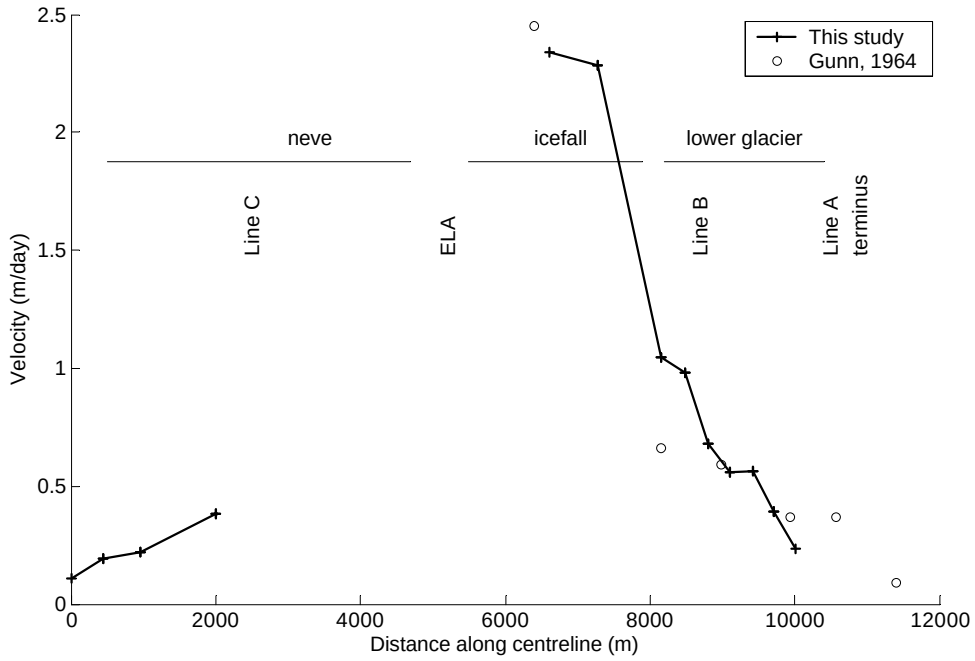

Figure 4.5. Longitudinal variations in ice velocity along the centreline shown in Figure 4.3.

On the lower glacier at line B the transverse variation is higher (Figure 4.7). Stake B5 is moving at 93% of the velocity of the central stakes, despite being only 100 m from the valley wall. This measurement indicates a high marginal slip rate. A lower marginal slip rate is evident at stake B1, which was sited in thin ice which appeared to be disconnected from the main flow through an area of extensive crevassing and has since (2003) melted. A better idea of marginal slip can be gained by examination of stake B2, which shows a velocity of 75% of the two central stakes. These high marginal slip rates indicate that sliding velocities may be high on the lower glacier

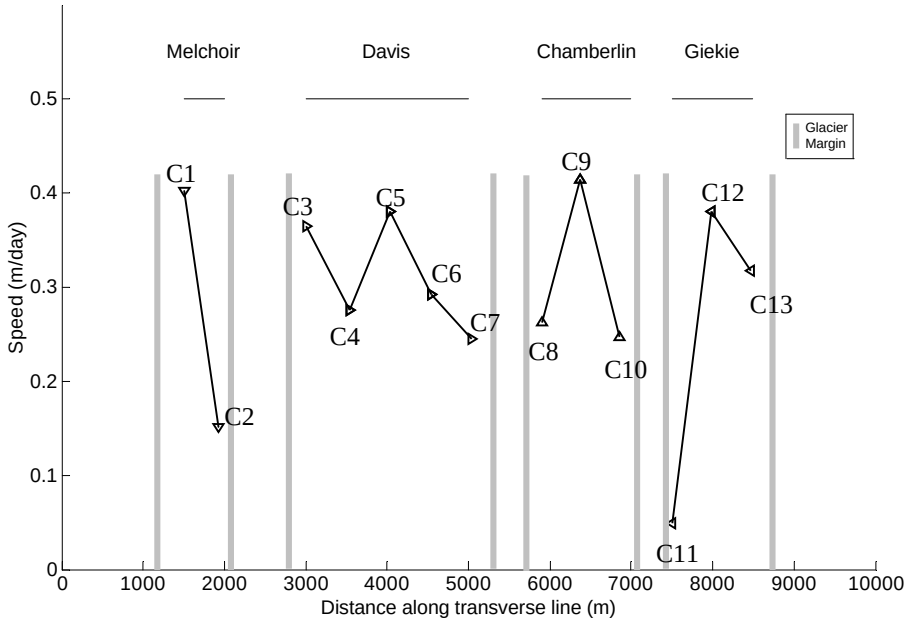

Figure 4.6. Transverse velocity variations on the glacier névé. Refer to Figure 4.2 for the locations of the transverse line C, stake labels, and the four névé basins, the Melchior Glacier, Davis, Chamberlin and Geikie Snowfields. The velocity is plotted from true left to true right.

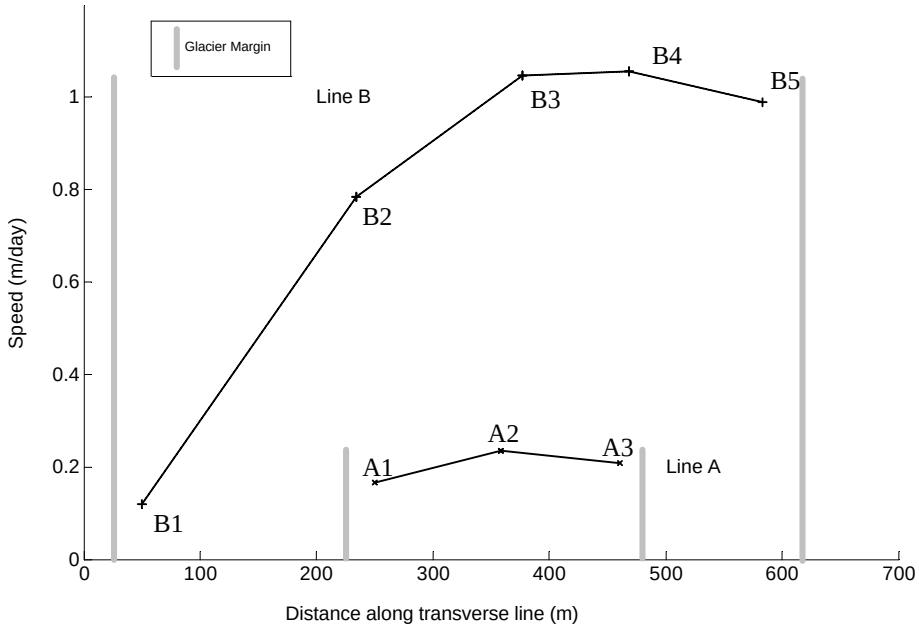

Figure 4.7. Transverse velocity variations on the lower glacier. Refer to Figure 4.3 for the locations of the transverse lines A and B and stake labels. The velocity is plotted from true left to true right.

Although there is no specific relationship between marginal and basal sliding rates (Andreason, 1983), these results indicate a high basal sliding velocity on the lower glacier, and a lower sliding velocity in the névé.

4.5 Temporal variations in measured ice velocity

Many glaciers show seasonal variations in velocity (Willis, 1995), largely as a result of seasonal changes in the amount of water available (Iken and Bindschadler, 1986; Mair and others, 2001). The large (up to 12 m/a) rainfall at Franz Josef Glacier (Figure 3.3) ensures that there is a plentiful supply of water at the bed of the glacier throughout the year, and we might expect that seasonal variations in velocity would not be as large as for other glaciers.

The spatial field of ice velocity varies continuously through time. Ice velocity measurements take a snapshot of this velocity field, averaged over the period of observation. As a consequence of this, the measured surface velocity of a glacier depends on the measurement interval – the shorter the measurement interval the greater the variation captured (Meier, 1974). Hence, there are difficulties in comparing velocities that have been averaged over different lengths of time, and the measurement interval must be considered in any interpretations.

4.5.1 Submonthly velocity variations on the lower glacier

On the sub-monthly time scale there are large variations in velocity (Figure 4.8). For example, the velocity of stake B3 was 0.66 m/day in early November 2000, but had increased to 1.34 m/day for the measurement period at the end of November 2000.

Studies of the velocity variations of other glaciers on short time scales have shown a correlation with water inputs from surface melt or rainwater (Willis, 1995, Mair and others, 2001). Ice deformation rates cannot change on such short time scales because glacier geometry does not change significantly on this time scale. Instead, these changes in velocity are most likely to be caused by changes in sliding velocities which are controlled, at least in part, by water pressure in the subglacial drainage system (Iken and Bindschadler, 1986; Iverson and others, 1995).

Different parts of the glacier have different patterns of temporal variation, and the stakes can be separated into two groups:

1. Stakes A1-A3, L1-L4, B1 and B5 show no major early season peak in velocity, rather a gradual rise in velocity through the summer (Figure 4.8a and b).
2. Stakes L5 and B2-B4 show a generally low velocity in late October, a peak in the early summer, and generally higher but less variable velocity through the summer (Figure 4.8b).

These velocity variations can be qualitatively linked with rainfall (Figure 4.8b). There was a rainfall event in late November 2000 which peaked with 125 mm of rain falling on November 25, within the period that the stakes near line B reached their maximum velocity.

Another period of heavy rainfall between December 15, 2000 and January 1, 2001 dropped 488 mm of rain. Almost all stakes on the lower glacier showed an increase in velocity during this period. The lack of dry periods during this time made GPS measurements difficult, so the velocity measurement period was 23 days, making the velocity peak appear to be smaller and broader than the November event, whereas the peak velocity may have been as high or higher.

The stakes in the first group do not show a velocity peak in November 2000, although there is a peak later, coincident with the large rainfall event in late December. Instead these stakes show steady increase in velocity through the summer. This increase in velocity may not be entirely due to sliding, but maybe due to an increase in the longitudinal strain rate caused by the velocity increase upglacier and corresponding increase in internal deformation (Willis, 1995).

4.5.2 Seasonal variations

Seasonal variations in ice velocity are examined by comparing the summer velocities from 2000/2001 with the winter velocities from 2002. The only winter velocities from the névé are from a 30 hour period in July 2002. Of the 14 stakes which had velocities measured during the winter, only 5 showed their minimum in winter (Figure 4.9). In general, winter velocities are within the short-term velocity variations evident in summer velocities (Section 4.5.1)

The velocity variation data in Figure 4.9 indicate that the Franz Josef Glacier does not show strong seasonal variation in velocity. Short-term velocity variations, probably a result of changes in water input and sliding velocity (Section 4.5.1), are larger than seasonal variations. Since seasonal velocity variations are commonly attributed to sliding velocity variations, it follows that sliding occurs year round at Franz Josef Glacier.

While glaciers often show seasonal variations in velocity (e.g. Hodge, 1974, Mair and others, 2001), this is by no means universal. For example, Jakobshavn Isbrae, Greenland, shows an almost complete lack of seasonal variation of velocity (Echelmeyer and Harrison, 1990), and the Blue Glacier, USA, shows less than 5-10% increase in the summer (Engelhart and others, 1978; Echelmeyer, unpublished cited in Echelmeyer and Harrison, 1990).

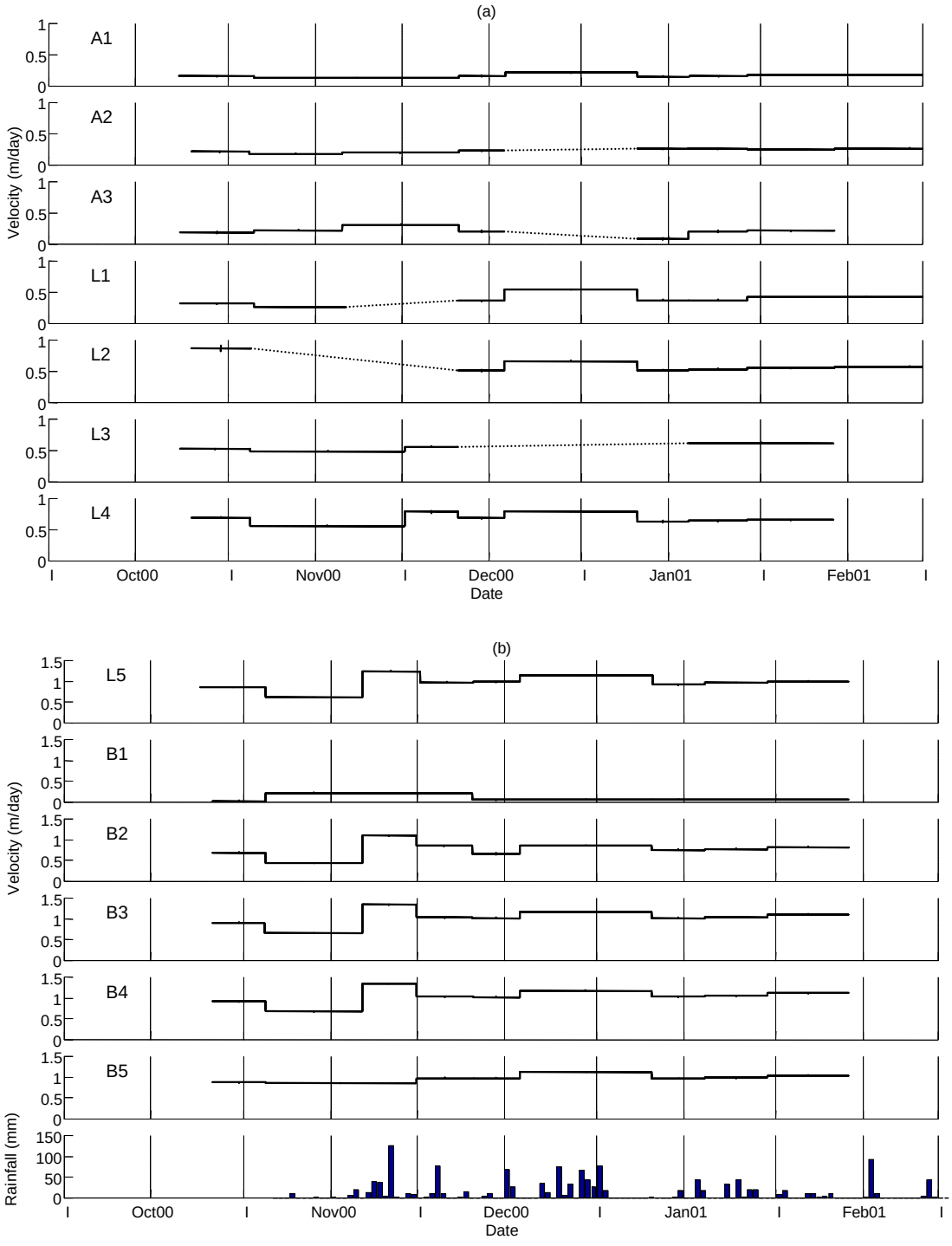

Figure 4.8. Velocity variations of selected stakes with time during the summer October 2000 – March 2001. a) stakes on line A, and the four nearest stakes on the longitudinal line upglacier. b) stakes on line B, and the stake nearest on the longitudinal line downglacier. Plotted in the lower pane of (b) is the daily rainfall total, measured with a tipping bucket raingauge at stake B3. Note that the vertical scale is different in (a) and (b). A dotted line is plotted where there is a measurement gap.

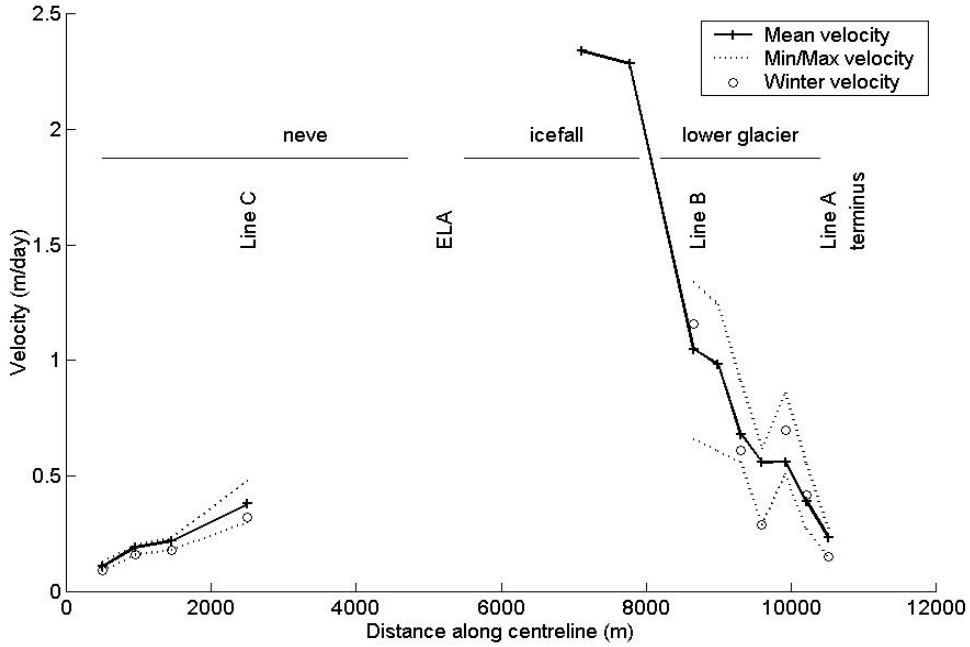

Figure 4.9. Minimum, mean and maximum velocity for each of the stakes down the centerline. Velocities for stakes which had velocity measurements during winter are also shown.

The 4 névé stakes, C5 and L9-L11, were at or near their minimum velocity during the winter measurement period (Figure 4.9). However, due to difficulties of measuring winter velocity in the névé, these measurements are based on stake displacements over 30 hours and the uncertainty in measured winter velocity encompasses the entire range of velocities measured for each stake. Hence there is no strong evidence of a winter minimum in ice velocity in the névé.

Studies on other glaciers suggest that temporal velocity variations in the névé are not due to variations in sliding velocities (Hodge, 1974; Andreason, 1983; Willis, 1995). Sliding velocity on glacier névés are generally lower and less variable, and it is expected that winter velocities may be higher than summer velocities because of increased internal deformation due to increased glacier thickness (Hodge, 1974; Andreason, 1983; Willis, 1995). Due to the non-linearity of the flow law, a small change in ice thickness can result in a large change in ice velocity.

Measurements of ice velocity in the névé through the summer months show a decrease from December 2000 to March 2001 (Figure 4.10). High-precision surface elevation measurements in the Davis Snowfield (at stakes C5 and L9-L11) indicate that ice thickness decreased 4m during the summer from a measured maximum in November/December 2000 to a minimum in March 2001. Glacier thickness varies between

150 m at L11 and 250 m at C5 in this area (Figure 4.4). Equation (1) indicates that internal deformation velocity varies with the fourth power of thickness; hence a 4 m thinning would result in an 11% decrease in deformation velocity at L11 and 8% at C5. The timing of the thickness change is in general agreement with the timing of the velocity change, except for the winter velocities which have large uncertainties associated with them. The winter velocities were measured during a short period in July, a time when the winter snowpack was still shallow. At this time the Davis Snowfield had thickened by about 3 m since February, which should result in an increase in velocity of about 5 - 8%. This increase is not shown in the data, but is within the uncertainty of the measurements.

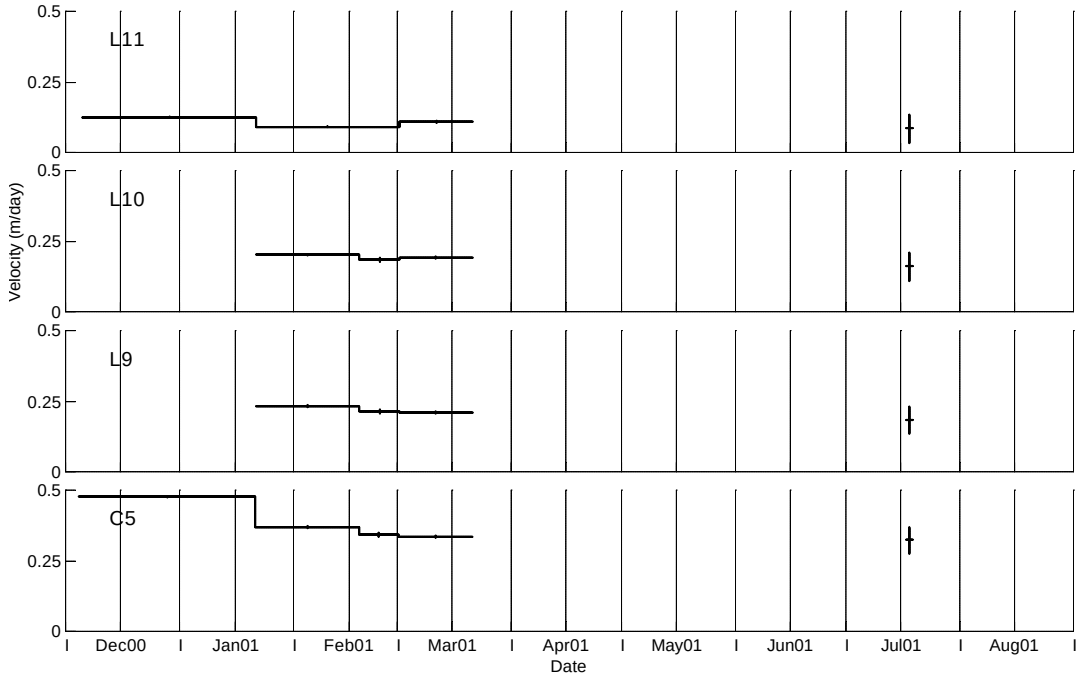

Figure 4.10. Velocity measurements from the névé. The measurements plotted in July 2001, were made in July 2002, but are plotted 1 year earlier for comparison with summer measurements from 2000/2001.

Measured velocity of the stakes in the névé varies by 10% at L11 and 25% at C5 (Figure 4.9), more than can be explained solely by internal deformation rate changes. Hence variations in sliding velocity do play a role in velocity variations in the névé.

The analysis of temporal variations of ice velocity at Franz Josef Glacier indicates that sliding occurs throughout the year. Temporal variations in ice velocity on the lower glacier in summer are clearly linked to water inputs (Figure 4.8) and are therefore a result of varying sliding velocities. Four out of six winter velocity measurements on the lower glacier are higher than the summer minimum velocities (Figure 4.9),

indicating that sliding must also be a significant component of winter velocities on the lower glacier. In the névé, a calculation of the variation in velocity due to ice thickness changes indicates that not all of the measured variability is a result of changes in internal deformation rates, indicating that there is a variable component of ice movement which must be basal sliding. Since there is only weak evidence for a winter minimum in velocity in the névé, and this minimum is partly a result of thickness changes it follows that there is probably year round sliding in the névé as well. The temporal variations in velocity also indicate that here is no strong seasonal pattern to measured velocities.

4.6 Ice velocity modelling

Having established the general patterns of ice velocity at Franz Josef Glacier, the next objective is to determine the values of the deformation parameter f_d in equation (1) and the sliding flow parameter f_s and exponent q in equation (5) which best model measured ice velocity patterns. We can then quantify the proportion of surface velocity which results from internal deformation and that which results from basal sliding.

4.6.1 Tuning flow parameters

The flow parameters f_d and f_s and flow exponent q are tuned so that the modelled velocities match the measured velocities. Equation (1) is used to calculate velocity due to internal deformation, including longitudinal stresses (equation 4), and equation (5) to calculate sliding velocities. The parameters values $f_d = 1.5 \times 10^{-24}$ $Pa^{-3}s^{-1}$, $f_s = 4.5 \times 10^{-20}$ $Pa^{-3}\,m^2\,s^{-1}$ and exponent $q = 3$ result in a generally good match between modelled and measured velocity (Figure 4.11).

The only major discrepancy is the velocity maximum at 6 km along the centreline where calculated velocity is approximately 10% less than measured velocity. There are a number of possible reasons for the difference:

- Ice thickness has not been measured here and the calculated ice thickness may not be realistic,
- The long and steep icefall results in longitudinal stress decoupling. The velocity comparison with and without the longitudinal stress calculation (Figure 4.13) indicates that stress decoupling in the ice fall would result in velocities 12% higher, matching the measured velocity peak value, but upstream of the measured peak.
- The may be enhanced sliding in the icefall because of its length and steepness, which cannot be accounted for with a constant sliding parameter f_s.

The relatively small departure from measured velocity does not warrant special treatment of the icefall area to account for these possibilities. Overall, the root-mean-square (RMS) difference between modelled and measured ice velocity is 4%

The choice of flow parameters is constrained by the different dynamics of the névé and lower glacier. The different proportions of sliding velocity to total velocity in these two areas means that there is no other choice of flow parameters which simulates the measured velocities as well as those chosen here.

These velocity calculations suggest that most of the glacier surface velocity is a result of basal sliding for almost all of the glacier length (Figure 4.11). This is especially so in the icefall and near the terminus (from 6 - 11 km along the centreline) where almost all of the surface velocity is a result of basal sliding.

The deformation and sliding equations (1) and (5) can be used to calculate velocities averaged over a period of several months. Shorter term variations cannot be captured because the effective pressure *N* has been neglected by taking *r*=0 in equation (5).

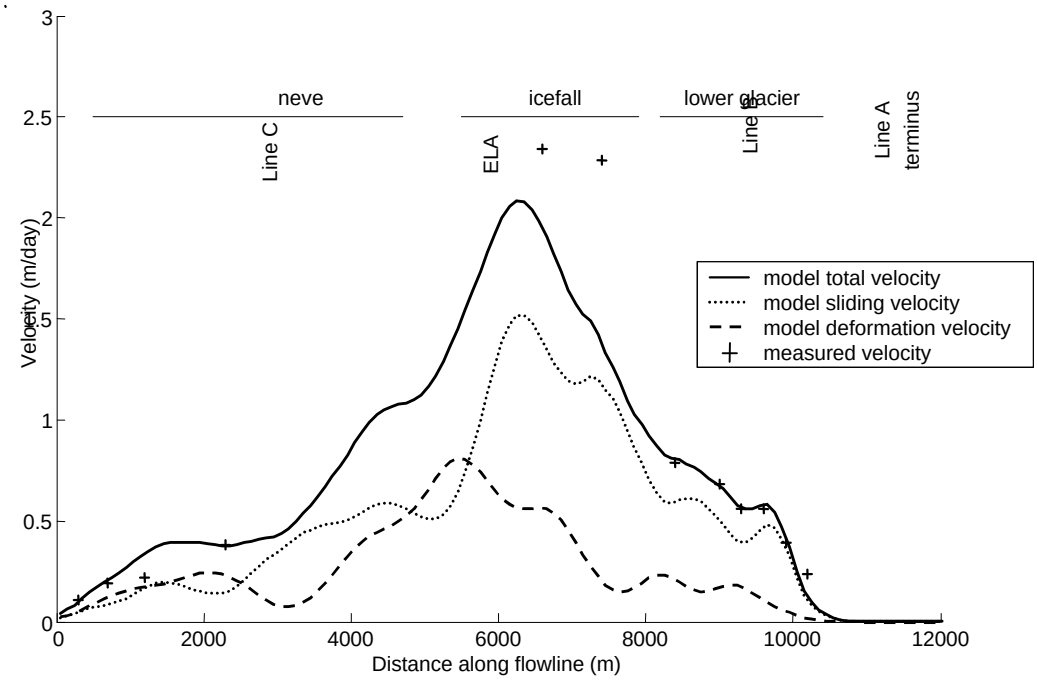

Figure 4.11. The velocity calculated along the glacier length.

The velocities calculated by the model in this study, Ruddell (1995) and Oerlemans (1997b) are now compared (Figure 4.12). The velocity modelled by Ruddell (1995) is erratic and shows little correspondence with measured velocity. The velocity modelled by Oerlemans (1997b) is better, with a reasonable general agreement, which would be closer if his model glacier was the same length as the 2001 glacier for which the velocity measurements are made. However, the low velocities in the névé predicted by Oerlemans (1997b) are a result of the single flowline used which has a large width and therefore low

velocity for the same ice flux. The model velocities calculated in this chapter fit measured ice velocities better than either Ruddell (1995) or Oerlemans (1997b).

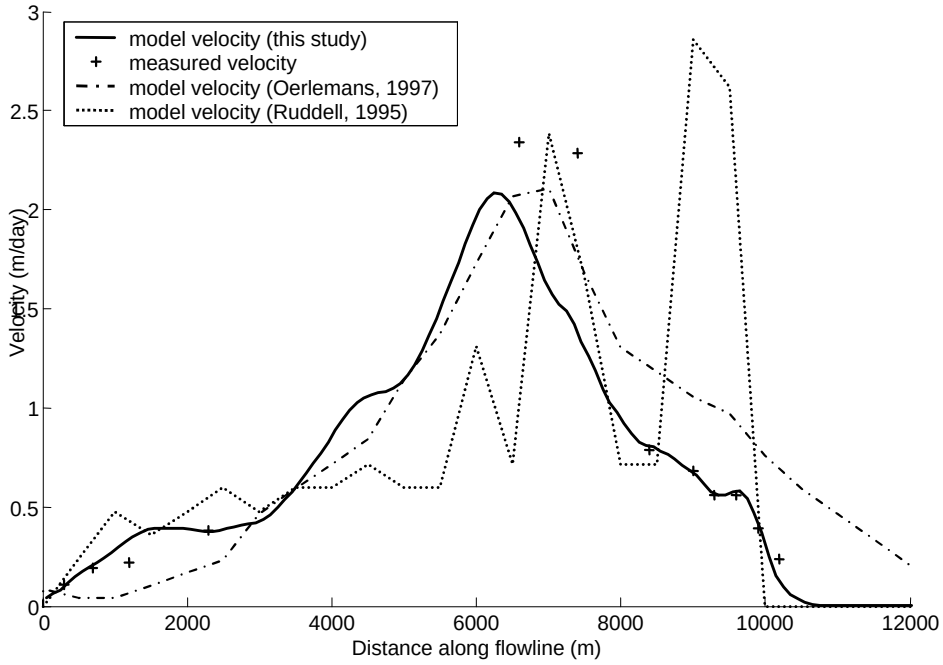

Figure 4.12. A comparison of model velocities from this study with that of previous studies.

4.6.2 The role of longitudinal stresses

The velocity calculation described above includes the effects of the longitudinal deviatoric stress t'_{xx}. The velocity calculation using just the driving stress approximation (equation 3) is compared in Figure 4.13. The driving stress approximation results in velocity variations which are unrealistic when compared to observations, while the calculation including longitudinal stresses shows a much smoother and more realistic velocity profile which fits the measured profile well. The smoother velocity profile is partly a result of smoothing required to make the longitudinal stress calculation converge.

(a)

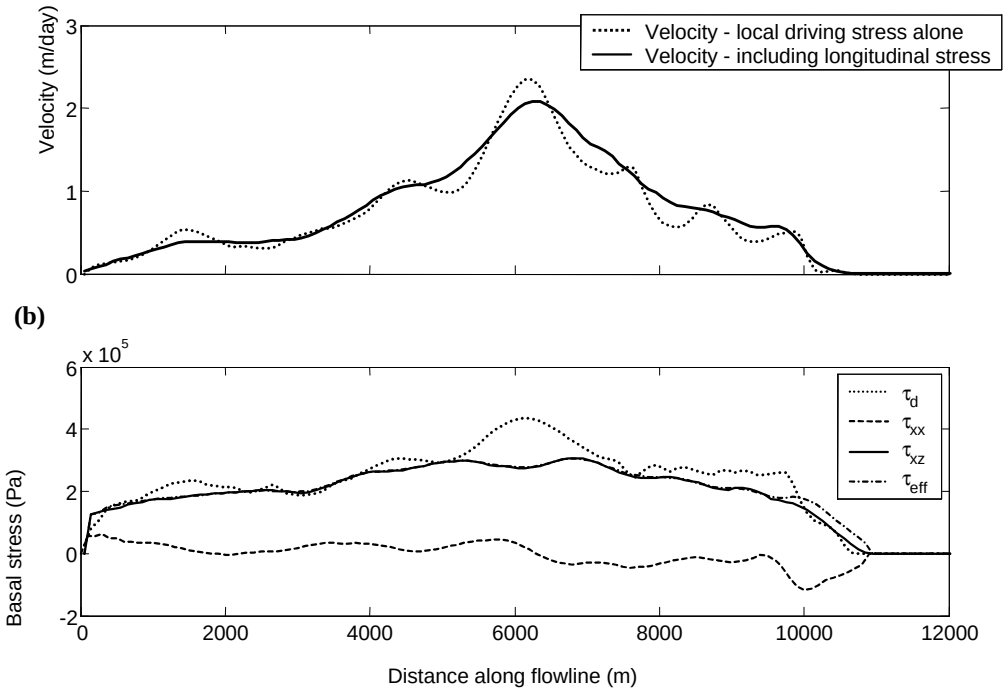

Figure 4.13. Stresses and velocity calculated along the centreline. (a) the velocity calculated using the driving stress alone is compared to velocity calculated including longitudinal stresses. (b) the magnitude of the various stresses calculated by the model; t_d is the driving stress as calculated in equation (2), t_{xz} includes the effects of the longitudinal stress t_{xx}, which along with the effective stress t_{eff} is defined by Hubbard (2000).

The longitudinal stress is small compared to the driving stress except for between 10 km and 11 km along the flowline (Figure 4.13) where it becomes greater than the driving stress. This result is comparable with the results of Hubbard (1997, 2000) who found that longitudinal stress became greater than local driving stress near the terminus. This result indicates that longitudinal stress should be incorporated into flow models for this, and other mountain glaciers.

4.7 Conclusion

The lower part of Franz Josef Glacier experiences significant velocity changes on short time scales (Figure 4.8). In November 2000 ice velocity doubled in the centre of the glacier below the main ice fall between the first and second halves of the month. These variations in velocity are ascribed to variations in sliding velocity resulting from changes in subglacial drainage. Short-term velocity variations are greater than seasonal variations (Figure 4.9). The lack of a systematic and widespread seasonal velocity variation and lack of a winter minimum in velocity indicates that sliding occurs throughout the year on the lower glacier.

In the névé, there is weak evidence for a winter minimum in velocity (Figure 4.10), and most of the seasonal velocity variation is the result of changes in internal deformation rates as the glacier thickness changes during the year. However, changes in internal deformation do not explain all of the measured variation in ice velocity, indicating that there is year round sliding in the névé as well.

These temporal variations in glacier velocity indicate that sliding velocity is low in the névé, and high on the lower glacier, although there are not enough field data to quantify the proportions of surface velocity resulting from basal sliding and from internal deformation.

To quantify the spatial patterns of sliding and internal deformation in the glacier, velocities are modelled using equation (1), for internal deformation and equation (5), the generalised sliding law (Figure 4.11). Measured velocity of the glacier was simulated with an RMS error of 4%, using the flow parameters f_d = 1.5×10^{-24} $Pa^{-3}s^{-1}$, f_s = 4.5×10^{-20} $Pa^{-3}\,m^2\,s^{-1}$. This choice of parameters is well constrained by the different proportions of sliding in the névé and lower glacier. Sliding makes up about half of the surface velocity in the névé, but as the glacier thins and steepens towards the terminus, the sliding proportion increases and makes up almost all of the surface velocity near the terminus. This result is consistent with measured temporal variations in ice velocity, which indicate a significant sliding velocity in the névé, and highly variable velocity on the lower glacier.

There are a lack of measurements of velocity between 3000 and 6000 m along the flowline. Future work could remedy this by using remote methods of measurement. These methods might include theodolite measurement of serac displacement (Ruddell, 1995) or feature tracking from repeat satellite imagery (Kääb and others, 2003).

We neglected the effect of subglacial sediment deformation on glacier motion in this analysis. Modelled velocity matches the patterns of measured velocity well (Figure 4.11), suggesting that sediment deformation is of little importance overall, or if it does exist it can be sucessfully modelled using equations (1) and (5).

The inclusion of a longitudinal stress calculation using the 'ice-stretching' approximation (Hubbard, 2000) changes the calculated ice velocity significantly, removing the large variations in velocity apparent when velocity is calculated using a basal shear stress calculated from local surface slope. The modelled velocity then matches the measured velocity much more closely. Despite the significant changes in overall ice velocity profile, the only area where the longitudinal stress is large is near the terminus. It is apparent that longitudinal stresses play an important role in the dynamics of Franz Josef Glacier and should be included when calculating glacier velocities.

The model described in this chapter successfully captures the dynamics of the Franz Josef Glacier. The correspondence between measured and modelled ice velocity is close. Combined with the mass balance model constructed for Franz Josef Glacier in Chapter 1, we can now examine the response of the Franz Josef Glacier to climate change with confidence.

5 Response of Franz Josef Glacier *Ka Roimata O Hine Hukatere* to climate change

5.1 Introduction

With the results of the previous two chapters we have a mass balance model verified with field measurements and an ice-flow model tuned to present-day measured ice velocity. In this chapter these models are coupled to evaluate the response of Franz Josef Glacier to climate change.

Previous attempts to link past climate changes to advance and retreat of Franz Josef Glacier have not been very successful. Early studies attempted to separate the effects of temperature and precipitation on glacier advance and retreat (Suggate, 1950, 1952; Soons, 1971; Hessell, 1983; Gellatly and Norton, 1984; Brazier and others; 1992), but none found a convincing relationship. Woo and Fitzharris (1992) applied a mass balance model using both temperature and precipitation as input data, and compared terminus position to mass balance variations in a qualitative way. A quantitative link between climate and terminus position was established by Ruddell (1995) who applied an ice-flow model to an independently calculated mass balance series. However, the results of these models have been demonstrated to be unrealistic, with Woo and Fitzharris (1992) overestimating accumulation by a factor of 2 and Ruddell (1995) overestimating ablation by a factor of 2 (Chapter 1).

A major goal of understanding past glacier variations is to allow us to predict future glacier variations. Little work has been done on the expected future variations of New Zealand glaciers. Ruddell (1995) predicted a loss of 80-90% of glacier ice in New Zealand over the next 100 years. Oerlemans and others (1998) predicted a reduction in volume for the Franz Josef Glacier of 40%, although that was based on an overestimate of mass balance and a climate warming greater than expected for New Zealand. With the recent availability of future climate scenarios for the next century (IPCC, 2001) which have been regionally downscaled (Mullan and others, 2001) it is time for the future behaviour of Franz Josef Glacier to be re-examined.

The objective of this chapter is to examine the response of the Franz Josef Glacier to climate change in the past and in the future. Specific goals are to:

1. Test the ability of a coupled mass balance - ice-flow model to simulate glacier behaviour for the period of reliable local climate data, from 1894-2003,
2. Predict short-term future glacier behaviour using the current (2003) dynamic state of the glacier, and

3. Predict long-term glacier behaviour to 2100 using future climate scenarios constructed within the IPCC framework.

These objectives will be realised by the application of a coupled mass balance - ice flow model to the Franz Josef Glacier. This model will be verified by comparison with the record of terminus position. The mass balance input to the model is derived from a degree-day mass balance model constructed in Chapter 1 which has been verified with mass balance and climate measurements. Ice thickness and temporal and spatial variations in ice velocity have been measured in Chapter 1 and provide input and tuning data for the model.

5.2 Ice-flow model

The ice flow model used in this study is a simple one-dimensional flowline model solved on a finite difference grid. The model is an improvement over those used previously on Franz Josef Glacier, by the use of measured ice thickness, multiple flowlines, the calculation of longitudinal stresses and the use of a 100 m grid spacing. Velocity measurements in Chapter 1 provide a sound basis for flow parameter choice.

The required inputs for the model are an initial glacier geometry, and mass balance to force the model. The outputs are ice thickness changes, terminus position and ice velocity.

5.2.1 Description

The dynamic behaviour of the glacier is described in terms of changes in ice thickness which are calculated from a continuity equation (Paterson, 1994). Glacier velocity is calculated from basal shear stress with contributions from internal deformation and basal sliding, which has previously been described in Section 4.2.

The glacier cross-section *S* is represented by a trapezium, described by the ice thickness, *H* the width of the bed w_b, and the slope of the valley sides θ , here taken as being equal on both sides (Figure 5.1)

The width at the surface w_s is given by:

$$w_s = w_b + 2\tan\theta \qquad (1)$$

and the surface area of the trapezium *S* by:

$$S = H(w_b + H\tan\theta) \qquad (2)$$

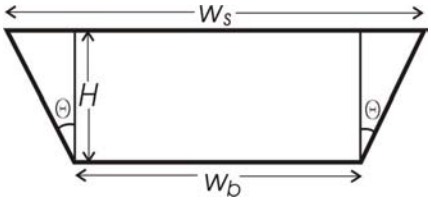

Figure 5.1. Glacier cross-section representation.

Assuming constant density, the continuity equation is integrated over the transverse cross-section to give the change in cross-section area due to mass balance and ice transport (Paterson, 1994):

$$\frac{\partial S}{\partial t} = \frac{\partial}{\partial x}(US) + w_s B \qquad (3)$$

where B is the specific mass balance, t is time, x is in the direction of flow and U mean velocity through the cross-section. The equation is reformulated in terms of ice thickness change by substituting (2) into (3) (Budd and others, 1979; Paterson, 1994):

$$\frac{\partial H}{\partial t} = \frac{1}{w_b + 2H \tan q} \frac{\partial}{\partial x}(US) + B \qquad (4)$$

where U and S both depend on H. The mean cross-section velocity U is calculated as described in Section 4.2, using equations (4.1) and (4.5), and includes the effect of longitudinal stresses.

Equation (4) is solved on a staggered finite difference grid using a forward explicit time step. The time step is controlled by the stability condition:

$$\Delta t \le \frac{\Delta x^2}{2n \max D} \qquad (8)$$

where x is oriented in the direction of flow, Δx is the grid spacing and

$$D = \frac{HU}{\sin a} \qquad (9)$$

is the effective diffusion (Hindmarsh, 2001). The time step Δt changes with changing glacier geometry and is typically 0.02 a, or approximately 7 days.

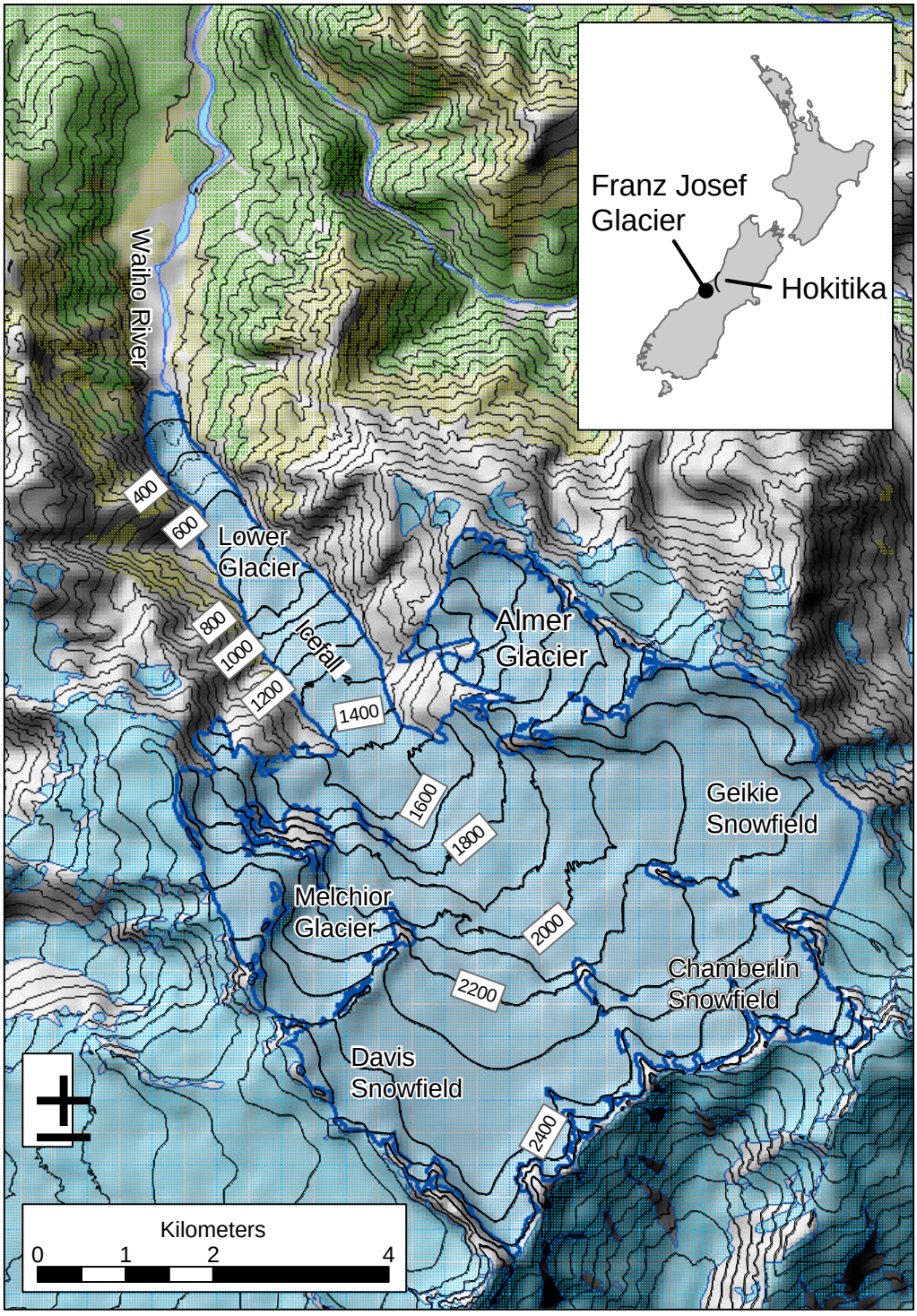

Figure 5.2. Franz Josef Glacier and its location in the South Island. Contours are at 100m intervals.

5.2.2 Model configuration

It is reasonable to parameterise the shape of the tongue of the glacier using a single flowline because of its relatively simple geometry. However, the rest of the glacier is more complicated, with the névé of the Franz Josef Glacier being comprised of three major basins, and another three glaciers join or nearly join the glacier further downstream near 1600 m a.s.l. (Figure 5.2). In order to account for such complex geometry, a common scheme is to use more than one flowline (Greuell, 1992; Zuo and Oerlemans, 1997), and this approach is followed here. Six flowlines are defined for the Franz Josef Glacier (Figure 5.3), one main flowline and 5 subsidiary flowlines. The boundary condition at the head of all but one of these flowlines is zero thickness where the flowline starts on steep mountain sides. The flowline for the Geikie Snowfield has a zero flux condition at the head as it begins at an ice divide. Flux in the last segment of each of the subsidiary flowlines is converted to a change in ice thickness and distributed to the adjacent grid points in the main flowline.

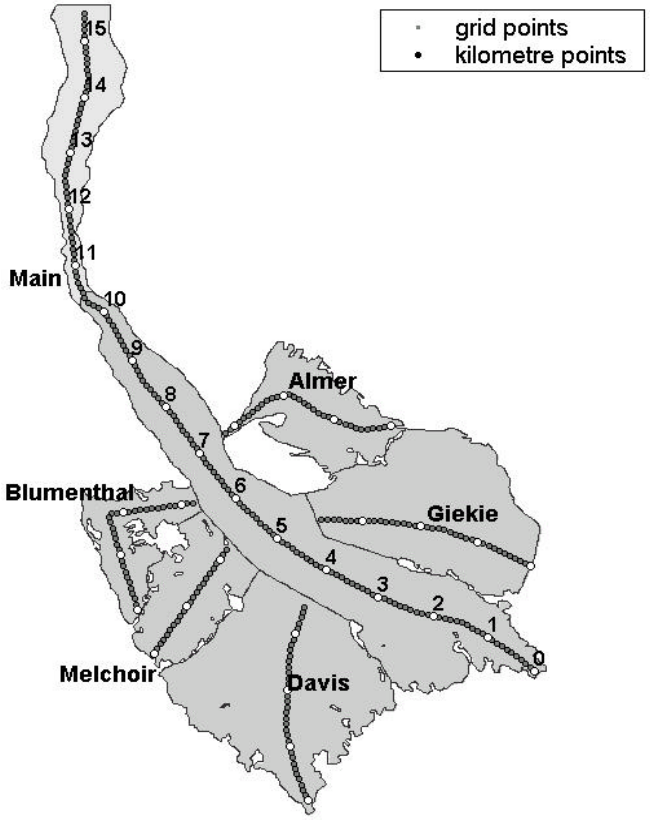

Figure 5.3. The flowlines used to parameterise the glacier geometry. Grid points are every 100 m, and kilometres from the glacier head are marked. The main flowline is not glacierised past 10.5 km (1986), and the Almer flowline is not glacierised after 3 km. In these cases the width of the flowline is defined by the width of the valley floor.

5.2.3 Input Data

The input data required for the model described above are the glacier geometry and mass balance. Glacier geometry is defined by the surface elevation h, the bedrock elevation b (Figure 5.4), the glacier width w_s and w_b, and the valley side slopes q . These data have been calculated from a 1:50 000 map as described in Section 4.3.2.

As the ice-flow model is now integrated through time, the mass balance B is required for the model at each grid point and each time step. The mass balance is calculated using a degree-day model which has been constructed for the Franz Josef Glacier and is explained in detail in Chapter 1. In this chapter mass balance changes are described by changes in elevation of the end of summer snowline (EOSS).

5.2.4 Model tuning

In addition to the input data detailed above, the flow parameters f_d and f_s also have to be determined for the model. Present-day (2000-2002) glacier velocity has been measured in Chapter 1 and flow parameters tuned to fit the velocity distribution. A good match between modelled and measured ice velocity was found when the flow parameters are set to $f_d = 1.5 \times 10^{-24}$ $Pa^{-3}s^{-1}$ and $f_s = 4.5 \times 10^{-20}$ $Pa^{-3}\,m^2\,s^{-1}$.

5.3 Past glacier response

The mass balance model described in Chapter 1 and ice flow model described in Chapter 1 have been constructed with present day (2000-2003) measurements of climate, mass balance and ice velocity. We now test the coupled mass balance - ice flow model for the period of long-term climate and terminus position records, 1894-2003, to assess whether together they can simulate glacier processes on a longer time scale.

The Franz Josef Glacier has a good record of terminus position since 1893 (Chinn, 1989; Ruddell, 1995; this study), and mass balance has been reconstructed since 1894 (Section 3.9.3). In order to test the coupled model, the mass balance reconstruction is used to drive the flow model, and the resulting modelled terminus position compared with the measured record. As a first step in this test, a dynamic calibration is performed which ensures that the glacier is in the correct dynamic state before the coupled model is used (Oerlemans, 1997b).

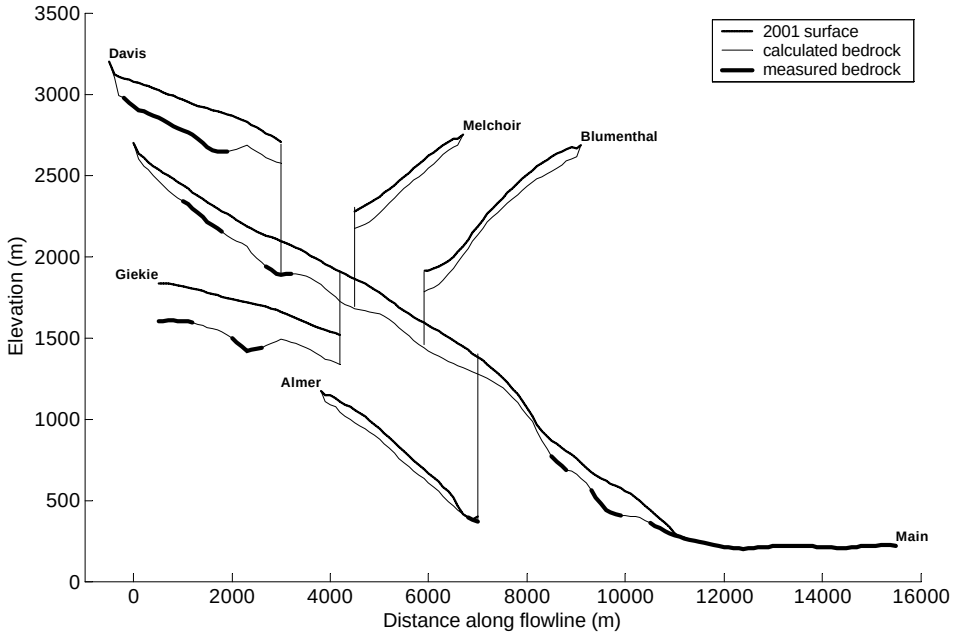

Figure 5.4. Surface and bed elevation of each of the flowlines. Note that the plotted elevation of the tributary flowlines has been adjusted for clarity, and the point of connection shown with a vertical line.

5.4 Dynamic calibration

The purpose of dynamic calibration is to ensure that at the start of the period where the mass balance and ice flow models are coupled the glacier is in the correct dynamic state, rather than assuming an equilibrium state. Dynamic calibration is a simple form of inverse modelling where a mass balance record is reconstructed from a terminus position record using an ice flow model. Typically a trial and error approach is taken to match a long-term, low temporal resolution, terminus position record by using a few step changes in mass balance (Oerlemans, 1997b; Mackintosh and others, 2002) and this approach is taken here.

The terminus position record (Figure 5.5) for the dynamic calibration starts with the revised LIA chronology for Franz Josef Glacier of McKinzey (2001) and includes the measured terminus position records from 1867 (Chinn 1989) and 1893 (Harper, 1894).

The flow model is driven by varying the mass balance. The year to year changes in mass balance can be approximated by shifting the mass balance curve vertically (Oerlemans, 1997a), and the mass balance curve is defined by a quadratic (Fountain and Vecchia, 1999):

$$B(z) = 4.3 \times 10^{-6} z^2 + 0.025 z - 31 \qquad (11)$$

which has been fitted to the mass balance measurements from 2000-2003 (Chapter 1).

The model glacier is run to equilibrium at the LIA 1 stand, before a series of step changes in mass balance is imposed on the model to simulate the glacier retreat up to 1894, the start of the reconstructed mass balance record. The required changes in mass balance (expressed as changes in EOSS) and resulting modelled glacier length in Figure 5.5 indicate that 11 step changes, found by trial and error, are sufficient to reconstruct the length record from 1495 to 1894, and that the model glacier is then in the correct dynamic state for the start of the coupled mass balance - ice-flow model integration from 1894 to 2003.

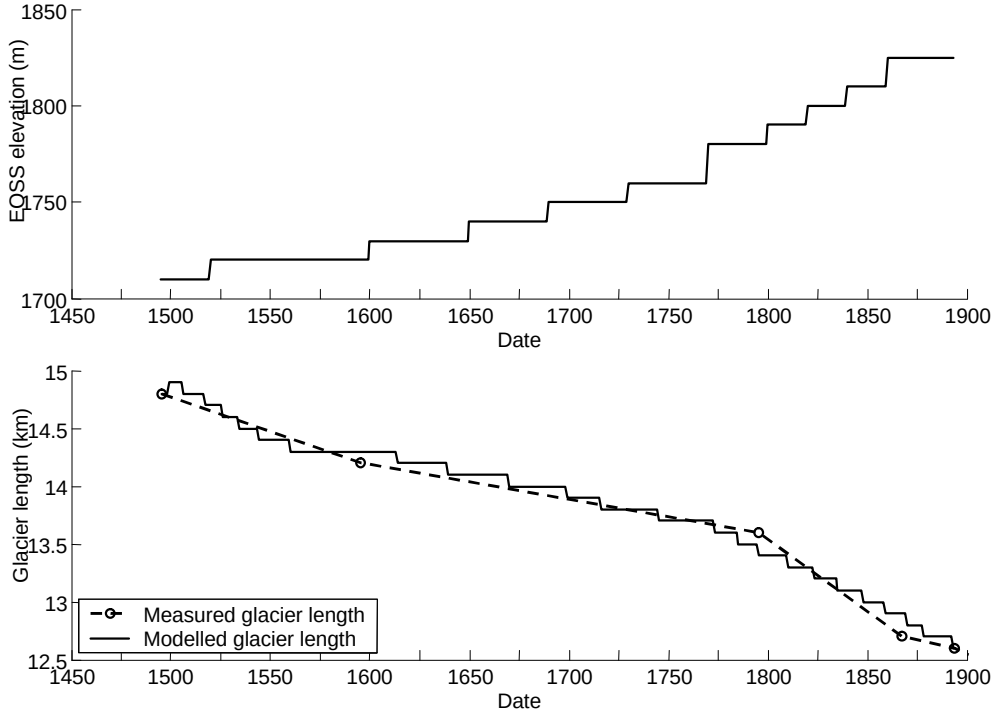

Figure 5.5. Dynamic calibration of the Franz Josef Glacier ice flow model. The EOSS perturbation in the upper plot is constructed to drive the model for the period 1480-1894 in such a way that the resulting glacier length, plotted as the continuous line in lower plot, matches the measured length record, plotted as the dashed line in the lower plot.

5.5 Coupled mass balance - ice-flow model 1894-2003

The ability of the coupled mass balance - ice-flow model to simulate the recorded variations of the glacier from 1894 to 2003 is now tested. The annual mass balance for the Franz Josef Glacier has been reconstructed from 1894 to 2003 (Section 3.7) and is expressed as an EOSS variation in Figure 5.6. The model starts in 1894 with the glacier geometry previously defined by the dynamic calibration, and run forward in time to 2003.

The coupled glacier model does not simulate the recorded glacier length well (Figure 5.6). The glacier advances from its state at the end of the dynamic calibration in 1894 immediately once the modelled mass balance is applied, and the advance continues for approximately 1400 m. The five year running mean of the EOSS forcing (Figure 5.6a) shows a marked lowering of the EOSS (increased mass balance) in the 1940s, but the model does not reflect the measured advance in the late 1940s, although the retreat does slow. Similarly, the subsequent periods of EOSS lowering in the 1960s and 1980s are not sufficient to make the model glacier advance, although advances were recorded for the glacier. The measured general retreat of the glacier is paralleled by the model glacier length, with the model glacier approximately 1500m longer than measured. Towards 1995 the measured and modelled glacier lengths converge.

The major problem with the model appears to be an unduly positive mass balance in the early part of the simulation. The problem is ascribed to the mass balance model rather than the ice flow model, since the uncertainties in the mass balance model are much greater than in the ice flow model. In order to test whether the model works for the later half of the simulation, an attempt was made to run the model from 1935, and then 1955, to 2003 after a short dynamic calibration. In both cases the glacier model advanced significantly, despite being starting in a retreating phase and maintained the 1 500 m difference between measured and modelled glacier length until 1985 where it begins to converge with the measured length.

It is clear from Figure 5.6 that modelled mass balance must be close to correct from 1995 onwards as the glacier length is close to that measured. Hence it appears that the coupled mass balance – ice flow model works well for present day conditions. Without measurements of mass balance before 2000, there is no way to test definitively whether the mass balance model predicts past mass balance accurately. The strongest test we have is the coupled glacier model, which strongly suggests that past mass balance is not accurately modelled.

The reasons for the poor modelling of past mass balance can only be speculated at. The problem almost certainly relates to the stability of model parameters through time. Since the main sensitivity of the model relates to precipitation variation with elevation (Section 3.5.3) this relationship is an obvious candidate for examination. The glacier is known to respond to changes in circulation patterns including the strength of the westerly flow and orographic precipitation (Fitzharris and Hay, 1989; Fitzharris and others, 1992). It is quite possible that the peak in precipitation identified in Section 3.4.1 moves up and down glacier with varying strength of the westerly flow. This would have quite a large effect on mass balance, but is difficult to model since even long term mean precipitation is not entirely known, let alone annual or decadal changes.

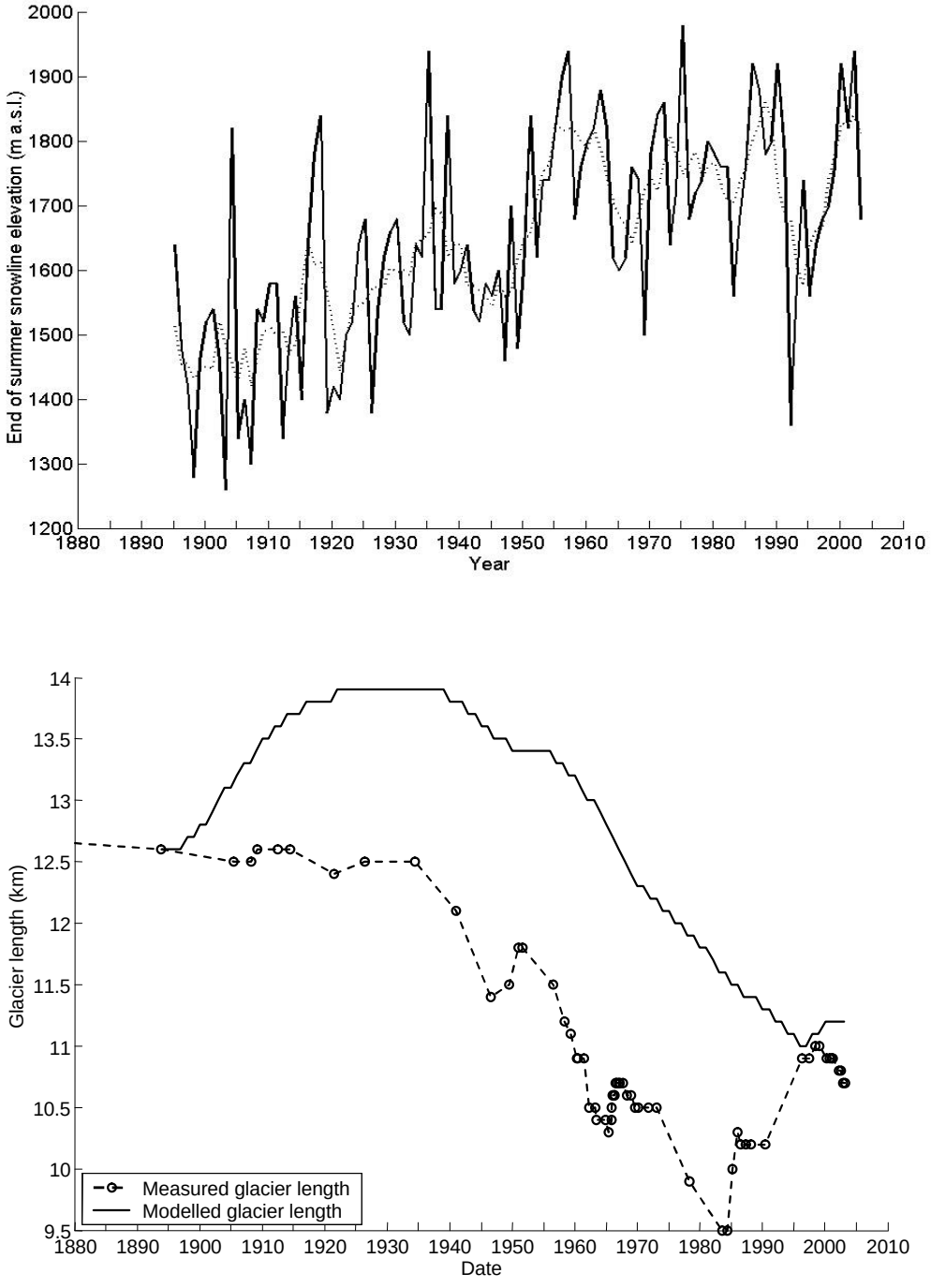

Figure 5.6. (a) The mass balance, expressed as EOSS, calculated from Hokitika climate data (Section 3.7) and used to drive the flow model. The dotted line is a five-year running mean. (b) The modelled and measured glacier length.

Another possibility is highlighted in Section 3.5.2 where a single June rainfall event that occurred in Franz Josef Village, but not in Hokitika, resulted in the significant difference in the total glacier mass balance calculation of 0.66 m/a w.e. The Hokitika climate data may simply not contain the signals required to reconstruct mass balance precisely, because of the spatial variability of precipitation. A possibility here for future work is to include precipitation data from Milford Sound, over 300 km to the south (for location see Figure 3.1), which may show correlate more closely with Franz Josef Village precipitation in some weather conditions.

5.6 Future prediction

Predicting the future is an uncertain business, and dealing with the uncertainty is a central issue in making future predictions of glacier advance and retreat (Van der Veen, 2002). Ideally, one would construct a probability density function which indicates the probability of any particular outcome occurring (Van der Veen, 2002). This approach is taken here when predicting the short-term (10 year) future behaviour of the glacier based on the present day geometry of the glacier.

For longer term predictions (100 years), the long-term changes in mass balance are important and future glacier behaviour projections are based on future climate projections. The uncertainty in future climate projections is managed by the use of scenarios, which cover a range of possibilities, but give no indication of the probability of any particular scenario occurring. Because of this limitation in the input data, a probability density function of future glacier behaviour cannot be constructed (Van der Veen, 2002), and so a series of glacier behaviour scenarios are constructed.

5.6.1 Short-term future prediction

Having established that the coupled mass balance - ice flow model at least captures the present day processes of mass balance and ice flow at the glacier (Figure 5.6), the third objective, to assess the short-term future behaviour of the glacier, is addressed.

The theory behind dynamic calibration is that the evolution of glacier geometry through time depends not only on the mass balance but also on the dynamic state of the glacier at the start of the period (Oerlemans 1997a). Here we ask the question: for what period of time can we predict the future behaviour of the glacier from the present day dynamics alone, and as a corollary: when does the mass balance signal become important? We use this dynamic constraint to predict the future behaviour of the glacier for a short time into the future without making any assumptions about the mass balance in that period, although clearly the mass balance must stay within the bounds of its interannual variability.

A short dynamic calibration procedure (as in Section 5.4) is performed for 1983-2003, a period at least as long as the 16-20 year response time of the glacier (Oerlemans 1997b, 2001). Measurements of surface

elevation and terminus position during 2000-2003 are used to ensure that the glacier model is in as close a state to the measured state of the glacier as possible in the dynamic calibration process. A Monte Carlo simulation is then performed, where the model is then run for a further 10 years to 2013, with the mass balance for each year specified as a random choice of one year of the climate normal period, 1970 – 1999, which is considered to be the 'present day' climate. The model is run in this way a large number of times, in order that the probability distribution of the short-term future behaviour of the glacier be determined, which for some time into the future is independent of the mass balance.

We can also use this process to determine the short-term future behaviour of the glacier if we do make some assumptions about climate changes in the next 10 years. The greatest influence on inter-annual climate, and therefore mass balance, variability is due to the El Niño southern oscillation, ENSO, (Mullan and others, 2001). A strong relationship between the southern oscillation index (SOI) and Franz Josef Glacier retreat and advance has been found (Fitzharris and others, 1997; Hooker and Fitzharris, 1999). Another, longer term climate oscillation, the Interdecadal Pacific Oscillation occurs on a 20 year timescale. A positive IPO index results in more El Niño (negative SOI) events (Figure 5.7), and the variability due to the IPO is within the variability of ENSO.

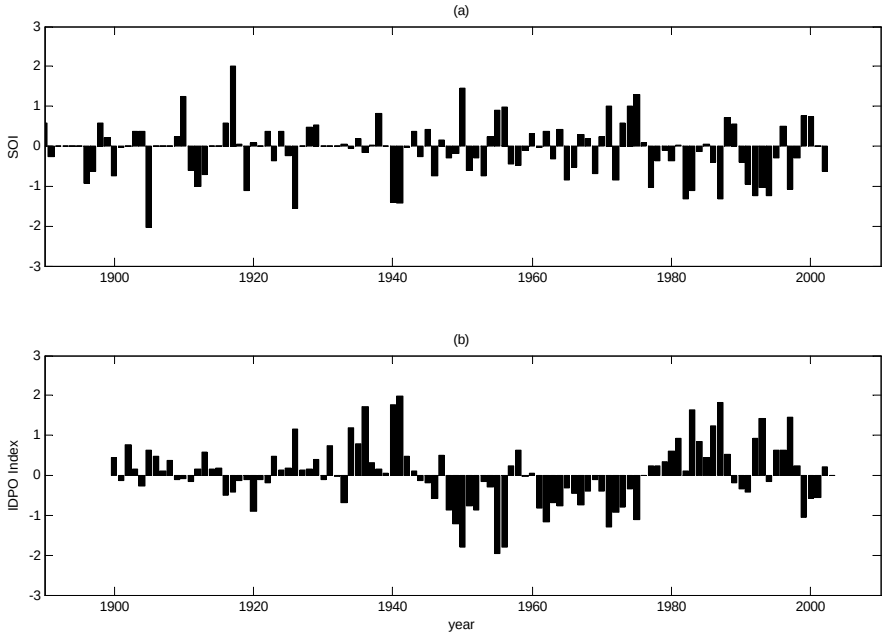

Figure 5.7. The SOI and IDPO index from 1890 to the present. *Source* Mantua (2003) and Shea (2003).

It is not possible to predict the future behaviour of ENSO more than a few months in advance (van Oldenborgh, 2003). A simple way to examine the possible short-term future glacier behaviour under positive or negative SOI scenarios to is run the Monte Carlo simulation again, with mass balance series

chosen only from years in the period 1970-1999 where the SOI is positive or negative. For the case where the model is run with a free choice of mass balance from the period 1970-1999, for the first five years, up to 2008, the glacier length shows little response to different mass balance specification (Figure 5.8a). After five years, different mass balance forcings result in widely different glacier length.

This pattern indicates that the glacier response is predetermined by glacier geometry for the first five years in the future, but the mass balance has an increasing influence after this time. Independent of the glacier mass balance, the glacier will continue to retreat for the next five years by approximately 1000 m. After this time no prediction can be made without assumptions about future mass balance, except to say that the glacier is likely to continue to retreat until 2013.

The probability distribution of glacier length for the El Niño (negative SOI) case is similar to that of the full period 1970-1999, although there is a slightly larger probability of an advance towards 2013 (Figure 5.8b). The similarity between Figure 5.8(a) and Figure 5.8(b) is a reflection of the fact that the period 1970-1999 was one of more El Niño than La Niña. The probability distribution of glacier length for a more La Niña like future is quite different, with the likelihood of further recession beyond 2008 to at least 2013 (Figure 5.8c).

5.6.2 Long-term future prediction

The final objective of this chapter is to determine the long-term future behaviour of the glacier. The time frame used is that of the IPCC climate change scenarios (IPCC, 2001) which provide projections to 2100. Mullan and others (2001) have statistically downscaled these climate change scenarios, and presented them in terms of monthly changes in temperature and precipitation per degree global warming.

These scenarios have been used to examine the effect of climate change on the mass balance curve at Franz Josef Glacier (Section 3.8). This mass balance variation is shown in terms of EOSS in Figure 5.9 for four scenarios:

1. the 'no warming' scenario where temperature and rainfall are kept at their means for the 1970-1999 period,
2. the 'mean warming' scenario where the mean global warming scenario and monthly changes are used,
3. the 'minimum warming' scenario which is the minimum global warming scenario, minimum monthly temperature change and maximum monthly precipitation change, and
4. the 'maximum warming' scenario which is the maximum global warming scenario, maximum monthly temperature change and minimum monthly precipitation change.

The ice-flow model is run with the EOSS derived for these future climate scenarios, and the resulting glacier length is shown in Figure 5.9, volume in Figure 5.10 and a map of 2100 terminus position in Figure 5.11.

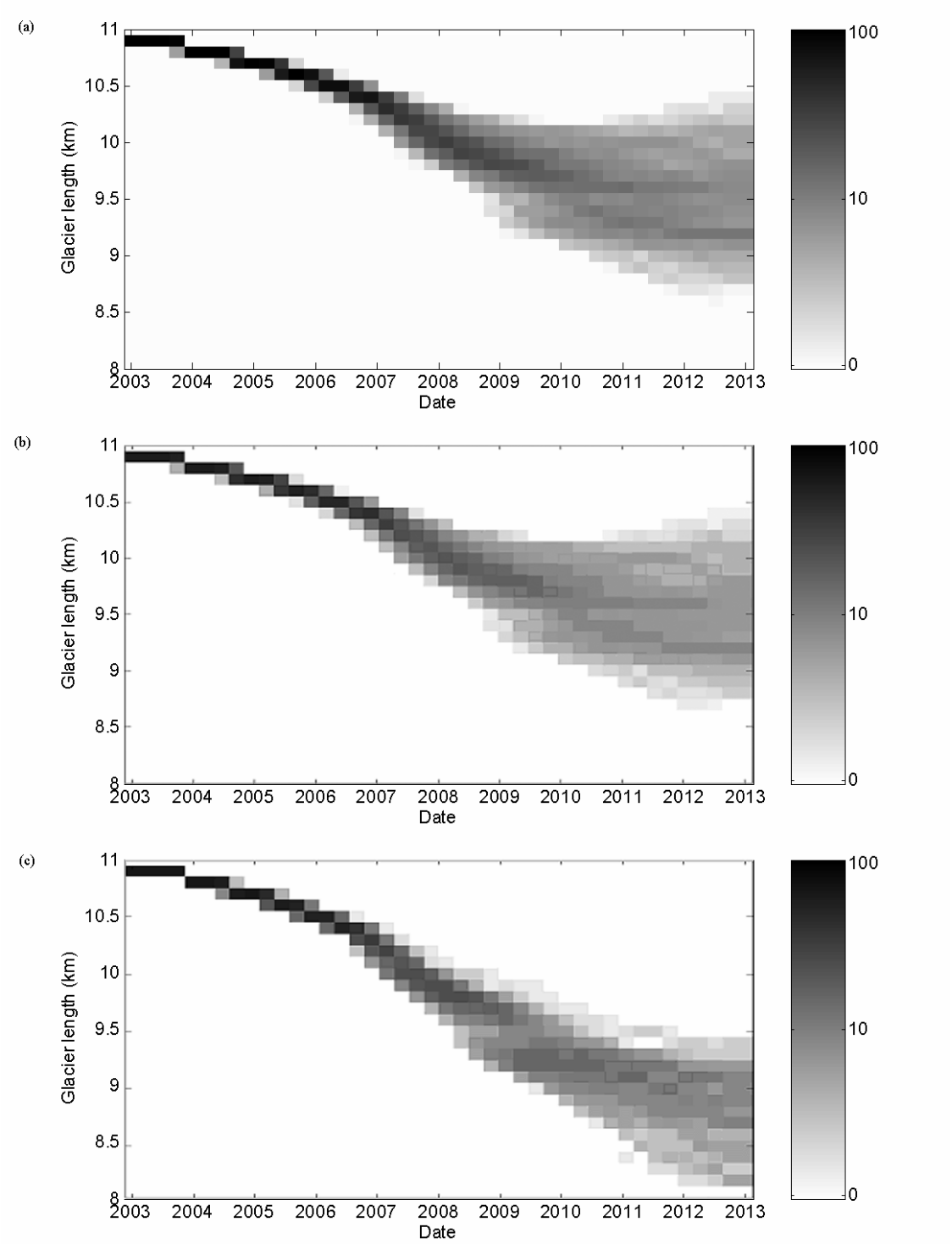

Figure 5.8. Probability distribution of glacier length for the period 2003-2013. The bar on the right indicates the percentage of model runs which result in each terminus position. The model was run 500 times. (a) no restriction (b) negative SOI (El Niño). (c) positive SOI (La Niña).

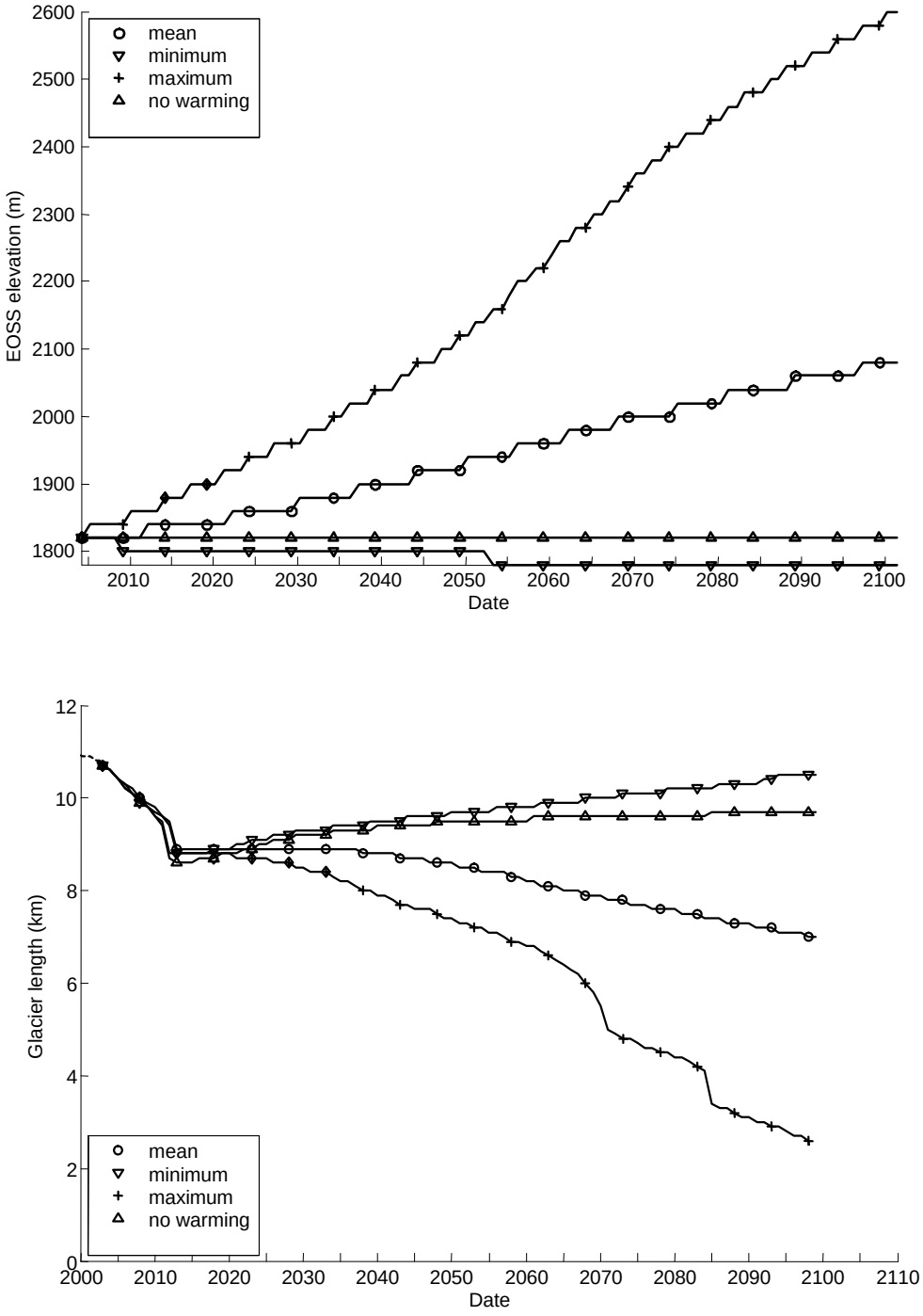

Figure 5.9. The EOSS in the upper pane resulting from each of the 4 climate scenarios is used to drive the ice-flow model. The glacier length is plotted in the lower pane.

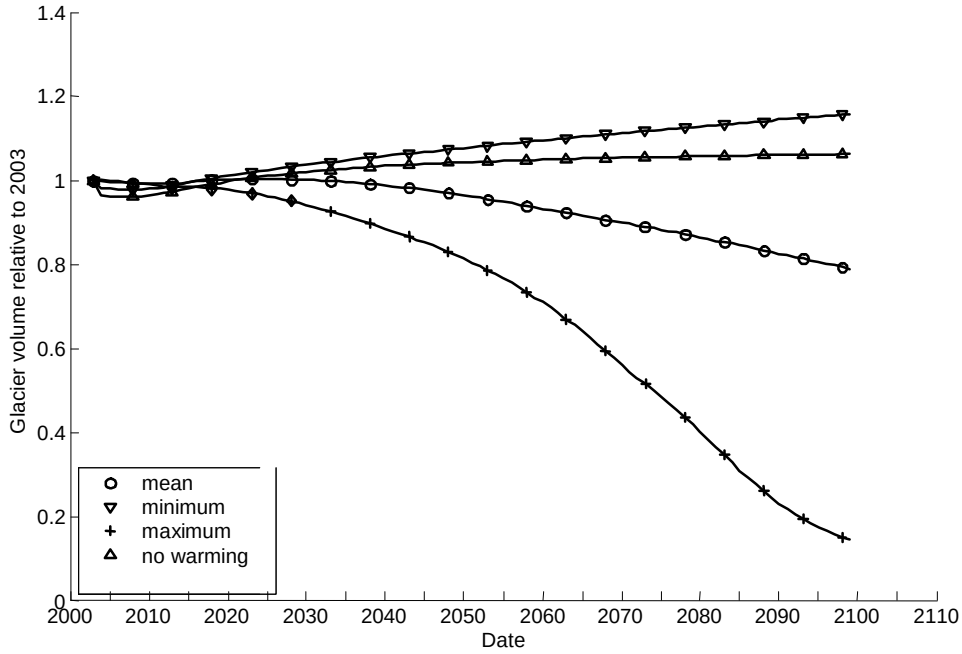

Figure 5.10. Glacier volume changes relative to the 2003 volume.

As expected from the short-term future predictions presented in the previous Section, in all cases the glacier continues to retreat for a few years after 2003. The retreat continues over two bedrock steps (Figure 5.9) to a stable length of 9 km by 2015. After this time the different scenarios diverge rapidly as the long-term mass balance signal from the climate change scenarios become important.

The 'no warming' scenario shows a slight advance of the glacier back over these bedrock steps (Figure 5.9) to 9.6 km, a length somewhat shorter than present. The 'mean warming' scenario forces a continued slow recession to a length of 7 km by 2100, and a reduction in volume to 80% of the 2003 volume. The 'maximum warming' scenario forces a drastic retreat to 3.3 km in glacier length, and 15% of the 2003 volume. Note the steps in glacier length around 2065 and 2085 which occur when the glacier retreats over bedrock steps (Figure 5.9).

An interesting aspect of the scenarios plotted in Figure 5.9 is that the 'minimum warming' scenario results in a slight lowering of EOSS and a glacier a similar length to present at 10.9 compared to 9.6 km for the 'no change' scenario. This result is because the effect of the slight warming in this scenario (0.4 K by 2100) is more than offset by the increase in precipitation (annual average increase of 26% by 2100).

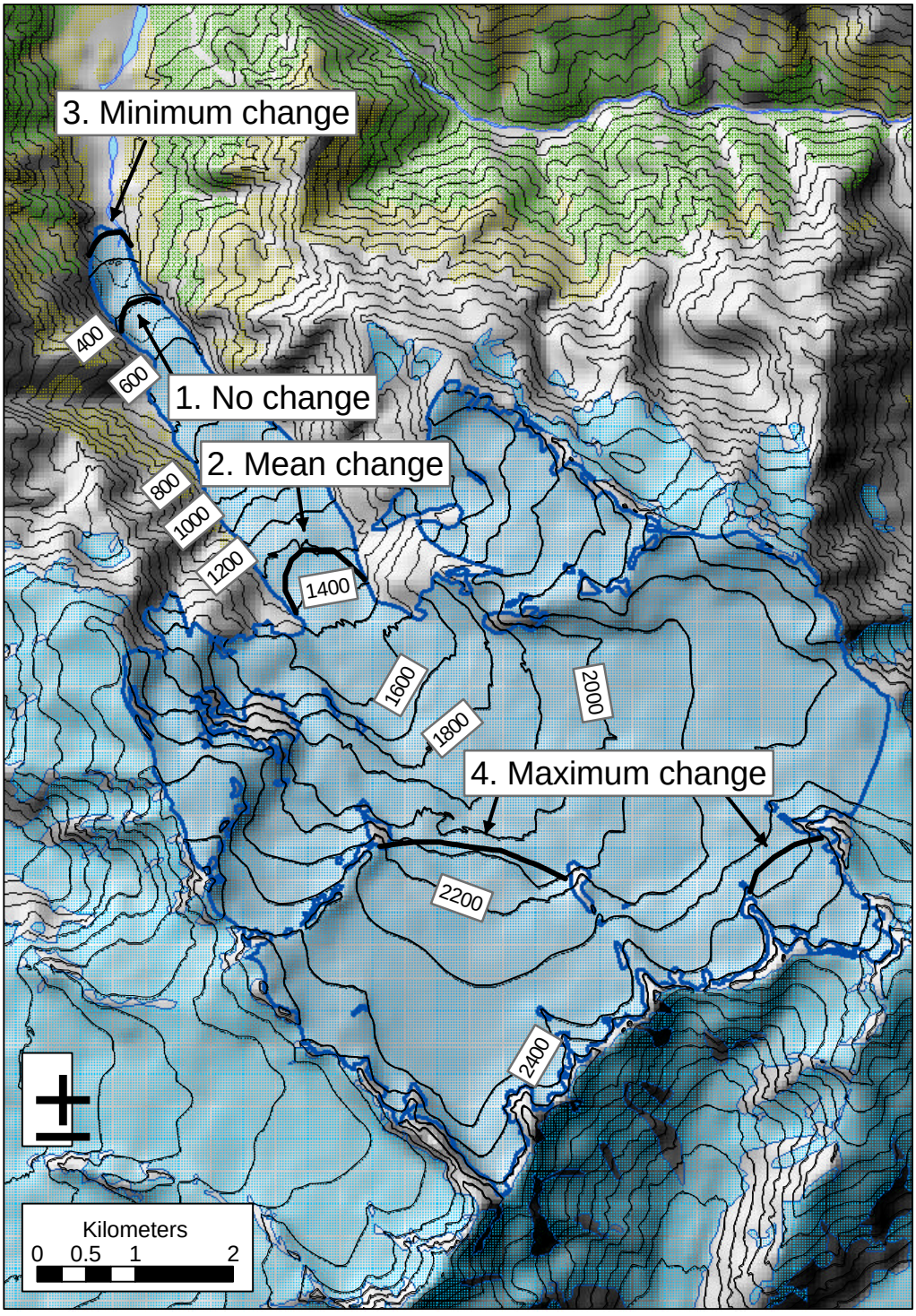

Figure 5.11. The approximate terminus position of the glacier in 2100 under different scenarios.

The length changes in Figure 5.9 are displayed in map form in Figure 5.11. The small volume of the glacier tongue means that the large retreat predicted from 2003-2015 is the result of only a small decrease in glacier volume (Figure 5.10).

5.7 Discussion

5.7.1 Simulation of past glacier response

Attempts to use mass balance reconstructions to drive ice-flow models have been made by a number of authors, with varying success. Studies which use a long-term climate reconstruction to calculate mass balance have generally shown a poor correspondence between measured and modelled glacier terminus changes (Oerlemans, 1986; Stroeven and others, 1989; Huybrechts and others, 1989). Simulations over shorter periods, using mass balance calculated directly from climate data have shown a better correspondence (Schlosser, 1997; Schmeits and Oerlemans, 1997).

Difficulties in simulating glacier terminus position are often put down to problems in calculating mass balance, rather than uncertainties in the flow model (Greuell, 1992; Oerlemans, 1997b). This appears to be the case for the simulation of Franz Josef Glacier presented in this chapter. The mass balance model in the period from 1894 to at least 1940 appears to overestimate mass balance, as indicated by the unrealistically long glacier predicted (Figure 5.6). Whether this overestimate is a result of poor quality climate data, or changes in mass balance model parameters that have been assumed to be constant, for example the variation of temperature and precipitation with elevation, is not clear.

5.7.2 Short-term future predictions

The relative importance of the present day glacier geometry/dynamics and future mass balance for the future advance and retreat of Franz Josef Glacier can be distinguished in Figure 5.8. For all assumptions about short future climate, namely no assumption, an El Niño restriction, and a La Niña restriction, it is apparent that the terminus position of the glacier is determined by the present day glacier geometry for about 5 years into the future. After 5 years the mass balance rapidly becomes of increasing importance and the envelope of the probability distribution of glacier length widens markedly.

It may be expected that the dynamic constraint dominates glacier behaviour for a period that is related to the response time of the glacier in some way. Depending on the definition and method for calculating response time, for Franz Josef Glacier it is between 6 and 24 years (Oerlemans, 2001), and so the dynamic constraint dominates glacier length for between 20-90% of the response time of the glacier.

The glacier will retreat 1000 m to 2008, and after that time the glacier length will depend increasingly on the particular mass balance experience since 2003.

5.7.3 Long-term future prediction

The range of possibilities of future glacier length is large, from 3.3 km to 10.9 km in 2100, and a volume change to between 15% and 120% of the 2003 volume. If we take the 'mean warming' scenario as the most likely outcome, the result for the 21st century is a retreat of the glacier of almost 4 km, more than the 3 km retreat measured in the 20th century. The volume change however, is quite small at 20% of the 2003 value, a result of the low volume tongue which can advance and retreat substantially with small overall volume changes (Soons, 1971).

Long-term glacier length and volume predictions must be approached with some caution. Uncertainties in future climate projections are compounded by uncertainties in the mass balance model, and uncertainties in the flow model before we arrive at projections of glacier length and volume. While it is possible to undertake a parametric uncertainty analysis to evaluate the probability density function of the uncertainties in the mass balance and ice-flow models (Van der Veen, 2002), the lack of probabilities associated with the climate scenarios negates the value of this approach. Hence all we can provide for future glacier projections is a broad range of possibilities.

5.8 Conclusion

With reference to the three objectives of this chapter, the following conclusions have been made:

1. The coupled mass balance - ice flow model simulates the general retreat of the glacier in the 20th century.
2. The details of glacier advance and retreat in the 20th century are not simulated by the model and the mass balance appears to be overestimated for the period 1894-1940 (Figure 5.6).
3. A Monte Carlo simulation of glacier length for the next 10 years indicates that the present-day glacier geometry constrains the glacier to retreat by 1 km in the next 5 years, independent of the climate (Figure 5.8a).
4. If the climate is strongly El Niño for the next decade, glacier length may stabilise after 5 years (Figure 5.8b).
5. If the climate is strongly La Niña for the next decade, the glacier is almost certain to continue to retreat after 5 years (Figure 5.8b).
6. Future climate scenarios to 2100, under the mean global warming scenario and applied to the coupled mass balance - ice flow model, indicate that the glacier will to retreat 4 km to a length of 7 km (Figure 5.9), and lose 20% of its volume (Figure 5.10).
7. If global warming is at the lowest end of the IPCC projections (IPCC, 2001), and the precipitation increase is at the high end of local projections (Mullan and others, 2001), the glacier will be close to its present (2003) length by 2100 (Figure 5.9), with a 20% increase in volume (Figure 5.10).

8. If global warming is at the highest end of the IPCC projections (IPCC, 2001), and the precipitation increase is at the low end of local projections (Mullan and others, 2001), the glacier will retreat 8 km to a length of 3 km (Figure 5.9), splitting into two remnant glaciers on the highest peaks, with an 85% decrease in volume (Figure 5.10).

6 Conclusion

The overall goal of this thesis was to examine the response of Franz Josef Glacier to climate change. The relationship between climate, mass balance, ice dynamics and terminus position of Franz Josef Glacier has been examined through the collection of an extensive set of field data, and the application of mass balance and ice-flow models. As indicated in Section 1.4, the specific objectives of this thesis were:

1. To synthesise the previous work regarding the climate - glacier linkages at Franz Josef Glacier in order to identify the key gaps and uncertainties in our knowledge of the response of the glacier to climate change;
2. To develop and verify a mass balance model which will explicitly account for the links between general climate, local glacier climate, and mass balance;
3. To develop and verify an ice-flow model which explicitly links net mass balance and glacier geometry changes; and
4. To predict future glacier behaviour using the coupled mass balance - ice-flow model.

These objectives have been achieved in each of the Chapters 2-5 respectively (see Sections 2.7, 3.10, 4.7 and 5.8). In this final chapter, we focus on synthesising the conclusions of these chapters to address the overall goal, that is the response of Franz Josef Glacier to climate change.

6.1 Response to past climate changes

Global warming in the last century of between 0.4 to 0.8^{o}C (IPCC, 2001) has led to widespread glacier recession. In terms of small glaciers, many glaciers in the continental setting of the European Alps have retreated 1 km or more in the last century. More maritime glaciers, which tend to be more sensitive, such as Nigardsbreen, Norway, and Franz Josef Glacier have retreated 3 km or more (IPCC, 2001). Assuming that glacier recession was driven by temperature changes alone, Ruddell (1995) attributed glacier recession in New Zealand to a 1^{o}C warming since the 1860s, and Oerlemans (2001) attributed the 20th century recession of Franz Josef Glacier to a 0.7^{o}C warming.

Simulations of the response of glaciers to past climate changes, in terms of historic terminus position, have been attempted for many glaciers with varying success (Table 6.1). There are three patterns that emerge in terms of the ability of these models to simulate historic terminus position variations. Firstly, the simulations that start in the 19th century are generally more successful that those that attempt to simulate glacier changes back to the 16th century. Secondly, and not surprisingly, the more successful of the simulations are for glaciers which have a long period of mass balance measurement for calibration. Thirdly, those models which are run with directly measured mass balance simulate glacier length variations particularly well. These patterns point to the importance of accurate mass balance data. In addition, it is clear that overall, the more recent studies have been more successful. The study of Schmeits and Oerlemans

(1997) stands out as a successful simulation for a long period for a glacier for which little is known apart from terminus length changes.

Table 6.1. A summary of published simulations of historic terminus position using ice-flow models.

Glacier	Reference	Period of simulation	Mass balance data source[(1)]	Measured mass balance used	Details simulated?
Nigardsbreen	Oerlemans, 1986	1710-1980 *270 years*	proxy climate	-	no
Argentiere	Huybrechts and others, 1989	1530-1980 *450 years*	proxy and instrumental climate	-	no
Rhône	Stroeven and others, 1989	1530-1980 *450 years*	proxy and instrumental climate	EOSS 1884-1910, 1979-1981 *2 years*	no
Hintereisferner	Greuell, 1992	1894-1985 *91 years*	instrumental climate and direct measurement	1953-1985 *32 years*	yes
Hintereisferner	Schlosser, 1997	1850-1985 *135 years*	instrumental climate and direct measurement	1953-1985 *32 years*	yes
Nigardsbreen	Oerlemans, 1997a	1961-1993 *32 years*	direct measurement	1961-1993 *32 years*	yes
Unterer Grindelwaldgeltscher	Schmeits and Oerlemans, 1997	1530-1992 *462 years*	proxy and instrumental climate	-	yes
Pasterze	Zuo and Oerlemans, 1997	1865-1990 *125 years*	instrumental climate	1979-1989 *10 years*	yes
Rhône	Wallinga and van de Wal, 1998	1600-2000 *400 years*	instrumental climate and direct measurement	EOSS 1884-1910, 1979-1981 *2 years*	yes
Storglaciären	Albrecht and others, 2000	1959-1990 *41 years*	direct measurement	1959-1990 *31 years*	yes
Franz Josef Glacier	this study	1894-2003 109 years	instrumental climate	2000-2003 *3 years*	no

[(1)] direct measurement refers to the direct measurement of mass balance by the glaciological method.

In this context, the past glacier length simulation for Franz Josef Glacier (Figure 5.6) is interesting. The simulation period is 109 years, shorter than other more successful simulations, the instrumental climate record used is of good quality (Salinger, 1981) and is closer to the glacier than that used in many of the studies in Table 6.1. However, the period of mass balance measurement at Franz Josef Glacier only 3 years, as the attempt to extend the record to 26 years by linking it to the EOSS measured on the Almer Glacier (Chinn, 1995; Chinn and Salinger, 2001) in Chapter 1 was not successful.

The dependence of the success of simulating historic response on having a good record of mass balance, both for Franz Josef and other glaciers, indicates that the lack of success in historic simulations cannot be ascribed to difficulties in ice-flow modelling, but rather to the mass balance specification. The lack of detailed simulation of historic terminus position at Franz Josef Glacier leads us to question why the mass balance model performs well for present-day conditions (Figure 3.8) but does perform well at times in the past. This may be the result of the maritime environment of Franz Josef Glacier, where temperature and precipitation are strongly controlled by circulation changes (Fitzharris and others, 1997) and the variation of temperature and precipitation with elevation may also change on a decadal scale as a result of the Interdecadal Pacific Oscillation (Figure 5.7). The common assumption that mass balance varies spatially with elevation alone (Fountain and Vecchia, 1999) does not appear to apply well to Franz Josef Glacier. The limitations of using terminus position as an indicator of glacier behaviour are apparent at Franz Josef Glacier, where significant advance and retreat (Figure 5.9) is the result of small changes in glacier volume (Figure 5.10).

6.2 Response to future climate changes

The variations in mass balance and glacier geometry over the last century have already determined the short-term future of the Franz Josef Glacier. The creation of a probability distribution of future glacier length (and volume), a novel method introduced in this thesis, indicates that the future response is only dynamically constrained for 5 years into the future. During this time the glacier will retreat 1 km, independent of the climate in this period, so long as it is within the variability experienced in the last 30 years. The calculation of a probability distribution of future glacier behaviour is a valuable tool in future prediction. For most glaciers, the period of dynamic constraint will be significantly longer than 5 years because on a global scale the Franz Josef Glacier has an unusually short response time (Oerlemans, 2001). The dynamic constraint may be a significant influence on small glacier behaviour in the coming century.

The longer term glacier response is less certain, and falls within a wide range as a result of the wide range of future climate scenarios. An additional factor when assessing the global response of glaciers to climate change is the varying regional climatic response to global warming (Gregory and Oerlemans, 1998; Mullan and others, 2001). For example, the annual mean warming predicted for Hokitika is only 40% of the mean global warming (Figure 3.13). Regionally variable global warming accounts for a large part of the

uncertainty in global sea level rise prediction from small glacier melt (Gregory and Oerlemans, 1998). We now compare the projected future changes of Franz Josef Glacier with those of other glaciers (Table 6.2). The length response of Franz Josef Glacier to its locally-projected warming is the median for this selection of glaciers, while the volume response is the smallest of the sample. These results can both be explained by the relatively small projected temperature increase and large precipitation increase, and the geometry of Franz Josef Glacier. While the EOSS of the Franz Josef Glacier is sensitive to climate change (Figure 3.15), the steep tongue also ensures that the recession for the mean warming scenario of 4 km results in an elevation rise for the terminus of 1200 m which then experiences less ablation. The consequent volume change is only 20% due to the low volume of the glacier tongue.

Table 6.2. A comparison of glacier change to 2100 under local downscaling of climate change scenarios.

Glacier	Reference	Annual temperature change	Precipitation change	Length change	Volume change
Franz Josef Glacier	this study	+1.5°C	+16%	-4 km	-20%
Rhônegletscher	Wallinga and van de Wal, 1998	+2°C	0	-4 km	-65%
Nigardsbreen	Oerlemans, 1997a	+2°C	0	-8 km	-90%
Pasterze	Zuo and Oerlemans, 1997	+2.2°C	0	-5 km	-60%
Blöndujökull/ Kvíslajokull	Jóhannesson, 1997	+3°C	+15%	-2 km	-40%
Illvidrajökull	Jóhannesson, 1997	+3°C	+15%	-1.5 km	-40%
Unterer Grindelwaldgeltscher	Schmeits and Oerlemans, 1997	+2°C	0	-2.7 km	-66%

6.3 Implications

On a global scale, the high mass turnover of the Franz Josef Glacier suggested by modelling studies has been confirmed by measurement and the Franz Josef Glacier appears to be the most extreme well studied maritime glacier that has been documented worldwide, in terms of the rates of accumulation and ablation. Questions have been raised in this thesis about the ability of mass balance models to simulate mass balance in this environment. The reasons for the problems encountered are not clear, but they are most likely to

relate to the calculation of mass balance using elevation as the only spatial variable, and the possible variation in temperature and precipitation patterns on a decadal time scale (Figure 5.7).

On a regional scale, the mass balance curve for Franz Josef Glacier (Figure 3.8) covers almost the entire elevation range of New Zealand glaciers (Figure 3.8) and can be used in conjunction with the EOSS monitoring programme (Chinn, 1995; Chinn and Salinger, 2001). Until this study there have been no measurements of annual mass balance covering such a large range of elevation, and the results of this thesis provide a basis for the estimation of mass balance and volume change for other glaciers in New Zealand

On a local scale, the retreat of Franz Josef Glacier will have a drastic effect on tourism. Guided walking and recreation on the glacier will become increasingly difficult and parts of the glacier may become impassable. Guided walks without helicopter support will be impossible after about 2015, when the glacier retreats back over two bedrock steps (Section 5.7.3). The entire area of the glacier currently used for guided walks will have disappeared by 2100 (Figure 5.11). As the Franz Josef Glacier is a major draw card for tourists to the entire West Coast region, a significant effect on the local economy can be expected.

6.4 Future research directions

In terms of the response of small glaciers to climate change, this thesis has raised some interesting questions. The spatial variation of mass balance, and its relationship to elevation and other controls warrant deeper examination. On a larger scale, the links between spatial variability of mass balance and the particular topographic and wider-scale setting, in terms of climate and continentality, could be further investigated.

This thesis has shown that the dynamic constraint on future glacier behaviour is an important control on short-term glacier response, independent of future climate. The probability-based approach of future glacier length using a Monte Carlo simulation is likely to be provide more information on glacier response further into the future for many glaciers than for Franz Josef Glacier, and may make up a large part of the response of glaciers with a long response time in the coming century.

The main impediment in the prediction of future glacier behaviour is the range of future climate change scenarios available. Further constraint on these models and the probabilities of different outcomes will improve better input for models of glacier response.

Finally, this conclusion has demonstrated that assessing the response of glaciers to climate change is difficult without good quality long term mass balance data. A high priority must be placed on the establishment of a long term mass balance monitoring programme on one or more New Zealand Glaciers.

7 References

Anderton, P.W. 1975. Tasman Glacier 1971-1973. *Hydrological research:* Annual report No. 33. Ministry of Works and Development for the National Water and Soil Conservation Organisation, Wellington, New Zealand, 28pp.

Anderton, P.W. and Chinn, T.J. 1978. Ivory Glacier, New Zealand, an IHD basin study. *Journal of Glaciology* **20**(82): 67-84.

Andreason, J.O. 1983. Basal sliding at the margin of the glacier Austre Okstindbre, Nordland, Norway. *Arctic and Alpine Research* **15**: 333-338.

Andrews, J.T. 1975. Glacial Systems: An Approach to Glaciers and their Environments. Duxbury Press, North Scituate, Massachusetts, 191 pp.

Bahr, D.B. 1997. Global distributions of glacier properties: A stochastic scaling paradigm. *Water Resources Research* **33**(7): 1669-1679.

Bahr, D. B., Pfeffer, W. T. and Meier, M. F. 1994. Theoretical limitations to englacial velocity calculations. *Journal of Glaciology*, **40** (136): 509-518.

Bahr, D.B., Meier, M.F. and Peckham, S.D. 1997. The physical basis of glacier volume-area scaling. *Journal of Geophysical Research* **102**(B9): 20355-20363.

Barringer, J.R.F. 1989. A variable lapse rate snowline model for the Remarkables, Central Otago, New Zealand. *Journal of Hydrology (New Zealand)* **28**(1): 32-46.

Bell, J.M. 1910. A geographical report on the Franz Josef Glacier, with topographical maps and data by R.P. Greville and botanical notes by Leonard Cockayne: New Zealand Geological Survey, Wellington, 14 pp

Benn, D.I. and Evans, D.J.A. 1998. *Glaciers and Glaciation.* Arnold, London.

Bindschadler, R. 1983. The importance of pressurized subglacial water in separation and sliding at the glacier bed. *Journal of Glaciology* **29**(101): 3-19.

Bishop, G. and Forsyth, J. 1988. *Vanishing Ice. An introduction to glaciers based on a study of the Dart Glacier.* J. McIndoe and New Zealand Geological Survey, DSIR.

Blake, E.W., Clarke, G.K.C. and Gérin, M.C. 1992. Tools for examining subglacial bed deformation. *Journal of Glaciology* **38**: 388-396.

Blatter, H. 1995. Velocity and stress fields in grounded glaciers: a simple algorithm for including deviatoric stress gradients. *Journal of Glaciology* **41**(138): 333-344.

Braithwaite, R.J. 1984. Can the mass balance of a glacier be estimated from its equilibrium-line altitude? *Journal of Glaciology* **30**(106): 364-368.

Braithwaite, R. J. 1985. Calculation of degree-days for glacier-climate research. *Zeitschrift für Gletscherkunde und Glazialgeologie* **20**(1984): 1-8.

Braithwaite, R. J. 1995. Positive degree-day factors for ablation on the Greenland ice sheet studied by energy balance modelling. *Journal of Glaciology* **41**(137): 153-160.

Braithwaite, R. J. and Zhang, Y. 1999. Modelling changes in glacier mass balance that may occur as a result of climate changes. *Geografiska Annaler* **81A**(4): 489-496.

Braithwaite, R. J. and Zhang, Y. 2000. Sensitivity of mass balances of five Swiss glaciers to temperature changes assessed by tuning a degree-day model. *Journal of Glaciology* **46**(152): 7-14.

Brazier, V., Owens, I.F., Soons, J.M. and Sturman, A.P. 1992. Report on the Franz Josef Glacier. *Z. Geomorph. N.F.* Suppl.-Bd. **86:** 35-49.

Broecker, W. 1997. Will our ride into the greenhouse future be a smooth one? *GSA Today* **7**(5):1-7.

Budd, W.F., Keage, P.L. and Blundy, N.A. 1979. Empirical studies of ice sliding. *Journal of Glaciology* **23**(89): 157-170.

Burrows, C.J. 1990. Processes of vegetation change. London, Unwin Hyman. 549 pp.

Chen J., and Funk M. 1990 Mass balance of Rhônegletscher during 1882/83-1986/87. *Journal of Glaciology* **36**(123): 199-209.

Chinn, T.J. 1969. Snow survey techniques in the Waitaki Catchment, South Canterbury. *Journal of Hydrology (New Zealand)* **8**(2): 68-76.

Chinn, T.J. 1979. How wet is the wettest of the wet West Coast? *New Zealand Alpine Journal* 1979: 85-78.

Chinn, T.J. 1989. Glaciers of New Zealand. U.S. Geological Survey Professional Paper 1386-H.

Chinn, T.J. 1995. Glacier fluctuations in the Southern Alps of New Zealand determined from snowline elevations. *Arctic and Alpine Research* **27**(2):187-198.

Chinn, T.J. and Salinger, J.M. 2001. New Zealand Glacier snowline survey, 2000. NIWA Technical report no. 98.

Conway, H., Rasmussen, L.A. and Marshall, H.P. 1999. Annual mass balance of Blue Glacier, USA: 1955-97. *Geografiska Annaler*, **81A**(4): 509-520.

Copland, L., Harbor, J., and Sharp, M. 1997. Borehole video observation of englacial and basal ice conditions in a temperate valley glacier. *Annals of Glaciology* **24**: 277-282.

Denton, G.H. and Hendy, C.H. 1994. Younger Dryas Age Advance of Franz Josef Glacier in the Southern Alps of New Zealand. *Science* **264**: 1434-1437.

Denton, G. H. and Hendy, C. H. 1995. The age of the Waiho Loop glacial event. *Science* **271:** 668-670. (1995).

Denton, G.H., Heusser, C.J., Lowell, T.V., Moreno, P.J., Andersen, B.G., Heusser, L.E., Schlüchter, C., and Marchant, D.R. 1999. Interhemispheric linkage of paleoclimate during the last glaciation. *Geografiska Annaler*, **81A**:107–153.

Douglas, C.E. 1894. On the Westland Alps. *Appendix to the Journal of the House of Representatives of New Zealand.* C-1, Appendix No 6: 71-75.

Dyurgerov, M.B. and Bahr, D.B. 1999. Correlations between glacier properties: finding appropriate parameters for global glacier monitoring. *Journal of Glaciology* **45**(149): 9-16.

Echelmeyer, K. and Harrison, W.D. 1990. Jakobshavns Isbrae, west Greenland: seasonal variations in velocity - or lack thereof. *Journal of Glaciology* **33**: 83-98.

Engelhart, H.F., Harrison, W.D. and Kamb, B. 1978. Basal sliding and conditions at the glacier bed as revealed by bore-hole photography. *Journal of Glaciology* **20**: 469-508.

Engeset, R.P., Elvehøy, H., Andreassen, L.M., Haakensen, N., Kjøllmoen, Roald, L.A. and Roland, E. 2000. Modelling of historic variations and future scenarios of the mass balance of Svartisen ice cap, northern Norway. *Annals of Glaciology* **31**: 97-103.

Fitzharris, B.B. and Hay, J.E. 1989. Glaciers - can they weather the storm of climate change? In Welch, R. (ed) *Proceedings of the 15th New Zealand Geography Conference, Dunedin.* New Zealand Geographical Society: 284-291.

Fitzharris, B., Hay, J. and Jones, P. 1992. Behaviour of New Zealand glaciers and atmospheric circulation changes over the past 130 years. *The Holocene* **2**(2): 97-106.

Fitzharris, B., Chinn, T. and Lamont, G. 1997. Glacier balance fluctuations and atmospheric circulation patterns over the Southern Alps, New Zealand. *International Journal of Climatology* **17:** 745-763.

Fitzharris, B., Lawson, W. and Owens, I. 1999. Research on glaciers and snow in New Zealand. *Progress in Physical Geography* **23**(4): 469-500.

Fleming, K.M, Dowdeswell, J.A., and Oerlemans, J. 1997. Modelling the mass balance of northwest Spitsbergen glaciers and response to climate change. *Anals of Glaciology* **24**: 203-210.

Fountain, A.G. and Vecchia, A.V. 1999. How many stakes are required to measure mass balance of a glacier? *Geografiska Annaler* **81A** (4): 563-573.

Fowler, A.C. 1987. Sliding with cavity formation. *Journal of Glaciology* **33**: 255-267.

Gellatly, A.F. and Norton, D.A. 1984. Possible warming and glacier recession in the South Island, New Zealand. *New Zealand Journal of Science* **27:** 381-388.

Gellatly, A.F. 1985. Historical records of glacier fluctuations in Mt Cook National Park, New Zealand: a century of change. *Geographical Journal* **151**(1): 86-99.

Glen, J. W. 1955. The creep of polycrystalline ice. *Proceedings of the Royal Society Series* A **228**: 513-38.

Goldthwait, R.P. and McKellar, I.C. 1962. New Zealand Glaciology. *In* Wexler, H., Rubin, M.J. and Caskey, J.E. Jr., eds, *Antarctic Research* (Geophysical Monograph Series No. 7); Washington D.C., American Geophysical Union, Publication No. **1036**: 209-216.

Goodsell, B., Hambrey, M.J. and Glasser, N.F. 2002. Formation of band ogives and associated structures at Bas Glacier d'Arolla, Valais, Switzerland. *Journal of Glaciology* **48**(161): 287-300.

Gregory, J.M. and Oerlemans, J. 1998. Simulated future sea-level rise due to glacier melt based on regionally and seasonally resolved temperature changes. *Nature* **391**: 474-476

Greuell, J.W. 1992. Hintereisferner, Austria: mass-balance reconstruction and numerical modelling of the historical length variations. *Journal of Glaciology* **38**: 233-244.

Griffiths, G.A. and McSaveney, M.J. 1983. Distribution of mean annual precipitation across some steepland regions of New Zealand. *NZ Journal of Science* **26:** 197-209.

Grove, J.M. 1988. *The Little ice age*. Methuen.

Gunn, B.M. 1964. Flow rates and secondary structures of Fox and Franz Josef Glaciers, New Zealand. *Journal of Glaciology* **5**(38): 173-190.

Haeberli, W., Frauenfelder, R. and Hoelzle, M. 2001. *Glacier Mass Balance Bulletin No. 6 (1998–1999)*. IAHS (ICSI) – UNEP – UNESCO – WMO 2001. pp93.

Harper, A.P. 1894. The Franz Josef Glacier. *Appendix to the Journal of the House of Representatives of New Zealand.* C-1, Appendix No 6: 75-79.

Harper, A.P. 1926. Variations of the Franz Josef Glacier. *New Zealand Alpine Journal* **3**(15): 343-349.

Henderson, R.D. 1998. The Southern Alps experiment. *New Zealand Alpine Journal* 1998: 106-109.

Henderson, R. D. and Thompson, S.M. 1999. Extreme Rainfalls in the Southern Alps of New Zealand. *Journal of Hydrology (NZ)* **38**(2): 309-330.

Hessell, J.W.D. 1982. *The climate and weather of Westland.* NZ Meteorological Service miscellaneous publication **115**(10).

Hessell, J.W.D. 1983. Climatic effects on the recession of the Franz Josef Glacier. *New Zealand Journal of Science* **26:** 315-320.

Hindmarsh, R.C.A. 2001. Notes on basic glaciological computational methods and algorithms, in Greve R., Ehrentraut, Y. Wang, and B. Straughan (eds.), *Continuum Mechanics in Geophysics and the Environment* (in press).

Hodge, S.M. 1974. Variations in the sliding of a temperate glacier. *Journal of Glaciology* **13**:349-369.

Holmlund, P. 1987. Mass balance of Storglaciären during the 20th century. *Geografiska Annaler* 69 A (3-4): 439-447.

Hooke, R. Le B., Pohjola, V.A., Jansson, P. and Kohler, J. 1992. Intra-seasonal changes in deformation profiles revealed by borehole studies, Storglaciären, Sweden. *Journal of Glaciology* **34**: 228-231.

Hooker, B.L. and Fitzharris, B.B. 1999. The correlation between climatic parameters and the retreat and advance of Franz Josef Glacier, New Zealand. *Global and Planetary Change* **22**: 39-48.

Hubbard, A. 1997. Modelling climate, topography and palaeoglacier fluctuations in the Chilean Andes. *Earth Surface Processes and Landforms* **22**: 79-92.

Hubbard, A. 2000. The verification and significance of three approaches to longitudinal stresses in high-resolution models of glacier flow. *Geografiska Annaler* **82A** (4): 471-487.

Hubbard, B. 2002. Direct measurement of basal motion at a hard-bedded, temperate glacier: Glacier de Tsanfleuron, Switzerland. *Journal of Glaciology* **48**(160): 1-8.

Huybrechts, P. Nooze de P. Decleir H. 1989. Numerical modelling of Glacier d'Argentiere and its historic front variation. In: Oerlemans J (ed) *Glacier fluctuations and climatic change*. Reidel. Dordrecht p 373-389.

Iken, A., Röthlisberger, H., Flotron, A. and Haeberli, W. 1983. The uplift of Unteraargletscher at the beginning of the melt season - a consequence of water storage at the bed? *Journal of Glaciology* **29**: 28-47.

Iken, A. and Bindschadler, R.A. 1986. Combined measurements of subglacial water pressure and surface velocity of the Findelengletscher, Switzerland: conclusions about drainage system and sliding mechanism. *Journal of Glaciology* **32**: 101-119.

IPCC. 2001. Climate Change 2001: The Scientific Basis Contribution of Working Group I to the Third Assessment Report of the Intergovernmental Panel on Climate Change (IPCC). Cambridge University Press, UK

Ishikawa, N., Owens, I.F. and Sturman, A.P. 1992. Heat balance characteristics during fine periods on the lower parts of the Franz Josef Glacier, South Westland, New Zealand. *International Journal of Climatology* **12:** 397-410.

Ivy-Ochs, S. Schlüchter, C., Kubik, P.W. and Denton, G.H. 1999. Moraine exposure dates imply synchronous Younger Dryas glacier advance in the European Alps and in the Southern Alps of New Zealand. *Geografiska Annaler* **81A:** 313-323.

Iverson, N. R., B. Hanson, R. LeB. Hooke, and Jansson, P. 1995. Flow mechanism of glaciers on soft beds. *Science* **267:** 80-81.

Jóhannesson, T., Sigurdsson, O., Laumann, T. and Kennett, M. 1995. Degree-day glacier mass-balance modelling with applications to glaciers in Iceland, Norway and Greenland. *Journal of Glaciology* **41**(138): 345-358.

Jóhannesson, T. 1997. The response of two Icelandic glaciers to climate warming computed with a degree-day glacier mass balance model coupled to a dynamic glacier model. *Journal of Glaciology* **43**(144): 321-327.

Kääb A., C. Huggel, F. Paul, R. Wessels, B. Raup, H. Kieffer and J. Kargel (2003): Glacier Monitoring from ASTER Imagery: Accuracy and Applications. EARSeL Proceedings. LIS-SIG Workshop. Berne, March 11-13, 2002.

Kamb, B. 1970. Sliding motion of glaciers. *Review of Geophysics and Space Physics* **8**: 673-728.

Kelliher, F.M., Owens, I.F., Sturman, A.P., Byers, J.N., Hunt, J.E. and McSeveny, T.M. 1996. Radiation and ablation on the névé of the Franz Josef Glacier. *NZ Journal of Hydrology* **35**(1): 131-150.

Kirkbride, M.P. 1995. Relationships between temperature and ablation on the Tasman Glacier, Mount Cook National Park, New Zealand. *New Zealand Journal of Geology and Geophysics* **38**: 17-27.

Laumann, T. and Reeh, N. 1993. Sensitivity to climate change of the mass balance of glaciers in southern Norway. *Journal of Glaciology* **39**: 656-665.

Lawrence, D.B. and Lawrence, E.G. 1965. Glacier studies in New Zealand. *Mazama* **47**: 17-27.

Mabin, M. 1995. The age of the Waiho Loop glacial event. *Science* **271**: 688.

Mackintosh, A.N., Dugmore, A.J. and Hubbard, A.L. 2002. Holocene climatic changes in Iceland: evidence from modelling glacier length fluctuations at Sólheimajökull. *Quaternary International* **91**: 39-52.

Mair, D., Nienow, P., Willis, I. and Sharp, M. 2001. Spatial patterns of glacier dynamics during an early melt-season high velocity event: Haut Glacier d'Arolla, Switzerland. *Journal of Glaciology* **47**(156): 9-20.

Mayo, L.R. 1984. Glacier mass balance and runoff research in the USA. *Geografiska Annaler* **66A**: 215-227.

Mantua, N. 2003. *Digital values of the JISAO PDO index*. Online. Available http://jisao.washington.edu/pdo/PDO.latest

Marcus, M.G., Moore, R.D., and Owens, I.F. 1985. Short-term estimates of surface energy transfers and ablation on the lower Franz Josef Glacier, South Westland, New Zealand. *New Zealand Journal of Geology and Geophysics* **28:** 559-567.

Marcus, M.G., Moore, R.D., and Owens, I.F. 1985. Short-term estimates of surface energy transfers and ablation on the lower Franz Josef Glacier, South Westland, New Zealand. *New Zealand Journal of Geology and Geophysics* **28:** 559-567.

Mackintosh, A.N., Dugmore, A.J. and Hubbard, A.L. 2002. Holocene climatic changes in Iceland: evidence from modelling glacier length fluctuations at Sólheimajökull. *Quaternary International* **91**: 39-52.

McKinzey, K.M. 2001. *A new Little Ice Age chronology of the Franz Josef Glacier, West Coast, New Zealand*. Masters thesis, University of Canterbury.

McSaveney, M.J., and Gage, M. 1968. Ice flow measurements on Franz Josef Glacier, New Zealand, in 1966. *New Zealand Journal of Geology and Geophysics*, **11**(3): 564-592.

Meier, M.F. and Post, A.S. 1962. Recent variations in mass net budgets of glaciers in western North America. IASH Publication, **58**: 63-77.

Meier, M. 1974. Flow of Blue Glacier, Olympic Mountains, Washington, U.S.A. *Journal of Glaciology* **13**(68): 187-212.

Meier, M.F. 1984. Contribution of small glaciers to global sea level. *Science* **226**: 1415-1421.

Meier, M.F., Armstrong, R. and Dyurgerov, M.B. 1997. Comments on "Annual net balance of North Cascade glaciers, 1984-94" by Mauri S. Pelto. *Journal of Glaciology* **43**(143): 192-193

Moore, R.D. and Owens, I.F. 1984. Modelling alpine snow accumulation and ablation using daily climate observations. *Journal of Hydrology (NZ)* **23**(2): 73-83.

Mullan, A.B., Wratt, D.S., and Renwick, J.A. 2001. Transient model scenarios of climate changes for New Zealand. *Weather and Climate* (21): 3-34.

Murray, T., Stuart, G.W., Fry, M., Gamble, N.H. and Crabtree, M.D. 2000. Englacial water distribution in a temperate glacier from surface and borehole radar velocity analysis. *Journal of Glaciology* **46**(154): 389-398.

Narod, B. and Clarke, G.K.C. 1994. Miniature high-power impulse transmitter for radio-echo sounding. *Journal of Glaciology* **40**(134): 190–194.

Naruse, R., Skvarca, P., and Takeuchi, Y. 1997. Thinning and retreat of Glaciar Upsala, and an estimate of annual ablation changes in southern Patagonia. *Annals of Glaciology* **24**: 38-42.

Nesje, A., and Dahl, S.O. 2000. *Glaciers and Environmental Change*. Arnold, London

New Zealand Meteorological Service. 1973. *Rainfall normals for New Zealand, 1941 to 1970 : stations in New Zealand and outlying islands, including the Cook group, Pitcairn Island, Niue Island and Western Samoa*. New Zealand Meteorological Service Miscellaneous publications 145.

Nye, J.F. 1951. The flow of glaciers and ice sheets as a problem in plasticity. *Proceedings of the Royal Society, Series A* **207**:554-572.

Nye, J.F. 1952. The mechanics of glacier flow. *Journal of Glaciology* **2**: 103-107.

Nye, J.F. 1953. The flow law of ice from measurements in glacier tunnels, laboratory experiments and the Jungfraufirn borehole experiment. *Proceedings of the Royal Society, Series A* **219**: 477-489.

Nye, J.F. 1957. The distribution of stress and velocity in glaciers and ice sheets. *Proceedings of the Royal Society, Series A* **239**: 113-133.

Nye, J.F. 1965. A numerical method of inferring the budget history of a glacier from its advance and retreat. *Journal of Glaciology* **5**(41): 589-607.

Nye, J.F. 1969. A calculation of the sliding of ice over a wavy surface using a Newtonian viscous approximation. *Proceedings of the Royal Society, Series A* **311**: 445-467.

Nye, J.F. 1970. Glacier sliding without cavitation in a linear viscous approximation. *Proceedings of the Royal Society, Series A* **315**: 381-403.

Odell, N.E. 1955. Franz Josef Glacier, New Zealand speed of flow. *Journal of Glaciology* **2**(18): 598.

Oerlemans, J. 1986. An attempt to simulate historic front variations of Nigardsbreen, Norway. *Theoretical and Applied Climatology* **37**: 126-135.

Oerlemans, J. and Fortuin, J.P.F. 1992. Sensitivity of glaciers and small ice caps to greenhouse warming. *Science* **258**: 115-117.

Oerlemans, J. 1997a. A flow-line model for Nigardsbreen: projection of future glacier length based on dynamic calibration with the historic record. *Annals of Glaciology* **24**: 382-389.

Oerlemans, J. 1997b. Climate sensitivity of Franz Josef Glacier, New Zealand, as revealed by numerical modelling. *Arctic and Alpine Research* **29**: 233-239.

Oerlemans, J., Anderson, B., Hubbard, A., Huybrechts, P., Jóhannesson, T., Knap, W.H., Schmeits, M., Stroeven, A.P., van de Wal, R.S.W., Wallinga, J. and Zuo, Z. 1998. Modelling the response of glaciers to climate warming. *Climate Dynamics*, **14**, 267-274.

Oerlemans, J. 2001: Glaciers and climate change. Balkema Publishers. Lisse, etc.

Owens, I.F., Marcus, M.G., and Moore, R.D. 1984. Temporal variations of energy transfers over the lower part of the Franz Josef Glacier. In Geography for the 1980s. *Proceedings of the Twelfth New Zealand Geography Conference, Christchurch, January 1983.* New Zealand Geographical Society: 83-87.

Owens, I.F., Sturman, A.P. and Ishikawa, H. 1992. High rates of ablation on the lower part of the Franz Josef Glacier, South Westland. *Proceedings of the Inaugural Joint Conference New Zealand*

Geographical Society and Institute of Australian Geographers Conference Auckland January 1992. NZ Geographical Society: Palmerston North.

Paterson, W.S.B. 1977. Secondary and tertiary creep of glacier ice as measured by borehole closure rates. *Reviews of Geophysics and Space Physics* **15**: 47-55.

Paterson, W.S.B. 1994. *The physics of glaciers*. Pergamon. Oxford. 3rd edn. 480 pp

Pelto, M.S. 1996. Annual net balance of North Cascade glaciers, 1984-94. *Journal of Glaciology* **42**(140): 3-9.

Pelto, M.S. 1997. Reply to the comments of Meier and others on "Annual net balance of North Cascade glaciers, 1984-94" by Mauri S. Pelto. *Journal of Glaciology* **43**(143): 193-196.

Porter, S.C. 1975. Glaciation limit in New Zealand's Southern Alps. *Arctic and Alpine Research* **7**(1): 33-37.

Röthlisberger, H. 1972. Water in intra- and sub-glacial channels. *Journal of Glaciology* **11**: 177-203.

Ruddell, A. 1995. *Recent glacier and climate change in the New Zealand Alps*. PhD Thesis, University of Melbourne.

Russell, P.G. 1987. Spatial and temporal analysis of the complex wind regime of Westland National Park, New Zealand. *Proceedings of the Fifteenth New Zealand Geography Conference Dunedin, August, 1989.* **15**:246-253.

Salinger, M.J. 1981. *New Zealand Climate: The instrumental record*. Unpublished PhD thesis, Victoria University of Wellington.

Sara, W.A. 1968. Franz Josef and Fox Glaciers, 1951-1967. *New Zealand Journal of Geology and Geophysics* **11:** 768-780.

Sara, W.A. 1979. Glaciers of Westland National Park. *New Zealand Department of Industrial and Scientific Research Information Series No. 75 Second Edition.*

Schlosser, E. 1997. Numerical simulation of fluctuations of Hintereisferner, Ötztal Alps, since AD 1850. *Annals of Glaciology* **24**: 199-202.

Schmeits, M.J. and Oerlemans, J. 1997. Simulation of the historical variations in length of the Unterer Grindelwaldgletscher. *Journal of Glaciology* **43**:152-164

Shea, D. 2003. *Southern Oscillation Index Based Upon Annual Standardization*. Online. Available http://www.cgd.ucar.edu/cas/catalog/climind/soiAnnual.html

Singer, C., Shulmeister, J. and McLea, B. 1998. Evidence against a significant Younger Dryas cooling event in New Zealand. *Science* **281**: 812-814.

Soons, J.M. 1971. Recent changes in the Franz Josef Glacier, *in* Johnston, R.J., and Soons, J.M., eds., *Proceedings of the Sixth New Zealand Geography Conference, Christchurch, August 1970*: New Zealand Geographical Society, Conference Series No. **6**(1): 195-200.

Speight, R. 1914. Recent changes in the position of the terminal face of the Franz Josef Glacier. *Transactions of the New Zealand Institute* **47**: 317-342.

Speight, R. 1921. Recent changes in the position of the terminal face of the Franz Josef Glacier. *Transactions of the New Zealand Institute* **53**: 53-57.

Speight, R. 1935. Notes on the Franz Josef Glacier, February 1934. *Transactions of the New Zealand Institute* **64**: 315-382.

Speight, R. 1941. Notes on the Franz Josef Glacier, December 1940. *Transactions of the New Zealand Institute* **71**(2): 131-133.

Stocker, T.F. 2002. North-south Connections. *Science* **297** (5588): 1814-1815.

Stocker, T.F. 2003. Global change: South dials north. *Nature* **424**(6948): 496-499.

Stroeven, A.P., van de Wal, R.S.W. and Oerlemans, J. 1989. Historic front variations of the Rhône Glacier: simulation with an ice flow model. In: J. Oerlemans (ed.), *Glacier Fluctuations and Climatic Change*. Kluwer (Dordrecht): 391-406.

Stroeven, A.P. 1996. The robustness of one-dimensional, time-dependent ice-flow models: a case study from Storglaciären, northern Sweden. *Geografiska Annaler* **78A** (2-3): 133-146.

Suggate, R.P. 1950. Franz Josef and other glaciers of the Southern Alps, New Zealand. *Journal of Glaciology* **1**(8): 422-429.

Suggate, R.P. 1952. Franz Josef Glacier, March 1951. *New Zealand Journal of Science and Technology* **33**(4): 299-304.

Tangborn, W. 1980. Two models for estimating climate-glacier relationships in the North Cascades, Washington, U.S.A. *Journal of Glaciology* **25**(91): 3-21.

Thompson, R.D., and Kells, B.R., 1973, Mass balance studies on the Whakapapanui Glacier, New Zealand, *in* The role of snow and ice in hydrology, Banff Symposium (1972), Proceedings: International Association of Hydrological Sciences, IAHS-AISH Publication No. 107, v. 1, no. 1 (Symposium on Properties and Processes (UNESCO)): 383-393.

Tyson, P.D., Sturman, A.P., Fitzharris, B.B., Mason, S.J. and Owens, I.F. 1997. Circulation changes and teleconnections between glacial advances on the west coast of New Zealand and extended spells of drought years in South Africa. *International Journal of Climatology* **17:** 1499-1512.

van der Veen, C.J. 1987. Longitudinal stresses and basal sliding: a comparative study. In C.J. van der Veen and J.Oerlemans (eds.), *Dynamics of the West Antarctic Ice Sheet*, 223-248. D. Riedel Publishing Company.

van der Wal, R.S.W. and Wild, M. 2001. Modelling the response of glaciers to climate change, applying volume-area scaling in combination with a high resolution GCM. *Climate Dynamics* **18**: 359-366.

van der Veen, C.J. 2002. Polar ice sheets and global sea level: how well can we predict the future? *Global and Planetary Change* **32**:165-194.

van Oldenborgh, G. J. 2003. To what extent have ENSO forecast models breached the spring barrier? *Geophysical Research Abstracts.* **5**

Vincent C, Vallon M., Reynaud L. and Le Meur E. 2000. Dynamic behaviour of the glacier de Saint Sorlin, France, from 40 years of observations, 1957-1997. *Journal of Glaciology* **46** (154): 499-506.

Wallinga, J. and van de Wal, R.S.W. 1998. Sensitivity of the Rhone glacier to climate change: experiments with a one-dimensional flow-line model. *Journal of Glaciology* **44**(147): 383-393.

Wardle, P. 1973. Variations of the glaciers of Westland National Park and the Hooker Range, New Zealand. *New Zealand Journal of Botany* **11:** 349-388.

Warrick, R.A. and Oerlemans, J. 1990. Sea Level Rise. Chapter 10 in J.T. Houghton, G.J. Jenkins and J.J. Ephraums (eds.), *Climate Change: The IPCC Scientific Assessment*. WMO/UNEP Intergovernmental Panel on Climate Change Working Group 1. Cambridge University Press, 365 p.

Weertman, J. 1964. The theory of glacier sliding. *Journal of Glaciology* **5**: 287-303.

Weka, H. 2003. *Hine Hukatere*. Online. Available http://www.angelfire.com/realm/aiam/maori.html.

Wigley, T.M.L. and Raper, S.C.B. 1993. Future changes in global mean temperature and sea level. In: Climate and Sea Level Change: Observations, Projections and Implications (Eds. R.A. Warrick, E.M. Barrow and T.M.L. Wigley), pp.111-133 Cambridge University Press, Cambridge, UK.

Willis, I.C. 1995. Intra-annual variations in glacier motion: a review. *Progress in Physical Geography* **19**(1): 61-106.

Woo, M. and Fitzharris, B.B. 1992. Reconstruction of mass balance variations for Franz Josef Glacier, New Zealand, 1913 to 1989. *Arctic and Alpine Research* **24:** 281-290.

Zuo, Z. and Oerlemans, J. 1997. Numerical modelling of the historic front variations and the future behaviour of the Pasterze glacier. *Annals of Glaciology* **24**:234-241.